

A Macro-Finance model with Realistic Crisis Dynamics*

Goutham Gopalakrishna[†]

October 3, 2022

Abstract

What causes deep recessions and slow recovery? I revisit this question and develop a macro-finance model that quantitatively matches the salient empirical features of financial crises such as a large drop in the output, a high risk premium, reduced financial intermediation, and a long duration of economic distress. The model has leveraged intermediaries with stochastic productivity and a state-dependent exit rate that governs the transition in and out of crises. A model without these two features suffers from a trade-off between the amplification and persistence of crises. I show that my model resolves this tension and generates realistic crisis dynamics.

*I thank my advisor Pierre Collin-Dufresne for invaluable guidance. I am grateful to Markus Brunnermeier for continued support. I also thank Jonathan Payne, Moritz Lenel, Wenhao Li, Semyon Malamud, Peter Maxted, Andrea Modena (discussant), Fernando Mendo (discussant), Paymon Khorrami, Andrei Zlate (discussant), Jerome Detemple, Diogo Mendes (discussant), Alejandro Van der Gote, Sebastian Merkel, Qian Yang (discussant), and participants at CESifo Area conference on Macro, Money, and International Finance, Princeton University Finance seminar, RiskLab/BoF/ESRB conference, DGF doctoral tutorial, and Day-Ahead workshop (University of Zurich) for helpful comments.

[†]EPFL and Swiss Finance Institute. Email: goutham.gopalakrishna@epfl.ch.

1 Introduction

It is well known that recessions are marked by high equity risk premia, low investment rates, and low output. The great recession of 2007-2008 emphasized the importance that financial intermediaries play in propagating shocks to the real economy. Since then, there has been a growing literature on the leverage of intermediaries as a key factor in moving asset prices and the real economy.¹ Recessions that feature a sharp decrease (increase) in the investment rate and output (risk premium) also feature a sharp increase in the leverage of BHCs. While the intermediaries take a central role in the recent macro-finance literature, the financial constraints that they face are of particular importance (see, example, [Brunnermeier and Sannikov \(2014\)](#) (BS2014 henceforth), [He and Krishnamurthy \(2013\)](#), [Di Tella \(2017\)](#), etc.). In these models, the financial constraints bind only at certain times which leads to non-linearity in the asset prices. In normal times, the financial markets facilitate capital allocation to the most productive agents. In such states, the intermediaries are sufficiently capitalized and the premium on the risky asset is low. In bad times, financial constraints bind and the capital gets misallocated to the less productive agents, who do not value capital as much. This leads to a deterioration of the intermediary balance sheet and pushes the system into a crisis region where the premium on risky assets shoots up. These models explain a high risk premium in the crisis periods but the contribution has largely been qualitative except [Maxted \(2020\)](#) and [Krishnamurthy and Li \(2020\)](#).²

The contribution of this paper is two-fold. First, I build an overlapping-generation incomplete-market asset pricing model with stochastic productivity and state-dependent exit of the experts that occasionally generates capital misallocation and fire sales. I solve the model using a novel deep learning-based numerical method that encodes the economic information as regularizers.³ This methodology, as shown in the companion paper [Gopalakrishna \(2021\)](#), is scalable and can be applied to similar high-dimensional problems. The fluctuating productivity of experts is a crucial driver of systemic instability along with capital shocks. In addition, I introduce state-dependent exit of experts

¹See, for example, [Brunnermeier and Sannikov \(2014\)](#), [He and Krishnamurthy \(2013\)](#), [Di Tella \(2017\)](#), [Adrian, Etula and Muir \(2014\)](#), [Phelan \(2016\)](#), [Moreira and Savov \(2017\)](#), etc.

²[Gertler, Kiyotaki and Prestipino \(2020\)](#) incorporates bank run into a standard New Keynesian model that explains financial crisis quantitatively. However, they focus on matching a specific crisis episode- the great recession of 2008.

³Regularizer is a commonly used tool in machine learning to reduce overfitting. See [Glorot and Bengio \(2010\)](#) for details.

as a parsimonious way of capturing bank defaults. The data from Federal Deposit Insurance Corporation (FDIC) shows that a total of 297 banks failed in the period 2009-2010 in the United States, which is a strikingly large number compared to 25 bank failures in the 7 years that preceded the crisis, and 23 bank failures between 2015-2020. Similarly, when measured by default volume, around 80% of the Moody's rated issuers' defaults in the year 2008 came from the financial institutions.⁴ Figure (1) shows the evolution of bank failures from 2001 till 2020. Both in terms of the count and the default volume, bank failures during the Great Recession were far greater than the other years. While a lot of non-financial institutions failed too during the Great recession, the fact that 80% of Moody's issuer defaults in terms of volume came from financial institutions alone indicates that the intermediaries default to a large extent, particularly during financial crises. I capture this empirical phenomenon through an expert exit rate that is calibrated to observed bank default rates.

The second contribution is the quantification of my model to dissect the mechanisms of the financial crisis. To this end, I show that a simpler model with constant productivity and no exit of experts, which reduces to Brunnermeier and Sannikov (2016) (BS2016 henceforth), suffers from a tension between the *amplification* and the *persistence* of financial crises. In particular, there is a trade-off between the conditional risk premium and the duration of crisis.⁵ During bad times, the premium on the risky asset shoots up due to capital misallocation and fire-sale. The leveraged experts earn the higher conditional risk premium allowing them to rebuild sufficient wealth and recover quickly from the crisis. Such a fast rebound is at odds with the data since recessions are empirically long-lasting. Auxiliary features of the model that generate longer crises necessarily attenuate the conditional risk premium (i.e., amplification gets dampened). This is because crises tend to be long when the experts recapitalize slowly, which can only happen when the risk premium that the experts earn is low in the model. To give a concrete example, when the simpler model is calibrated to generate a realistic 18-month duration of the crisis, the model implied conditional risk premium is 2%, which is much lower than

⁴Source for bank failures: <https://www.fdic.gov/bank/historical/bank/>, and Moody's Corporate Default and Recovery Rates, 1920-2008. Financial institutions include Bank holding companies, Real estate, and insurance companies. The list of banks includes only those that are insured by the FDIC. Failure of investment banks such as Lehman Brothers in 2008 is not included.

⁵Another interesting trade-off that emerges from this simpler model is between the unconditional risk premium and the probability of a crisis. This is explored in detail in Section 3.

the empirically observed premium of 25%.⁶ On the other hand, when the model is calibrated to generate a realistic conditional risk premium of 25%, the model-implied average duration of crisis is 5 months, well short of 18-month crisis duration observed in the data. The model with stochastic productivity and state-dependent exit rate resolves this tension and provides reasonable crisis dynamics along three key dimensions: a) *crisis likelihood*, which represents the occupation time of the economy in a crisis state, b) *amplification*, that represents a large conditional risk premium and low output, and c) *persistence*, that represents slow recovery from the crisis. When the economy is in a stochastic steady state, all capital is held by the experts, and the risk premium is low. A negative shock to the level of capital also decreases the productivity of experts, increasing the frequency of crisis by exerting downward pressure on the wealth share of experts. Once the wealth share falls below an endogenous crisis threshold, an amplification mechanism is triggered generating a large risk premium and low output. The model implies an 8% probability of a crisis, matching the empirical value of 7% from [Reinhart and Rogoff \(2009\)](#). In this crisis state, the rate at which the experts exit and become households is high, reflecting large empirical bank bankruptcies, reducing the proportion of agents who manage capital more productively. This force has a dominating impact on the experts' wealth compared to the effect coming from increased risk premium and pushes the economy deeper into crisis. The productivity eventually mean reverts, and the economy reaches a point where the increased productivity dominates the exit effect, helping the economy climb out of the crisis. The speed of mean reversion in productivity is low, forcing the system to spend a long amount of time in distress before the increase in productivity ends the gloomy phase. The model implies a crisis duration of 17 months, close to the empirical value of 18 months from the NBER recessionary cycle data. At normalcy, all capital in the economy is held by intermediaries again, and the financial amplification channel is shut down, where the exit rate is small. Thus, the twin forces of stochastic productivity and exit match the empirical moments in all three categories, bringing the model closer to data.

The model is solved using a deep learning-based numerical algorithm that takes advantage of the universal approximation theorem by [Hornik, Stinchcombe and White](#)

⁶See Table (3) in Section 3 for the estimated conditional risk premium. The average contraction period from the NBER website is around 18 months. Source: <https://www.nber.org/cycles.html>. This is a conservative measure compared to around 3 years peak to trough period reported in [Muir \(2017\)](#).

(1989), which states that a neural network with one hidden layer can approximate any Borel measurable function. This method is scalable since it alleviates the curse of dimensionality that plagues the finite-difference schemes in higher dimensions. The main difficulty that arises from grid-based solutions such as finite-difference schemes is the combination of an explosion in the number of grid points and the need for a reduced time step size as the dimensions grow large. My solution side-steps these limitations since it is mesh-free.⁷ This algorithm dominates the finite-difference method used in BS2016, Hansen, Khorrami and Tourre (2018), etc., since it has the advantage of being easier in scaling to higher dimensions.⁸ The companion paper Gopalakrishna (2021) discusses the algorithm in detail and applies it to similar problems with the a number of dimensions as high as five.

The simpler benchmark model with constant productivity and no exit is similar in spirit to BS2016 but there is an overlapping generation of agents (OLG) with recursive preference. The assumption of OLG offers a non-degenerate stationary distribution of the state variable (Cârleanu and Panageas (2015)), while recursive preference helps with obtaining realistic asset pricing moments.⁹ I quantify this benchmark model, similar in spirit to He and Krishnamurthy (2019) (HK2019 henceforth) and Krishnamurthy and Li (2020) but with notable differences. The model that I consider has both the households and the experts consuming by solving an infinite horizon optimization problem, whereas, in HK2019 the experts do not consume and solve a myopic optimization problem. Both models feature non-linear asset prices arising due to occasionally binding financial intermediary constraints. However, the transition from the normal to the crisis state is smooth in HK2019. On the contrary, the model that I consider, similar to BS2016, features an endogenous jump in the risk prices that reflects the fact that periods prior to financial crises are typically calm with an exceedingly low risk premium (Baron and Xiong (2017)) and rises dramatically once the crisis period begins. The endogenous jump in the model is caused by the fire-sale effect where the experts sell capital to households that have a lower valuation of the capital due to their lower productivity rate. The effect of fire sales on the asset markets is crucial in times of distress, as is emphasized in

⁷I rely on Tensor-flow, a deep learning library developed by Google Brain, that computes the numerical derivatives efficiently.

⁸Appendix C.4.1 shows that the solution obtained from this algorithm matches the solution from the finite difference method when applied to a simpler model with one state variable. I also demonstrate how one can modify a few lines of code and jump from solving a low to a high-dimensional state space problem.

⁹The OLG assumption provides a non-degenerate distribution even when there is no discount rate heterogeneity.

Kiyotaki and Moore (1997), Shleifer and Vishny (2011), and Kurlat (2018). Importantly, due to the endogenous jump, the point in the state space at which the financial crisis occurs is well-defined. In models where the transition is smooth, one has to rely on an exogenously defined threshold at which the system enters the crisis region. Krishnamurthy and Li (2020) considers the model with an endogenous jump similar to this paper but focuses on matching credit spreads across several financial crisis episodes with an emphasis on the pre-crisis froth in credit markets. While the agents in their model have log utility with the capital subjected to Brownian and Poisson shocks, I consider a recursive utility function and focus on matching a broader set of macroeconomic and asset pricing moments such as the intermediary leverage patterns, the risk-free rate, the equity risk premium, the investment rate, the GDP growth rate, the probability and duration of crisis among others. The recursive utility has the advantage of separating the risk aversion from the IES (Bansal and Yaron (2004)) and also helps with obtaining better asset pricing moments. Maxted (2020) analyzes a quantitative model of financial intermediation and sentiment, similar to Krishnamurthy and Li (2020) where intermediaries do not consume and have mean-variance preferences over their reputation.

Models of intermediary asset pricing highlight the *persistence* and the *amplification* of shocks caused by the leveraged agents. A measure of persistence and amplification is the duration of the crisis and conditional risk premium, respectively. The quantification of the benchmark model reveals two key trade-offs. First, there is tension between the unconditional risk premium and the probability of a crisis. A high level of risk aversion means that the experts earn a large risk premium in the stochastic steady state. Small negative shocks to the capital do not cause enough deterioration in their net worth to hit the crisis boundary, thereby diminishing the probability of a crisis. Second, conditional on being in crisis, there is tension between the risk premium and the duration of the crisis. This is because risk premium spikes as soon as the system enters a crisis state, enabling the experts to gain wealth quickly and revert to the normal regime leading to fast recovery. With larger values of risk aversion, the experts build wealth even faster through a higher risk premium, resulting in a quicker reversion to the normal state. This poses a direct challenge to the heterogeneous agent models with leveraged agents that are calibrated with high risk aversion since larger risk aversion levels mechan-

cally imply a lower probability and duration of crisis.¹⁰ The benchmark model has its strengths in capturing the non-linearity of the asset prices, the output growth, and the leverage patterns of intermediaries. The biggest weaknesses are the inability to jointly generate a realistic duration of crisis and risk premium, and sufficient variation in the risk prices.¹¹ The richer model with stochastic productivity and state-dependent exit rate of the experts generates reasonable asset pricing and crisis moments. Embedding these two features that have empirical support brings the model closer to the data in important aspects.

Related Literature This paper relates to several strands of the literature. On the modeling front, it is most closely related to BS2016 which introduces a continuous time macro-finance model based on capital misallocation and fire sales. It fits within a large body of intermediary based asset pricing models such as BS2014, [He and Krishnamurthy \(2013\)](#), [Di Tella \(2017\)](#), [Adrian and Boyarchenko \(2012\)](#), [Moreira and Savov \(2017\)](#), etc. While BS2014 assumes risk-neutral agents with an exogenous interest rate, the agents in BS2016 are risk averse with CRRA utility function, and the risk-free rate is endogenous. The capital misallocation in BS2016 occurs due to bad shocks and the subsequent fire-sale effect. [Moll \(2014\)](#) analyses a model where the inability of the productive agents to lever up due to collateral constraints causes capital misallocation.

The empirical evidence for intermediary-based asset pricing highlights the role that the banks and the hedge funds play in pricing assets ([He, Kelly and Manela \(2017\)](#), and [Adrian, Etula and Muir \(2014\)](#)). While these papers provide a theory based on intermediary leverage as a motivation for empirical findings, the literature that tightly tests the ability of general equilibrium asset pricing models with financial frictions to match the data is sparse. Two related papers that attempt to fill the gap are [Muir \(2017\)](#), and HK2019. However, the experts in their model do not consume and solve a myopic optimization problem, whereas, in my model both the households and the experts consume a fraction of the total output by solving an infinite horizon optimization problem. While HK2019 focus on matching the non-linearity of their model with the data and consider an exogenously defined probability of a crisis, the goal of this paper goes beyond match-

¹⁰It is common in asset pricing literature to assume a high risk aversion. See, for example [Gârleanu and Panageas \(2015\)](#), who set risk aversion of leveraged agents equal to 10.

¹¹Since the q-theory result tightly ties the investment rate to the capital price, a low model implied volatility of price translates to a low variation in the investment rate too.

ing just the non-linearity and deals with an endogenous crisis boundary- a slightly more daunting task since there is one less degree of freedom. In this regard, this paper comes closer to [Krishnamurthy and Li \(2020\)](#) which attempts to match the pre-crisis froth in the credit market through a Bayesian learning model. [Muir \(2017\)](#) analyses risk premia during downturns for a large panel of countries and finds that financial crises are crucial in understanding the variation in risk premium. Also, the intermediary-based asset pricing model is shown to fare better compared to the consumption-based representative agent models with long-run risk ([Bansal and Yaron \(2004\)](#)), habit ([Campbell and Cochrane \(1999\)](#)), and rare disaster ([Barro \(2006\)](#)) features. This paper also relates to [Khorrami \(2016\)](#), who shows that the implied cost of entry to participate in the stock market is as large as 90% of the wealth of the agents. Another interpretation of this result is that the costs of risk concentration are unreasonably large to match the empirically observed level of risk premium. While he focuses on a limited asset market participation model with costly entry, my model features capital misallocation with stochastic productivity that is calibrated to match both the amplification as well as the duration of crisis in the data. [Bigio and D’Avernas \(2021\)](#) build a risk capacity-based model with information asymmetries to explain slow recovery from the financial crisis. The state-dependent exit of experts in this paper relates to [Eisfeldt, Lustig and Zhang \(2017\)](#) who introduce endogenous entry and exit of participants in complex asset markets.¹²

[Hansen, Khorrami and Tourre \(2018\)](#) provide a framework that nests several models based on financial frictions. Even though the frictions prevent the economy from achieving the first-best outcome, their model features a dynamically complete market since the households can hedge their risk exposures through the derivative market. Their contribution is largely to provide qualitative insights by comparing different nested models, whereas, this paper is guided by quantitative analysis. While they consider a multi-dimensional problem with auxiliary shocks to the volatility and long-run growth, my model has stochastic productivity and exit rate of experts. More importantly, I conduct extensive simulations to test the model performance in matching both unconditional and conditional macroeconomic and asset pricing moments. My model assumes that the productivity of experts is a function of its size (wealth share of experts) which holds empirical relevance ([Hughes, Mester and Moon \(2001\)](#), [Feng and Serletis \(2010\)](#)). I con-

¹²In [Eisfeldt, Lustig and Zhang \(2017\)](#), the decision to enter and exit is endogenous and hence the agents solve an optimal stopping time problem. In this paper, the exit rate is assumed to be state-dependent.

sider a parsimonious way to capture bank defaults through an exogenous exit rate of experts which complements a large literature on the endogenous bank runs and defaults ([Gorton and Ordoñez \(2014\)](#), [Gertler, Kiyotaki and Prestipino \(2020\)](#), [Li \(2020\)](#)).

Lastly, this paper also relates to the literature on global solution methods for heterogeneous agent models using continuous time machinery (see [Achdou et al. \(2014b\)](#) for an overview). The assumption that the agents can consume and invest continuously in response to their instantaneous change in wealth not only greatly simplifies the computation, but also reflects the reality that people do not take these decisions only at the end of a quarter. Another advantage of the continuous-time method is the analytical tractability of equilibrium prices up to a coupled or decoupled system of partial differential equations. [Achdou et al. \(2014a\)](#), BS2016, and [Fernández-Villaverde, Hurtado and Nuno \(2020\)](#) offer a solution technique involving an implicit scheme with up-winding to solve the PDEs that ensures faster convergence. [D’Avernas and Vandeweyer \(2019\)](#) document that finite difference methods are difficult to implement in higher dimensions not only because of the curse of dimensionality but also due to the difficulty in preserving the monotonicity of the finite difference scheme. They offer a solution method based on [Bonnans, Ottenwaelter and Zidani \(2004\)](#) that involves rotating the state space and finding the right direction to approximate the cross partial derivatives such that the monotonicity of the scheme is preserved. With the advancements in machine learning, recent papers have turned to neural networks to solve equilibrium models. [Duarte \(2017\)](#) considers a method based on deep learning to solve asset pricing problems in high dimensions. [Fernández-Villaverde, Hurtado and Nuno \(2020\)](#) solves for the high dimensional law of motion of households using a deep neural network.¹³ The algorithm proposed in this paper is similar in spirit but also incorporates prior information from the crisis boundary as regularizers and is particularly geared toward solving heterogeneous agent incomplete market problems with capital misallocation and *endogenous* jump in prices. It also seeks inspiration from active machine learning where the algorithm learns to sample points from the state space in an informed manner. To the best of my knowledge, this is the first paper to apply a deep learning-based algorithm to solve such type of a model.

¹³There is a substantial literature on the deep-learning techniques to solve PDEs in Applied Mathematics, which I cover in the companion paper [Gopalakrishna \(2021\)](#). For the application of deep learning techniques to solve discrete-time DSGE models, see [Azinovic, Gaegauf and Scheidegger \(2019\)](#).

The paper is organized as follows. Section 2 introduces the model. Section 3 presents the benchmark model and quantifies it to shed light on the tension between the amplification and the persistence of crises. Section 4 shows that the model with stochastic productivity and exit rate of experts resolves the tension and brings the model closer to the data. Section 5 concludes. The proofs and details on numerical methodology can be found in Online Appendix B.

2 Model

In this section, I present a heterogeneous agent model with stochastic productivity and state-dependent exit rate of experts. There is an infinite horizon economy with a continuum of agents, who are of two types: Household (\mathbb{H}) and Expert (\mathbb{E}). The aggregate capital in the economy is denoted by K_t , where $t \in [0, \infty)$ denotes time. Within each group, the agents are identical and hence we can index the representative household and the expert by $h \in \mathbb{H}$ and $e \in \mathbb{E}$ respectively.¹⁴ The experts can issue risk-free debt, and obtain a higher return to holding capital as they are more productive than households. The friction is such that the experts have to retain at least some amount of equity on their balance sheet. In the absence of this friction, the experts should hold all capital as they are more productive users. Also, the agents are precluded from shorting the risky capital. The production technology can be written as

$$y_{j,t} = a_{j,t} k_{j,t} \quad j \in \{e, h\} \quad (1)$$

where the capital evolves as¹⁵

$$\frac{dk_{j,t}}{k_{j,t}} = (\Phi(\iota_{j,t}) - \delta)dt + \sigma dZ_t^k \quad (2)$$

with $\iota_{j,t}$ as the investment rate, and $\{Z_t \in \mathbb{R}; \mathcal{F}_t, \Omega\}$ is the standard Brownian motions representing the aggregate uncertainty in $(\Omega, \mathbb{P}, \mathcal{F})$. The parameter σ denotes the exogenous volatility of the capital process. The investment function $\Phi(\cdot)$ is concave and captures the decreasing returns to scale, and δ is the depreciation rate of capital. As in

¹⁴This is also due to the homogeneity of preferences of agents within each group as explained later.

¹⁵Note that $k_{j,t}$ is the capital held by agent j .

BS2016, $\Phi(\cdot)$ captures the technological illiquidity. The depreciation rate is the same for both households and experts. I assume that the investment cost function takes the logarithmic form¹⁶ $\Phi(\iota) = \frac{\log(\kappa\iota+1)}{\kappa}$ where κ is the adjustment cost parameter that controls the elasticity of the investment technology. I assume that the productivity of the experts is governed by the following stochastic differential equation

$$da_{e,t} = \pi(\hat{a}_e - a_{e,t})dt + \underbrace{\nu(\bar{a}_e - a_{e,t})(a_{e,t} - \underline{a}_e)}_{\sigma_{ae,t}} dZ_t^a \quad (3)$$

where the Brownian shock dZ_t^a has a correlation φdt with the Brownian shock dZ_t^k with $\varphi > 0$. That is, the expert productivity follows an Ornstein–Uhlenbeck process with stochastic volatility such that it moves between a lower level \underline{a}_e and an upper level \bar{a}_e with a persistence parameter π and mean $\hat{a}_e \in (\underline{a}_e, \bar{a}_e)$. Since $a_h < \underline{a}_e < \bar{a}_e$, the productivity of the experts is always higher than that of the households even though it fluctuates between \underline{a}_e and \bar{a}_e .¹⁷ The capital price q_t follows

$$\frac{dq_t}{q_t} = \mu_t^q dt + \sigma_t^{q,k} dZ_t^k + \sigma_t^{q,a} dZ_t^a$$

The return process for each type of agent is given by $dR_{j,t} = \frac{d(q_t k_{j,t})}{q_t k_{j,t}} + \frac{(a_{j,t} - \iota_{j,t})k_{j,t}}{q_t k_{j,t}} dt$ where the first component of the R.H.S is capital gain, and the second component is the dividend yield. Note that the dividends are agent-specific due to different productivity rates, and possibly due to different investment rates.¹⁸ Applying Ito's lemma, we get

$$dR_{j,t} = \underbrace{\left(\mu_t^q + \Phi(\iota_{j,t}) - \delta + \sigma \sigma_t^{q,k} + \varphi \sigma \sigma_t^{q,a} + \frac{a_{j,t} - \iota_{j,t}}{q_t} \right)}_{\mu_{j,t}^R} dt + (\sigma_t^{q,k} + \sigma) dZ_t^k + \sigma_t^{q,a} dZ_t^a \quad (4)$$

¹⁶This is a valid investment cost function since $\Phi(0) = 0$, $\Phi' > 0$, and $\Phi'' \leq 0$.

¹⁷I denote $(a_{j,t}; j \in \{e, h\})$ to have concise notation but it is to be understood that $a_{h,t}$ is just a constant a_h , whereas $a_{e,t}$ follows equation (3).

¹⁸It turns out that the optimal investment rate is the same for both types of agent since it depends on the capital price and the adjustment cost parameter κ . For now, I assume that the investment rate is agent-specific and show later in (13) that it is the same for all agents.

The aggregate output in the economy is given by $y_t = A_t K_t$, where $K_t = \int_{\mathbb{E} \cup \mathbb{H}} k_{j,t} dj$, and A_t is the aggregate dividend that satisfies

$$A_t = \int_{\mathbb{E} \cup \mathbb{H}} a_{j,t} \frac{k_{j,t}}{K_t} dj$$

Let the capital share held by the expert sector be denoted by

$$\psi_t := \frac{\int_{\mathbb{E}} k_{j,t} dj}{\int_{\mathbb{H} \cup \mathbb{E}} k_{j,t} dj}$$

The experts and the households trade capital and the experts face a skin-in-the-game constraint that forces them to retain at least a fraction $\underline{\chi} \in [0, 1]$ of the equity on their balance sheet. The agents can also trade in the risk-free security that pays a return r_t that is determined in the equilibrium. The stochastic discount factor (SDF) process for each type of agent is given by

$$\frac{d\xi_{j,t}}{\xi_{j,t}} = -r_t dt - \zeta_{j,t}^k dZ_t^k - \zeta_{j,t}^a dZ_t^a \quad (5)$$

where $\zeta_{j,t}^k$ and $\zeta_{j,t}^a$ are the prices of risk for the shocks dZ_t^k and dZ_t^a respectively.

Preferences and equilibrium I assume that the agents have recursive utility with IES=1. That is, the utility is given by

$$U_{j,t} = E_t \left[\int_t^\infty f(c_{j,s}, U_{j,s}) ds \right]$$

with

$$f(c_{j,t}, U_{j,t}) = (1 - \gamma) \rho U_{j,t} \left(\log(c_{j,t}) - \frac{1}{1 - \gamma} \log((1 - \gamma) U_{j,t}) \right) \quad (6)$$

where γ and ρ are the risk aversion and the discount rate coefficients respectively. Following [Gârleanu and Panageas \(2015\)](#), I assume that some agents are born and die at each time instant with a probability λ_d . Let \bar{z} and $1 - \bar{z}$ denote the proportion of experts and households that are born each instant respectively. The death risk is not measurable under the filtration generated by the Brownian process \mathcal{F}_t and the agents do not have bequest motives. Hence, once the agents die, the wealth is pooled and distributed

on a pro-rata basis. As a result of the death risk, the rate of time preference parameter ρ can be thought of as inclusive of the death rate λ_d . I abstract away from the insurance market to hedge the death risk, similar to [Hansen, Khorrami and Tourre \(2018\)](#) for simplicity. I assume that at each time instant dt , a fraction $\tau_t dt$ of experts become households, where τ_t is state-dependent. This transition will be taken into consideration in the optimization problem of the agents.¹⁹ This assumption is a parsimonious way to capture bank failures, which are particularly high during financial crises, as seen in Figure (1). The experts optimize by maximizing their utility functions, subject to wealth constraints, starting from some initial wealth $w_{e,0}$.²⁰ Let τ' denote the time at which the experts exit and become households, that is exponentially distributed with the rate τ_t . They solve

$$\begin{aligned}
 U_{e,t} = & \sup_{c_{e,t}, k_{e,t}, \chi_{e,t}} E_t \left[\int_t^{\tau'} f(c_{e,s}, U_{e,s}) ds + U_{h,\tau'} \right] \\
 \text{s.t. } & \frac{dw_{e,t}}{w_{e,t}} = \left(r_t - \frac{c_{e,t}}{w_{e,t}} + \frac{q_t k_{e,t}}{w_{e,t}} (\mu_{e,t}^R - r_t - (1 - \chi_{e,t}) \epsilon_{h,t}) \right) dt \\
 & + \sigma_{w_{e,t}} \left((\sigma + \sigma_t^{q,k}) dZ_t^k + \sigma_t^{q,a} dZ_t^a \right)
 \end{aligned} \tag{7}$$

where $\frac{q_t k_{e,t}}{w_{e,t}}$ and $\chi_{e,t}$ denote the fraction of wealth invested in capital, and the experts' inside equity share, respectively. The experts obtain a continuation utility of $U_{h,\tau'}$ starting from the time of transition into households. While the experts obtain an expected excess return of $\mu_{e,t}^R - r_t$ by investing in the risky asset, they have to pay the outside equity investors $(1 - \chi_{e,t}) \epsilon_{h,t}$, where $\epsilon_{h,t}$ is the premium demanded by households defined in equation (12). Thus, the latter component is netted out from the total expected return on capital investment. The skin-in-the game constraint implies that experts choose the inside equity share $\chi_{e,t} \in [\underline{\chi}, 1]$. On the other hand, households do not issue outside equity implying that $\chi_{h,t} = 1$ always. I write $\chi_{e,t}$ simply as χ_t for notational convenience

¹⁹[Gomez \(2019\)](#) uses a similar assumption that applies to the leveraged wealthy households, and in [Di Tella \(2017\)](#), a similar exit rate is applied to the intermediaries to generate a non-degenerate stationary distribution. However, they do not model the exit rate as state-dependent. The functional form of τ_t is provided later in (22), after constructing of the state space.

²⁰Note that since all agents within the same group are identical, the wealth equation is presented for the aggregated agents. For wealth dynamics of individual agent within the group, see Appendix B.1.2.

henceforth. The households solve

$$U_{h,t} = \sup_{c_{h,t}, k_{h,t}} E_t \left[\int_t^\infty f(c_{h,s}, U_{h,s}) ds \right] \quad (8)$$

$$\text{s.t. } \frac{dw_{h,t}}{w_{h,t}} = \left(r_t - \frac{c_{h,t}}{w_{h,t}} + \frac{q_t k_{h,t}}{w_{h,t}} (\mu_{h,t}^R - r_t) \right) dt + \sigma_{w_{h,t}} \left((\sigma + \sigma_t^{q,k}) dZ_t^k + \sigma_t^{q,a} dZ_t^a \right)$$

The diffusion terms of the wealth equation are given by

$$\sigma_{w_e,t} = \frac{q_t k_{e,t}}{w_{e,t}} \chi_t \quad (9)$$

$$\sigma_{w_h,t} = \frac{q_t k_{h,t}}{w_{h,t}} + (1 - \chi_t) \frac{q_t k_{e,t}}{w_{h,t}} \quad (10)$$

The experts retain a fraction χ_t of risk in their balance sheet, and hence the fraction of capital invested in the diffusion terms is multiplied by this quantity. The households receive the remaining risk that enters into the second part of equation (10). The households face a no-shorting constraint $k_{h,t} \geq 0$. I define

$$\epsilon_{e,t} := \zeta_{e,t}^k (\sigma + \sigma_t^{q,k}) + \zeta_{e,t}^a \sigma_t^{q,a} + \varphi(\zeta_{e,t}^a (\sigma + \sigma_t^{q,k}) + \zeta_{e,t}^k \sigma_t^{q,a}) \quad (11)$$

$$\epsilon_{h,t} := \zeta_{h,t}^k (\sigma + \sigma_t^{q,k}) + \zeta_{h,t}^a \sigma_t^{q,a} + \varphi(\zeta_{h,t}^a (\sigma + \sigma_t^{q,k}) + \zeta_{h,t}^k \sigma_t^{q,a}) \quad (12)$$

There are two prices of risk for each type of the agent: $\zeta_{j,t}^k$ and $\zeta_{j,t}^a$, corresponding to the capital shock and the productivity shock, respectively. That is, by borrowing in the risk free market at a rate r_t and investing in the risky capital, they obtain the prices of risk $\zeta_{j,t}^k$ and $\zeta_{j,t}^a$. The exit rate of experts does not enter into the individual wealth equation, but it appears in the evolution of aggregated expert wealth as shown in Appendix B.1.2. In fact, there are an infinite number of agents in the economy, but each individual in types \mathbb{E} and \mathbb{H} is identical, hence they have the same preferences. Therefore, one can seek an equilibrium in which all agents in the same group take the same policy decisions. For completeness, I present the full version of the equilibrium first.

Definition 2.1. A competitive equilibrium is a set of aggregate stochastic processes adapted to the filtration generated by the Brownian motions Z_t^k and Z_t^a . Given an initial distribution of wealth between the experts and households, the processes are prices (q_t, r_t) , policy functions $(c_{j,t}, l_{j,t}, \psi_t; j \in \{e, h\})$ and net worth $(w_{j,t}; j \in \{e, h\})$, such that

- Capital market clears: $\int_{\mathbb{H}} (1 - \psi_t) K_t dj + \int_{\mathbb{E}} \psi_t K_t dj = \int_{\mathbb{H} \cup \mathbb{E}} k_{j,t} dj \quad \forall t$

- Goods market clear: $\int_{\mathbb{H} \cup \mathbb{E}} c_{j,t} dj = \int_{\mathbb{H} \cup \mathbb{E}} (a_{j,t} - \iota_{j,t}) k_{j,t} dj \quad \forall t$
- $\int_{\mathbb{H} \cup \mathbb{E}} w_{j,t} dj = \int_{\mathbb{H} \cup \mathbb{E}} q_t k_{j,t} dj \quad \forall t$

Asset pricing conditions The agents choose the optimal rate of investment by maximizing their return on holding capital. That is, $\iota_{j,t}$ solves²¹

$$\max_{\iota_{j,t}} \Phi(\iota_{j,t}) - \frac{\iota_{j,t}}{q_t}$$

The optimal investment rate is obtained as

$$\iota_{j,t}^* = \frac{q_t - 1}{\kappa} \quad (13)$$

The investment rate is the same for both types of agents since it depends only on q_t . This is a standard ‘q-theory’ result, which implies a tight relation between the price of capital and the investment rate. Thus, the growth rate of the economy is endogenously determined by the investment rate through the capital price. A higher price increases investment and causes output growth to accelerate (since $\Phi'(\cdot) > 0$). The asset pricing relationship for experts is given by²²

$$\frac{a_{e,t} - \iota_t}{q_t} + \Phi(\iota_t) - \delta + \mu_t^q + \sigma \sigma_t^{q,k} + \varphi \sigma \sigma_t^{q,a} - r_t = \chi_t \epsilon_{e,t} + (1 - \chi_t) \epsilon_{h,t} \quad (14)$$

where $\epsilon_{j,t}$ is defined in (11) and (12). The experts will issue the maximum allowed equity ($\chi_t = \underline{\chi}$) if the premium demanded by them is higher than that required by households. The pricing condition of households is given by

$$\frac{a_h - \iota_t}{q_t} + \Phi(\iota_t) - \delta + \mu_t^q + \sigma \sigma_t^{q,k} + \varphi \sigma \sigma_t^{q,a} - r_t \leq \epsilon_{h,t} \quad (15)$$

²¹Note that the only component in the expected return that contains investment rate is $\Phi(\iota_{j,t}) - \frac{\iota_{j,t}}{q_t}$.

²²This can be shown using a Martingale argument. See Appendix B.1.1 for the proof.

where the equality holds if $\psi_t < 1$. We can combine (14) and (15) and write the asset pricing condition as

$$\frac{a_{e,t} - a_h}{q_t} \geq \chi_t(\epsilon_{e,t} - \epsilon_{h,t}) \quad (16)$$

$$\min\{\chi_t - \underline{\chi}, \epsilon_{e,t} - \epsilon_{h,t}\} = 0 \quad (17)$$

Equation (16) holds with equality if $\psi_t < 1$. Equation (17) states that whenever the risk premium of experts is larger than that of households, experts issue the maximum outside equity (i.e., $\chi_t = \underline{\chi}$). When experts are wealthy enough such that the constraint is no longer binding, the risk premium becomes equal. I solve for the decentralized Markov equilibrium by summarizing the system in terms of two state variables: wealth share of the experts denoted by z_t , and the productivity of the experts $a_{e,t}$.²³ The equilibrium conditions map the optimal consumption, investment, capital share, and the capital price to the history of Brownian shocks Z_t^k and Z_t^a through state variables $(z_t, a_{e,t})$ which has a domain denoted by Ω . The wealth share is defined as

$$z_t = \frac{W_{e,t}}{q_t K_t} \in (0, 1)$$

where $W_{e,t} = \int_{\mathbb{E}} w_{j,t} dj$. Moving forward, I write $X_{h,t}$ and $X_{e,t}$ to denote the aggregated quantities $\int_{\mathbb{H}} x_{j,t} dj$ and $\int_{\mathbb{E}} x_{j,t} dj$ respectively and characterize the model with a representative household and expert.²⁴

Proposition 1. *The law of motion of the wealth share of experts is given by*

$$\frac{dz_t}{z_t} = \mu_t^z dt + \sigma_t^{z,k} dZ_t^k + \sigma_t^{z,a} dZ_t^a \quad (18)$$

²³All relevant objects scale with the capital K_t and hence we can summarize the economy in just two state variables.

²⁴That is, since each agent within their respective group are identical, solving for the aggregate agent policies are enough.

where

$$\begin{aligned}\mu_t^z &= \frac{a_{e,t} - l_t}{q_t} - \frac{C_{e,t}}{W_{e,t}} + \left(\frac{\chi_t \psi_t}{z_t} - 1 \right) \left((\sigma + \sigma_t^{q,k}) (\hat{\zeta}_{e,t}^1 - (\sigma + \sigma_t^{q,k})) + \sigma_t^{q,a} (\hat{\zeta}_{e,t}^2 - \sigma_t^{q,a}) - 2\varphi(\sigma + \sigma_t^{q,k}) \sigma_t^{q,a} \right) \\ &\quad + (1 - \chi_t) \left((\sigma + \sigma_t^{q,k}) (\hat{\zeta}_{e,t}^1 - \hat{\zeta}_{h,t}^1) + \sigma_t^{q,a} (\hat{\zeta}_{e,t}^2 - \hat{\zeta}_{h,t}^2) \right) + \frac{\lambda_d}{z_t} (\bar{z} - z_t) - \tau(a_{e,t}, z_t) \\ \hat{\zeta}_{j,t}^1 &= \zeta_{j,t}^k + \varphi \zeta_{j,t}^a; \quad j \in \{e, h\} \\ \hat{\zeta}_{j,t}^2 &= \zeta_{j,t}^a + \varphi \zeta_{j,t}^k; \quad j \in \{e, h\} \\ \sigma_t^{z,k} &= \left(\frac{\chi_t \psi_t}{z_t} - 1 \right) (\sigma + \sigma_t^{q,k}) \\ \sigma_t^{z,a} &= \left(\frac{\chi_t \psi_t}{z_t} - 1 \right) \sigma_t^{q,a}\end{aligned}$$

Proof: See Appendix B.1.2.

The parameters λ_d and \bar{z} denote the death rate and the mean proportion of experts in the economy at each time instant, respectively. The exit rate τ_t enters the drift of the wealth share.

2.1 Model solution

The solution method is similar to value function iteration, with an inner static loop used to solve the equilibrium quantities $(\chi_t, \psi_t, q_t, \sigma_t^{q,k}, \sigma_t^{q,a})$ using a Newton-Raphson method, and an outer static loop to solve the value functions $J_{j,t}$ using a deep neural network architecture. The first step begins from a time T and solves equilibrium policies from the value function, which is set to take an arbitrary value. This is analogous to ‘policy improvement’ in the reinforcement learning literature. In the second step, the neural network solves for the value function, taking policies computed in first step as given, which is then used to update policies in the subsequent step. This corresponds to the ‘policy evaluation’ in the language of reinforcement learning.²⁵ The two-step procedure is performed repeatedly until the value function converges. I present and discuss the equilibrium policies, and relegate the methodological details to Appendix B.1.5.

²⁵While there are similarities between the value function iteration and reinforcement learning, the state space in my model is known ahead. A large part of the reinforcement learning deals with exploring new state space which is not relevant for the setup considered in this paper.

Static decisions and HJB equations: The value function is given by $U_{j,t}$ and the HJB for optimization problem (7) can be written as

$$\sup_{C_{j,t}, K_{j,t}} f(C_{j,t}, U_{j,t}) + E[dU_{j,t}] = 0 \quad (19)$$

Homothetic preferences imply that the value function is of the form

$$U_{j,t} = \frac{(J_{j,t}(z_t, a_{e,t})K_t)^{1-\gamma}}{1-\gamma}$$

with the process for the stochastic opportunity set defined as

$$\frac{dJ_{j,t}}{J_{j,t}} = \mu_{j,t}^J dt + \sigma_{j,t}^{J,k} dZ_t^k + \sigma_{j,t}^{J,a} dZ_t^a \quad (20)$$

The aggregate wealth dynamics of experts is given by

$$\begin{aligned} \frac{dW_{e,t}}{W_{e,t}} = & \left(r_t - \frac{C_{e,t}}{W_{e,t}} + \frac{q_t K_t}{W_{e,t}} \epsilon_{e,t} - \lambda_d + \frac{\bar{z} \lambda_d}{z_t} - \tau(z_t, a_{e,t}) \right) dt \\ & + \chi_{e,t} \frac{q_t K_t}{W_{e,t}} (\sigma + \sigma_t^{q,k}) dZ_t^k + \chi_{e,t} \frac{q_t K_t}{W_{e,t}} \sigma_t^{q,a} dZ_t^a \end{aligned} \quad (21)$$

The terms involving λ_d are due to the birth and death, and $\tau(z_t, a_{e,t})$ is the state dependent exit rate. I assume the following function for the exit rate.

$$\tau_t = \tau_n 1_{\Omega_n}(z_t, a_{e,t}) + \tau_c 1_{\Omega_c}(z_t, a_{e,t}) \quad (22)$$

where $\Omega_c = \{(z_t, a_{e,t}) | z_t \leq z^*(a_e)\}$ is the endogenous region in state space at which the capital gets misallocated, and the economy is in crisis. That is, $z^*(a_e)$ denotes the crisis boundary at which experts find it optimal to fire-sell the capital to households, triggering the financial amplification mechanism. The region $\Omega_n = \{(z_t, a_{e,t}) | z_t > z^*(a_e)\}$ corresponds to the normal regime with high output and low risk premium, and $\Omega = \Omega_c \cup \Omega_n$. The parameters (τ_c, τ_n) are calibrated to the observed bank default rates. The HJB equa-

tion is written as²⁶

$$\begin{aligned} & \rho \left[\log \frac{C_{j,t}}{W_{j,t}} - \log J_{j,t} + \log(q_t z_{j,t}) \right] + (\Phi(t) - \delta) - \frac{\gamma}{2} \sigma^2 + \mu_{j,t}^J - \frac{\gamma}{2} ((\sigma_{j,t}^{J,k})^2 + (\sigma_{j,t}^{J,a})^2 + 2\varphi \sigma_{j,t}^{J,k} \sigma_{j,t}^{J,a}) \\ & + (1 - \gamma)(\sigma \sigma_{j,t}^{J,k} + \varphi \sigma \sigma_{j,t}^{J,a}) + 1_{j \in \mathbb{E}} \frac{\tau_t}{1 - \gamma} \left(\left(\frac{J_{j',t}}{J_{j,t}} \right)^{1-\gamma} - 1 \right) = 0 \end{aligned} \quad (23)$$

where the last term on the left hand side is due to the exit.²⁷

Proposition 2. *The optimal consumption policy, and prices of risk are given by*

$$\hat{C}_{j,t} = \rho \quad (24)$$

$$\zeta_{e,t}^k = -(1 - \gamma) \sigma_{e,t}^{J,k} + \sigma_t^{z,k} + \sigma_t^{q,k} + \gamma \sigma \quad (25)$$

$$\zeta_{e,t}^a = -(1 - \gamma) \sigma_{e,t}^{J,a} + \sigma_t^{z,a} + \sigma_t^{q,a} \quad (26)$$

$$\zeta_{h,t}^k = -(1 - \gamma) \sigma_{h,t}^{J,k} - \frac{z_t}{1 - z_t} \sigma_t^{z,k} + \sigma_t^{q,k} + \gamma \sigma \quad (27)$$

$$\zeta_{h,t}^a = -(1 - \gamma) \sigma_{h,t}^{J,a} - \frac{z_t}{1 - z_t} \sigma_t^{z,a} + \sigma_t^{q,a} \quad (28)$$

Proof: See Appendix B.1.3.

The consumption-wealth ratio $\hat{C}_{j,t}$ is constant and is equal to the discount rate because IES=1. The optimal policies are given in terms of the other equilibrium quantities $(J_{j,t}, \chi_t, \psi_t, q_t)$ which are found by solving for a Markov equilibrium in the state space $\Omega := \mathbf{z}_t \in (0, 1) \times \mathbf{a}_{e,t} \in (\underline{\mathbf{a}}_e, \mathbf{a}_e)$.

Definition 2.2. A Markov equilibrium in Ω is a set of adapted processes $q(z_t, a_{e,t}), r(z_t, a_{e,t}), J_e(z_t, a_{e,t}), J_h(z_t, a_{e,t})$, policy functions $\hat{C}_e(z_t, a_{e,t}), \hat{C}_h(z_t, a_{e,t}), \psi(z_t, a_{e,t}), \chi_t(z_t, a_{e,t}), \iota_t(z_t, a_{e,t})$, and state variables $\{z_t, a_{e,t}\}$ such that

- $J_{j,t}$ solves the HJB equation and the corresponding policy functions $\hat{C}_{j,t}, \psi_t$

²⁶The value function is conjectured to be a function of aggregate capital K_t , instead of the wealth using the relation $z_t = \frac{W_{e,t}}{q_t K_t}$. Hence, the capital share does not enter the HJB equation directly. See Appendix B.1.3 for further details.

²⁷The index j' refers to the other type of agent. That is, for the case of experts, j' refers to households. Note that $z_{j',t}$ equals z_t in the case of experts and $1 - z_t$ in the case of households.

- Markets clear

$$(\hat{C}_{e,t}z_t + \hat{C}_{h,t}(1 - z_t))q_t = \psi_t(a_{e,t} - \iota_t) + (1 - \psi_t)(a_h - \iota_t) \quad (29)$$

$$\frac{q_t K_{e,t}}{W_{e,t}}z_t + \frac{q_t K_{h,t}}{W_{h,t}}(1 - z_t) = 1 \quad (30)$$

- z_t and $a_{e,t}$ satisfy (18) and (3) respectively

Similar to BS2016, there are three regions in the state space that describe the mechanisms of risk-sharing. In the first region (Ω_c), where z_t is low, the risk premium of experts is high enough such that condition (16) holds with equality. In this region, the experts issue maximum allowed equity $1 - \underline{\chi}$ to households since their risk premium is high. In the second region, the experts hold all capital in the economy. This corresponds to the case when $\psi = 1$ but the risk premium of experts is still larger than that of households. As a result, they issue the maximum allowed equity (i.e., $\chi_t = \underline{\chi}$). In the third region, experts still hold all the capital (i.e., $\psi = 1$) as before, but they now issue outside equity such that $\epsilon_{e,t} = \epsilon_{h,t}$. This is the region where experts are wealthy enough such that the skin-in-the game constraint is no longer binding, and the risk premium of experts and households are equal. The second and third region together form Ω_n .

Proposition 3. *The total return variance is given by*

$$\|\sigma_t^R\|^2 := (\sigma + \sigma_t^{q,k})^2 + (\sigma_t^{q,a})^2 = \frac{\sigma^2 + \left(\frac{\sigma_{ae,t}^2}{q_t} \frac{\partial q_t}{\partial a_{e,t}}\right)^2}{\left(1 - \frac{1}{q_t} \frac{\partial q_t}{\partial z_t} z_t \left(\frac{\psi_t \chi_t}{z_t} - 1\right)\right)^2} \quad (31)$$

Proof. See Appendix B.1.4.

The first term in the numerator on the R.H.S of equation (31) reflects the fundamental volatility while the second term captures the contribution of productivity shocks. There are two effects that drive the total volatility: (a) Since $\frac{\partial q_t}{\partial z_t} > 0$, and $\frac{\psi_t \chi_t}{z_t} \geq 1$ in equilibrium²⁸ in the crisis region, the denominator contributes towards a higher return volatility than the fundamental volatility σ (b) Since $\frac{\partial q_t}{\partial a_{e,t}} > 0$, the second part in the numerator adds to the amplification caused by (a). The equations (29), (31), and (16) are used to solve for $(q_t, \sigma_t^{q,k}, \sigma_t^{q,a}, \chi_t, \psi_t)$. The remaining equilibrium objects can be obtained

²⁸The quantity $\frac{\psi_t \chi_t}{z_t}$ is the experts exposure to the investment in risky capital. This quantity is larger than 1 whenever the expected return of experts is greater than that of households, which is the case in crisis region.

from these quantities. Appendix [B.1.5](#) explains the solution steps in detail.

2.2 Calibration

The calibration strategy follows the standard procedure in the literature where each model parameter is identified with a moment.

RBC parameters: The investment cost parameter is calibrated to generate an investment-capital ratio of 8%. The depreciation rate is chosen to match the average investment rate.²⁹ The conditional risk premium in the model is determined by the productivity gap between households and experts. The predictive regression results from (2) estimate the risk premium conditional on crises to be around 25%. I choose the gap between average expert productivity \hat{a}_e and a_h to target a 25% conditional risk premium. The correlation of shocks to the level of capital and expert productivity is chosen to be 0.5. This is guided by a -0.48 empirical correlation between bank efficiency and log GDP in the period from 1996Q1 to 2020Q4.³⁰

Preference parameters: The discount rate is taken to be 5% from the literature (closer to the 4% used in [Gertler and Kiyotaki \(2010\)](#)). The risk aversion parameter γ is chosen to be 7, which targets an unconditional risk premium of 5%. A larger risk aversion parameter implies a higher risk premium implied by the model, but too large a value can reduce the probability of crisis.³¹ I find the value of 7 to be a good balance between the unconditional risk premium and the crisis frequency. The death rate is chosen to be 3%, meaning that experts live on average for 37 years.³² The fraction of new born agents designated as experts is calibrated to 0.1 following [Hansen, Khorrami and Tourre \(2018\)](#).

Productivity parameters: The parameter π governs the persistence of productivity and is chosen to target the duration of crisis. The empirically bank efficiency cycle is highly persistent with an AR(1) correlation coefficient of 0.77. The parameter π is calibrated to generate a persistent productivity process. The volatility parameter ν is calibrated such that the variance of the simulated productivity process is approximately equal to the empirical bank efficiency variance of 7%.

²⁹The average investment rate in the data is around 14%, with a volatility of 4.7% between the year 1975 to 2015 ([He and Krishnamurthy \(2019\)](#)).

³⁰Bank efficiency is measured as the asset-weighted average ratio of non-operating income to cost ratio for bank holding companies in the US. The data is at quarterly frequency from 1984Q1 till 2020Q4.

³¹This tension is explored in detail in Section [3.2](#).

³²[Gârleanu and Panageas \(2015\)](#), and [Hansen, Khorrami and Tourre \(2018\)](#) use a value of 2% which is comparable to the value of 3% used in this paper.

Other parameters: Expert exit rates are parameterized by τ_n and τ_c ; these are important in governing the transition into and out of crisis. The baseline rate τ_n is set to 5%, comparable to the 6% rate in [Krishnamurthy and Li \(2020\)](#). Empirically, bank default volume is approximately 15 times larger compared to the periods outside of the crisis.³³ Taking into account a recovery rate of 20%, the exit rate during a crisis is around 12 times larger than during the normal period, implying a τ_c of 60%. Finally, the equity retention threshold is set to be 0.65. This is comparable to the value of 0.5 used in BS2016 and [Hansen, Khorrami and Tourre \(2018\)](#).

Figure (2) presents the equilibrium quantities obtained from the numerical solution. The productivity level has a large effect on the capital price. A lower level of expert productivity implies a lower capital price throughout the state space. The presence of productivity shocks allows the return volatility to be higher than the fundamental volatility even in the normal regime. When the wealth share of more productive experts is higher, capital is fully held by them. They always operate with leverage in equilibrium and, therefore, when a negative shock hits the capital, their net worth decreases disproportionately more than that of the households, resulting in a deterioration of their wealth share. When it falls below a threshold $\{z^*(a_e)\}$, the system endogenously enters into the crisis region featuring depressed asset prices, and higher asset volatility. The jump in prices occurs due to the fire sales. In the crisis zone, experts begin selling capital to households, who always place a lower value on it. Hence, the capital price has to fall enough for households to purchase it and clear the market. The fall in capital price is an inefficiency caused by the failure to internalize the pecuniary externality by the agents. This is because each individual in the economy takes prices as given in their respective decision-making process. To be more concrete, whenever experts choose not to hold capital, they fail to take into account the fact that households will be forced to hold it by market clearing. Since households value capital less, they will demand a higher premium resulting in a fall in the capital price. This feeds-back into the experts' balance sheet since they are leveraged and causes further inefficiency and misallocation of resources. There is a second externality that the experts do not take into consideration, which is the increased exit rate when the system enters the crisis region. The pricing

³³This is based on historical data from the FDIC between the year 2001 till 2020. During the period 2008-2011, the total bank default volume is approximately USD 667 billion, whereas outside this period, the total default volume is USD 44 billion.

dynamics is different from the heterogeneous risk aversion literature in complete markets (see [Gârleanu and Panageas \(2015\)](#), for example). With homogeneous productivity and heterogeneous risk aversion, experts will sell capital to household during periods of distress, who will demand a higher premium (and lower price) due to their *higher risk aversion*. Although both models feature a drop in prices during the crisis, the latter will be gradual.

The jump in prices due to the fire-sale effect can only be explained by the differences in productivity rates in an incomplete market setting and no-shorting constraint. There will be a state space where experts hold all the capital since the risk premium of households is lower than that of experts. In such states, households would desire to hold a negative quantity of capital, but since shorting is disallowed, they will hold no capital at all. In contrast, if the productivity of households is the same as experts, they will face the same risk premium as experts. Therefore, even if their risk aversion were smaller, they would still desire to hold some positive quantity of capital. This smooths the transition from the normal to the crisis regime.³⁴

3 Quantitative analysis

In this section, I consider a simpler model without stochastic productivity and exit rate of the experts that will serve as a benchmark model for the quantitative analysis. Through simulation studies, I show that there is a trade-off between the amplification and the persistence of financial crises in this simpler model. While there are many channels that generate this tension, I focus on the risk aversion channel.³⁵

3.1 Benchmark model

I assume that the productivity rate of both experts and households is constant such that $a_e > a_h$ holds, and the exit rate is zero. With these two simplifications, the model reduces to BS2016 augmented with recursive preference and OLG elements. While the agents have CRRA utility function in BS2016, I assume that they have recursive preference so as to disentangle the risk aversion and the inter-temporal elasticity of substitution. The rest

³⁴This dynamics is present in [Gârleanu and Panageas \(2015\)](#). [Hansen, Khorrami and Tourre \(2018\)](#) offer additional insights for the case of heterogeneous productivity vs heterogeneous risk aversion.

³⁵See Appendix C.3 for details on the skin-in-the-game constraint generating a similar trade-off.

of the assumptions carry over from the stochastic productivity model in Section 2. That is, the output is given by AK technology as in (1), with a_e and a_h as the productivity rates of the experts and the households respectively. The evolution of capital is governed by (2) as before. Appendix C.1 presents the model in detail along with the numerical procedure and the solution.

Comparative statics: Figure (3) depicts the risk premium of experts in the benchmark model, as well as the stationary density of expert wealth share.³⁶ The static comparison from the left hand side figure in (3) shows that as the risk aversion increases, so does the premium on the risky capital for experts. The other equilibrium objects, such as capital price, return volatility, capital share of experts, drift of wealth share, and volatility of wealth share are shown in Figure (11) in Appendix C.1. Even though the price volatility is lower for higher risk aversion, there is a region in the parameter space where it is much higher than in the case of lower risk aversion. That is, with lower risk aversion levels, the endogenous risk is higher but displays a smaller crisis region. Lastly, changes in the market price of risk induced by varying risk aversion translate into vast differences in the drift of the wealth share. This has a direct impact on how the system transitions into and out of the crisis region.

Stationary distribution: While Figure (3a) gives us a qualitative description of the economy, the stationary distribution of the wealth share is required to confront the model with the data. The stationary distribution represents the average location of the state variable z_t in the interval $[0,1]$ as $t \rightarrow \infty$ for any given starting point z_0 . I obtain this distribution by numerically simulating the model for 5000 years at a monthly frequency. The simulation maps the Brownian shocks Z_t^k to state variable z_t , which is governed by the law of motion given by equation (62) in Appendix C.1. I repeat the procedure 1000 times and ignore the first 1000 years so that the distribution is not sensitive to the arbitrarily chosen initial value z_0 . I annualize the result and repeat the procedure for different initial values to ensure that the economy has converged. I explain the numerical procedure in detail in Appendix C.2. I assess how well the model captures the salient empirical features of financial crises in the data. I define the crisis moments as follows

³⁶The parameters used for calibration are shown in Table (10) in Appendix C.1.

1. *Crisis event* is defined as a state where the capital is misallocated to households, and skin-in-the game constraints are binding. In this state, the risk premium is high, and GDP growth is low, reflecting the empirical nature of the financial crisis. This definition is similar to [Maxted \(2020\)](#), who defines crises as states where the capacity constraint is binding. The *amplification* in my model refers to the moments computed when the economy is in a crisis state.
2. *Probability of crisis*: The proportion of time that the economy spends in a crisis state. Analyzing a large set of advanced economies over several years, [Reinhart and Rogoff \(2009\)](#) estimate this value to be 7% empirically. They define a crisis as a recession accompanied by severe banking panic.
3. *Duration of crisis*: The average amount of months required to recover and revert to normalcy after entering the crisis state. The average length of contraction cycle from NBER recessionary data is around 18 months. The simulated mean duration of the crisis is taken to be the model-implied *persistence*.

Figure (3b) plots the stationary distribution of the wealth share for three different risk aversion levels. As risk aversion increases, the mass of wealth share that lies in the crisis zone diminishes. In fact, it shrinks rather quickly, and this result also holds if I allow for heterogeneous risk aversion, with the experts being less risk averse. The stationary distribution gives us additional insights that one cannot obtain from studying the comparative static plots. Looking at Figure (3a), it appears as if increasing risk aversion will not have a drastic impact on the frequency of a crisis since the boundary z^* , the point at which the risk premium jumps and the investment rate falls, moves only slightly to the right.³⁷ However, higher risk aversion increases the drift of wealth share a lot and pushes the stationary distribution away from the crisis region to a greater extent. Since the experts operate with leverage, a higher price of risk will have a positive effect on their wealth share. From figure (12) in Appendix C.1 that plots the stationary distributions along with the crisis boundary, we can see that the boundary z^* is far from the stochastic steady state \hat{z} for higher levels of risk aversion.³⁸ This means that a much longer sequence of negative shocks is required to push the system into the crisis region.

³⁷The point z^* denotes the point at which the experts start fire selling the capital to the households, and is defined to be the crisis boundary. Formally, $z^* = \sup\{z_t \mid \psi_t < 1\}$ where ψ_t is the share of capital held by the experts.

³⁸The stochastic steady state can be defined as $\hat{z} := \{z_t : \mu_t^z(z_t) = 0\}$.

Comparison to Data: While the crisis is well defined and endogenously determined in the model, defining the crisis episodes in the data is a challenge. [Reinhart and Rogoff \(2009\)](#) determine the frequency of crisis states to be around 7% for the advanced economy. This figure is much lower than the 29% of percentage NBER recessionary periods from the year 1874 till today.³⁹ The stark difference in the frequency between [Reinhart and Rogoff \(2009\)](#) and NBER data is due to the fact that in the former, recessionary periods need to feature severe banking panic to qualify as financial crises. This relates to the findings by [Muir \(2017\)](#) and [Gorton and Ordoñez \(2020\)](#) that not all recessions are financial crisis episodes. [Muir \(2017\)](#) finds that the risk premium is higher during financial crises than during recessions, where a financial crisis occurs when the wealth share of intermediaries deteriorates sufficiently, just like in the model considered in this paper. HK2019 argue that the past decade in the US featured roughly three financial crisis periods. I take the probability of being in the crisis period as 7% for the purpose of quantitative calibration. For each z_t simulated from the discretized version of its dynamics, the equilibrium quantities are computed using the mapping given by the equilibrium functions.⁴⁰ Following this, various model-implied moments are computed and compared to the data, as will be explained. Since the empirical risk premium is not observed, I estimate its mean and volatility using return forecasting regression (32).

$$R_{t+1}^e = a + \beta * D_t/P_t + \beta_{rec} * 1_{Rec} * D_t/P_t + \beta_{fin} * 1_{fin} * D_t/P_t + \epsilon_t \quad (32)$$

I split the NBER recessionary periods into crisis (financial recession) and non-crisis (non-financial recession) periods based on the definition of [Reinhart and Rogoff \(2009\)](#). I then run predictive regressions with dividend yield (D_t/P_t) as the regressor and 1-year ahead stock returns as the dependent variable. In Table (2), regression (I) uses only the dividend yield as a regressor, whereas regressions (II) and (III) include a dummy for non-financial recession and financial crisis, respectively. The dividend yield and stock return data are from Robert Shiller's website. I use a monthly frequency from the years 1945 to 2021. The indicator functions 1_{Rec} , and 1_{fin} take a value of 1 in months of NBER non-financial recession and financial recession, respectively. The dummy variable corresponding to the financial crisis is positive and statistically significant as seen in Table

³⁹The percentage of NBER recessionary periods since the beginning of Federal Reserve (1914) is around 20%.

⁴⁰See Appendix C.2.5 for details.

(2).⁴¹ The R-squared value is also higher when controlling for recession and financial crises, indicating better predictive power. This confirms the finding in Muir (2017) that the risk premium is much higher during financial crises and the predictive power is improved by conditioning on the recessionary periods. I take the fitted value from regression (III) in Table (2) and compute the standard deviation to obtain the volatility of the risk premium.

3.2 Tension between amplification and persistence of crises

A trade-off between the amplification and the persistence of financial crises arises in the benchmark model. One such channel that generates this trade-off is the risk aversion of the agents. The level of amplification required to match the empirical asset pricing moments leads to two related problems. First, the probability of a crisis implied by the model with high risk aversion becomes too small to reconcile with the data. Second, and more importantly, the higher the amplification, the less persistent the crisis episodes implied by the model. I first explain the trade-off between risk premium and crisis probability, and then explain how a higher amplification (conditional risk premium) can only be obtained at the expense of lower persistence.

Figure (4) plots the unconditional risk premium, the volatility of the risk premium, and the probability of crisis. With a risk aversion equal to 1, the parameters in Table (10) lead to a 7.8% probability of crisis. The unconditional mean risk premium is around 1.7%. One way to obtain even a higher risk premium is by pumping up the risk aversion. However, increasing the risk aversion causes the probability of crisis to fall rapidly. As the values in Table (3) suggest, to obtain an empirically observed unconditional risk premium of 7.5%, the risk aversion has to be around 20. For this high level of risk aversion, the economy almost never enters into a crisis state. The reason is that a higher risk premium increases the wealth share of experts in the stochastic steady state and, therefore, a series of large negative shocks is required for the wealth share to diminish enough to push the system into the crisis zone. The model-implied standard deviation of the risk premium is 3.1% (see column 5 of Table (3)) which occurs solely due to the non-linearity in the model between the normal and the crisis regime. The point is that

⁴¹This finding is robust to using different time periods such as 1871-2018 (time since Shiller's data is available), and 1914-2018 (since the start of Federal Reserve).

while the comparative static plots in Figure (3) feature a large risk premium in some regions of the state space, if the dynamics of the model is such that these regions are barely reached, then the model cannot match the high risk premium in the data.

The persistence of financial crises is as much an important empirical phenomenon as the amplification. A direct measure of persistence is the duration. Fixing the model implied frequency of crisis at 7%, the average length of the crisis that the model can generate is around 6 months, which is much shorter than observed in the data. While there is disagreement regarding the empirical length of crises in the literature, the consensus is that it is longer than eight months.⁴² Figure (5) plots the frequency distribution of the crisis length observed in the model. Most of the mass resides in periods less than 5 months, and a crisis length of more than 10 months is probabilistically very small. The reason for this is that the only shocks in the model are Brownian, whose increments are i.i.d normal. Hence, a negative shock that impairs the expert wealth share is on average followed by a positive shock that restores the lost wealth quickly. This is the case despite the model featuring leveraged experts. To be more concrete, imagine that the system has just entered the crisis period following a series of negative shocks. The capital price and investment rate are lower, putting a downward pressure on the net worth of experts. However, the risk premium is higher, and as the experts operate with leverage, they earn more since they hold a larger proportion of risky capital. The latter effect is larger than the former and makes the drift of the wealth share high enough to push the system back to the normal regime. When risk aversion is higher, the effect of the risk premium is even larger, resulting in the average length of the crisis falling even more. In other words, higher risk aversion creates higher amplification but dampens the persistence. Figure (5) shows the average length of a crisis for different values of risk aversion. As the risk aversion increases, the mass of crisis length that lies in the range of 1-2 months increases. As for the mass of crisis length that lies above 2 months, the opposite is true. This indicates that crisis periods are far too infrequent in the model when the agents are more risk averse. The dynamics explained above corroborate this observation.

This tension between persistence and amplification is unaffected by parameter values or utility functions. In the case of CRRA utility, and recursive utility with non-

⁴²See [He and Krishnamurthy \(2013\)](#), [Muir \(2017\)](#) for example.

unitary IES, the consumption-wealth ratio is time-varying and affects the drift of the wealth share in addition to the risk premium, capital price, and investment. However, the effect of the risk premium highly dominates the other effects, and therefore this tension is pervasive for more general preferences as well.⁴³ There are also other channels through which this tension becomes evident. In Appendix C.3, I show that decreasing the skin-in-the-game constraint leads to a more amplified crisis, but reduces the persistence. When the experts are constrained to keep a larger (smaller) fraction of the equity on their balance sheet, the risk premium becomes larger (smaller) in the crisis state, which increases (decreases) the wealth share of the experts, leading to a quick (late) recovery. This indicates that the tension observed is not a matter of calibration. Regardless of how one calibrates the model to generate a high amplification to the extent that is observed in the data, the high risk premium in the amplified crisis state causes the experts to repair their balance sheets by quickly building sufficient capital, thereby failing to match the prolonged crisis that we see in the data.

Other moments: Figure (4) presents the data moments that the model aims to match with the methodology to compute them. The benchmark model delivers an unconditional average GDP growth rate of around 2.3% and an investment rate of 6%. An important measure of model success is its ability to capture the observed non-linearity in the data. The GDP growth rate conditional on being in a crisis is around -8%. The empirical annualized GDP growth rate during the third quarter of 2008 was -8.2%. In this respect, the model captures the non-linearity quite well. However, the drop in investment rate implied by the model during the crisis is not sufficient to reconcile with the data. The private investment rate fell by 8% during the third quarter of 2008, whereas the model implied investment rate conditional on being in the crisis is 4%. Note that even though the output of experts and households individually moves in sync with the capital due to the assumption of AK technology, the aggregate output depends on the aggregate dividend, which is a function of the capital share. During the crisis period, less productive households hold capital, and hence the aggregate dividend drops to a large extent, and this causes the output to drop a lot as well. On the other hand, the investment rate is determined by capital prices alone. A drop in the capital price during

⁴³I experiment with log, CRRA, recursive utility with IES=1, and recursive utility with IES different from 1. Appendix C.1 solves the benchmark model with these utility functions using the finite difference up-winding scheme. The results from simulation studies for the case of all utility functions are not included in the paper but they display the same tension between the persistence and the amplification that is explained in the paper.

the crisis period is not large enough to generate the observed drop in the investment rate.⁴⁴ The volatility of investment rate implied by the model is close to zero. Overall, the model captures non-linearity in output growth but misses non-linearity in the mean and volatility of investment rates. This result is comparable to HK2019, which has a realistic consumption volatility but an excessively low investment volatility. This calls for future work to match both output and investment dynamics. The mean leverage of the expert sector implied by the model with unitary risk aversion is 3.23, comparable to the empirical leverage of 3.77.⁴⁵ The model also features counter-cyclical leverage. Even though the experts fire sell the assets to the households in periods of distress, the price of capital also drops, which depresses the experts' equity. Since the experts operate with leverage in equilibrium, the drop in expert equity is more than the drop in assets, which results in rising leverage. Table (11) shows that the correlation between the shock and the leverage ranges from -19% to -22% for different risk aversion levels. This matches the empirical correlation of -18% quite well. However, as risk aversion increases, the level of leverage falls. With a risk aversion level as high as 10, the leverage is 1.43, well short of the empirical leverage of 3.77. Overall, for lower risk aversion levels, the model seems to do well in matching the leverage patterns. Lastly, the model does not generate an excessive asset return volatility (Shiller (1981)). The unconditional return volatility is more or less the same as the exogenous fundamental volatility of 6%, even though it shoots up in the crisis state. This is because the endogenous risk σ_t^q becomes zero in the normal regime. The conditional volatility, albeit high, is not large enough to make the unconditional one match the data.

Table (5) summarizes the ability of the benchmark model to succeed in different aspects. By far, matching the intermediary leverage pattern and the non-linearity in output growth seem to be the strongest suits of the model. For any reasonable parameters in calibration, the model cannot resolve the tension between unconditional risk premium, conditional risk premium, and crisis persistence. The focus of the next section is to provide a resolution to this problem.

⁴⁴The result is not much quantitatively different if one assumes a quadratic functional form instead of logarithmic for the capital adjustment costs $\Phi(\cdot)$.

⁴⁵This number is taken from HK2019.

4 Resolution of the tension between amplification and persistence of crises

In this section, I quantify the model with stochastic productivity and exit of experts, and show that it resolves the tension between persistence and amplification of financial crises and provides reasonable time variation in the prices. The definition of a crisis event, probability, and duration of crisis is similar to the benchmark model.⁴⁶ Figure (6) plots the stationary marginal distribution of the wealth share obtained through simulation.⁴⁷ Table (6) presents the average duration of crisis in the benchmark model and the stochastic productivity model and compares them against the data. There is a substantial controversy in the literature regarding the duration of crises (Reinhart and Rogoff (2009)). The NBER reports that the Great Recession started in December 2007 and ended in June 2009, indicating an 18 month duration.⁴⁸ To facilitate comparisons, I adjust the parameters to generate a comparable probability of the crisis in the range of 7-8% across the the benchmark and my model. The numbers in Table (6) can be thought of as the ability of the models to generate the stated duration for a reasonable crisis probability of 7-8%. Both of the benchmark models deliver a duration of crisis that is much lower than observed in the data. The mean duration from my model matches the data quite well although the 10th and 50th percentile values are lower. The parameters used for calibrating my model are shown in Table (1).

Figure (8) plots the frequency distribution of the wealth share during the time the system spends in the crisis region. In the benchmark model (left panel), a lot of the mass lies near the crisis boundary of 0.125 compared to the interior region where the wealth share is close to zero. The reason for this is that the benchmark model has only one i.i.d Brownian shock. After a series of negative shocks hit the economy, the system enters a crisis, leading to a sharp increase in the risk premium. Since experts are always leveraged in equilibrium, the risk premium loads positively on the drift of wealth share of experts. Moreover, the assumption of i.i.d Brownian shock implies that a series of

⁴⁶Note that in this two-dimensional model, the crisis boundary is a function of expert productivity. The simulation results show that the economy enters crisis mostly when the productivity is well below its mean. This can also be verified by inspecting the joint density shown in Figure (7).

⁴⁷The simulation method is similar to the benchmark model except that the equilibrium objects are two-dimensional.

⁴⁸The average duration of recession in the past 33 cycles from year 1854 to 2020 is around 18 months. Source: <https://www.nber.org/cycles.html>.

negative shocks is often followed by a positive shock. Thus, the experts recapitalize quickly by capturing the high risk premium, leading to short-lived crises. In contrast, the frequency distribution of the wealth share in the crisis region in my model, as shown in the right panel in Figure (8), features fatter tails. The economic mechanisms that generate this result rest on three forces. Firstly, negative shocks to the capital impair the net worth of the experts just like in the benchmark model. This is the financial amplification channel that is widely covered in the literature. The second force comes from stochastic productivity. The aggregate banking sector productivity is lower during a crisis state. The key comparative advantage of the experts in my model is that they have a higher productivity rate of operating capital. During bad times, this comparative advantage diminishes.⁴⁹ A realistic crisis frequency is obtained even for higher risk aversion levels due to stochastic productivity. With a constant productivity as in the baseline model, the risk-averse experts will always remain wealthy by earning a large premium. Negative shocks to the capital in the stochastic steady state will not be enough to generate realistic crisis events. In my model, negative shocks to the capital also push the experts productivity down, which negatively impacts the risk premium. Hence, a series of negative shocks reduces the premium earned in the normal region and will put downward pressure on the drift of wealth share, eventually causing sufficient deterioration in the net worth of experts to generate crisis events.

The third force is the exit rate of experts, which is higher during bad times. While the overlapping generations capture the demographic changes relating to natural birth and death of agents, the exit rate captures the retirement of the experts. In normal times, experts retire at a rate of 5.0%. When they retire, they don't consume all of their wealth immediately. Instead, they transition into households until death. While the crisis is endogenously determined in my model, as soon as the crisis boundary is hit, the exit rate shoots up from 5.0% to 60%. A higher exit rate during a crisis parsimoniously captures the strikingly large number of bank failures during a financial crisis, as evident in figure (1). The fact that a large fraction of the experts retire and become households means that the proportion of the agents who operate capital more productively is lower in times of distress than in normal times. This has a dominating effect on the drift of wealth share and pushes the economy deeper into the crisis since the drift is negatively affected by

⁴⁹Simulation shows that the crisis zone features both a lower wealth share and a lower productivity of experts as seen in the right panel of Figure (7).

exit. The only way for the economy to break out of the crisis is for a remaining smaller proportion of the experts to be more productive again, since higher productivity pushes up the risk premium, enabling the experts to rebuild their wealth.⁵⁰ However, the rate at which expert productivity reverts to its mean is low, and this sluggish reversion means that the economy spends a long amount of time in a state of distress until the effect of increased productivity is dominant. This leads to delayed recovery from the crisis. Once the system is back to normalcy, all capital in the economy is held by the experts, and the financial amplification is shut down.

Table (8) compares the moments of key asset pricing and macroeconomic variables between my model and the benchmark model. The unconditional risk premium of 5.0% is comparable to the empirical value of 5.5%, whereas, the benchmark model generates a mere 1.7% premium. Importantly, my model allows for reasonable crisis dynamics by simultaneously generating a high conditional risk premium of 17.5% and long a duration of crisis of 18.5 months without compromising on the other dimensions. That is, the unconditional mean leverage, GDP growth rate, investment-capital ratio, and correlation between expert leverage and capital shock are comparable to the data.

To further understand the individual roles of stochastic productivity and exit rate in delivering quantitative results, I compare my model against two other benchmark models: a) Model B1, which considers stochastic productivity but without exit, and b) Model B2, which considers constant productivity and state-dependent exit. The trade-offs analyzed in the benchmark model also carry over to model B1. While stochastic productivity helps in generating more time variation in the risk premium compared to the benchmark model, the duration of crisis implied is lower compared to the data, as seen in Table (8). Without state-dependent exit, the proportion of experts who recapitalize their balance sheets by earning a large risk premium is high, and the economy recovers quickly from a crisis as a result. Hence, features related to the bankruptcy of intermediaries or bank runs are crucial in explaining the slow recovery from a crisis. This relates to [Gertler, Kiyotaki and Prestipino \(2020\)](#) who build a quantitative macroeconomic model with bank runs as the main driver behind the 2008 financial crisis. However, incorporating bankruptcy without stochastic productivity is not sufficient to gen-

⁵⁰The consumption-wealth ratio of the agents is constant due to the assumption of a unitary IES. For a non-unitary IES, the consumption-wealth ratio may also increase due to increased productivity of the experts and contribute positively towards the wealth share of experts.

erate realistic crisis dynamics. Table (8) presents the results of model B3 that includes state-dependent exit but with constant productivity. When the exit rate is calibrated to empirical default rates, the probability of crisis implied by the model is unrealistically large. During bad times, a higher exit rate of experts pushes the economy into crisis. Without the offsetting force of mean-reverting productivity, the effect of the exit rate continues to dominate the drift of wealth share, trapping the economy in a distressed state around 80% of the time.

My model generates a larger drop in the investment rate in the crisis period but falls short of the negative investment rate observed in the data. During the last quarter of 2008, private domestic investment in the United States fell by approximately 8%. The q-theory result in the model ties the investment rate tightly to the capital price. Hence, the capital price needs to fall drastically to generate a fall in the investment rate to the extent that is observed in the data. My model is certainly an improvement over the benchmark in this regard, but more work needs to be done in jointly matching the investment and output dynamics.⁵¹ Lastly, the variation in investment rate and risk free rate is higher in my model compared to the benchmark model due to time-varying experts productivity. Also, the model implied unconditional volatility of the risk premium is 5.3%, well in line with the empirical value of 5.1% reported in Table (3). Overall, my model does a good job of balancing the persistence and the amplification and delivers a reasonable time variation in the prices.

5 Conclusion

Financial recessions are typically characterized by a high risk premium and a slow revival. I have built a macro-finance asset pricing model with intermediaries facing productivity shocks and a state-dependent exit rate. A series of negative capital shocks reduces expert productivity, reflecting the experts' diminishing comparative advantage over households in terms of productivity differential. A simpler model with constant expert productivity and no exit rate cannot simultaneously generate amplified and persistent financial crises. There is a trade-off between the risk premium and the probability

⁵¹Note that I have assumed a simple logarithmic form to model technological illiquidity following Brunnermeier and Sannikov (2016). Using other functional forms, for example, as found in Di Tella (2017) also fail to generate a large drop in investment during crises periods.

and duration of crises. I show that auxiliary model features that improve the financial amplification channel dampen the persistence of the crisis.

The richer model with stochastic productivity and the exit rate of the experts can resolve this tension and quantitatively generate a high risk premium, a large drop in output, decreased financial intermediation, counter-cyclical leverage, and prolonged distress periods. The twin forces of state-dependent exit and stochastic productivity are at the core of improved dynamics in my model. In particular, a higher exit rate and lower productivity of experts in bad times forces the economy to dip deeper into recession, which eventually revives once productivity mean reverts. The model also generates a large time variation in the risk prices due to the stochastic nature of expert productivity, which is absent in the benchmark model. An interesting avenue for future research is to build a model that endogenously causes variation in the expert productivity, which is an exogenous force in my model. I have utilized a novel method of solving the model based on active machine learning that encodes the economic information as regularizers in a deep neural network. The algorithm is scalable and has the potential to solve high-dimensional problems with less effort in the numerical setup, opening up new avenues to model asset pricing with frictions in potentially large dimensions.

References

- Achdou, Yves, Francisco J. Buera, Jean-Michel Lasry, Pierre-Louis Lions, and Benjamin Moll. 2014a. "Partial differential equation models in macroeconomics." *Philosophical Transactions of the Royal Society A: Mathematical, Physical and Engineering Sciences*, 372(2028).
- Achdou, Yves, Jiequn Han, Jean-Michel Lasry, Pierre-Louis Lions, and Benjamin Moll. 2014b. "Heterogeneous agent models in continuous time." *Preprint*.
- Adrian, Tobias, and Nina Boyarchenko. 2012. "Intermediary Leverage Cycles and Financial Stability." *SSRN Electronic Journal*, , (August 2012).
- Adrian, Tobias, Erkki Etula, and Tyler Muir. 2014. "Financial Intermediaries and the Cross-Section of Asset Returns." *Journal of Finance*, 69(6): 2557–2596.

- Azinovic, Marlon, Luca Gaegauf, and Simon Scheidegger.** 2019. "Deep Equilibrium Nets." *SSRN Electronic Journal*.
- Bansal, Ravi, and Amir Yaron.** 2004. "Risks for the long run: A potential resolution of asset pricing puzzles." *Journal of Finance*, 59(4): 1481–1509.
- Baron, Matthew, and Wei Xiong.** 2017. "Credit expansion and neglected crash risk." *Quarterly Journal of Economics*, 132(2): 713–764.
- Barro, Robert J.** 2006. "Rare disasters and asset markets in the twentieth century." *Quarterly Journal of Economics*, 121(3): 823–866.
- Bigio, Saki, and Adrien D'Avernas.** 2021. "Financial Risk Capacity." *American Economic Journal: Macroeconomics*, 13(4): 142–81.
- Bonnans, J. Frédéric, Élisabeth Ottenwaelter, and Housnaa Zidani.** 2004. "A fast algorithm for the two dimensional HJB equation of stochastic control." *Mathematical Modelling and Numerical Analysis*, 38(4): 723–735.
- Brunnermeier, Markus K., and Yuliy Sannikov.** 2014. "A macroeconomic model with a financial sector." *American Economic Review*, 104(2): 379–421.
- Brunnermeier, M. K., and Y. Sannikov.** 2016. "Macro, Money, and Finance: A Continuous-Time Approach." In *Handbook of Macroeconomics*.
- Campbell, John Y., and John H. Cochrane.** 1999. "By force of habit: A consumption-based explanation of aggregate stock market behavior." *Journal of Political Economy*, 107(2): 205–251.
- Chen, Luyang, Markus Pelger, and Jason Zhu.** 2019. "Deep Learning in Asset Pricing." *SSRN Electronic Journal*.
- D'Avernas, Adrien, and Quentin Vandeweyer.** 2019. "A Solution Method for Continuous-Time Models." 1–33.
- Di Tella, Sebastian.** 2017. "Uncertainty shocks and balance sheet recessions." *Journal of Political Economy*, 125(6): 2038–2081.
- Duarte, Victor.** 2017. "Machine Learning for Continuous-Time Economics."

- Eisfeldt, Andrea L., Hanno Lustig, and Lei Zhang.** 2017. "Complex Asset Markets." *NBER Working Papers*, 123(5): 1177–1200.
- Feng, Guohua, and Apostolos Serletis.** 2010. "Efficiency, technical change, and returns to scale in large US banks: Panel data evidence from an output distance function satisfying theoretical regularity." *Journal of Banking and Finance*, 34(1): 127–138.
- Fernández-Villaverde, Jesús, Samuel Hurtado, and Galo Nuno.** 2020. "Financial Frictions and the Wealth Distribution." *SSRN Electronic Journal*.
- Gârleanu, Nicolae, and Stavros Panageas.** 2015. "Young, old, conservative, and bold: The implications of heterogeneity and finite lives for asset pricing." *Journal of Political Economy*, 123(3): 670–685.
- Gertler, Mark, and Nobuhiro Kiyotaki.** 2010. "Financial Intermediation and Credit Policy in Business Cycle Analysis." *Handbook of Monetary Economics*, 3(C): 547–599.
- Gertler, Mark, Nobuhiro Kiyotaki, and Andrea Prestipino.** 2020. "A Macroeconomic Model with Financial Panics." *The Review of Economic Studies*, 87(1): 240–288.
- Glorot, Xavier, and Yoshua Bengio.** 2010. "Understanding the difficulty of training deep feedforward neural networks."
- Gomez, Matthieu.** 2019. "Asset Prices and Wealth Inequality." *Working Paper*.
- Gopalakrishna, Goutham.** 2021. "ALIENs and Continuous Time Economies." *SSRN Electronic Journal*.
- Gorton, Gary, and Guillermo Ordoñez.** 2014. "Collateral Crises." *American Economic Review*, 104(2): 343–78.
- Gorton, Gary, and Guillermo Ordoñez.** 2020. "Good Booms, Bad Booms." *Journal of the European Economic Association*, 18(2): 618–665.
- Gu, Shihao, Bryan Kelly, and Dacheng Xiu.** 2020. "Empirical Asset Pricing via Machine Learning." *The Review of Financial Studies*, 33(5): 2223–2273.
- Hansen, Lars Peter, Paymon Khorrami, and Fabrice Tourre.** 2018. "Comparative Valuation Dynamics in Models with Financing Restrictions." *Working Paper*.

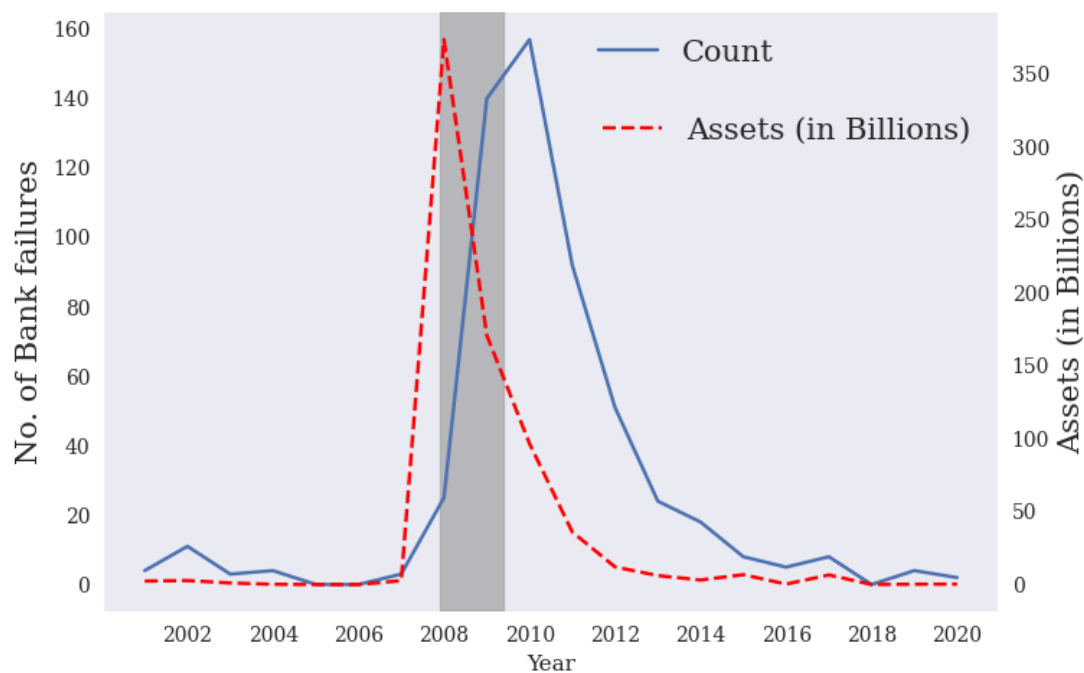
- He, Zhiguo, and Arvind Krishnamurthy.** 2013. "Intermediary asset pricing." *American Economic Review*, 103(2): 732–770.
- He, Zhiguo, and Arvind Krishnamurthy.** 2019. "A macroeconomic framework for quantifying systemic risk." *American Economic Journal: Macroeconomics*, 11(4): 1–37.
- He, Zhiguo, Bryan Kelly, and Asaf Manela.** 2017. "Intermediary asset pricing: New evidence from many asset classes." *Journal of Financial Economics*, 126(1): 1–35.
- Hornik, Kurt, Maxwell Stinchcombe, and Halbert White.** 1989. "Multilayer feedforward networks are universal approximators." *Neural Networks*.
- Hughes, Joseph P, Loretta J Mester, and Choon Geol Moon.** 2001. "Are scale economies in banking elusive or illusive?: Evidence obtained by incorporating capital structure and risk-taking into models of bank production." *Journal of Banking and Finance*, 25(12): 2169–2208.
- Khorrami, Paymon.** 2016. "Entry and Slow-Moving Capital: Using Asset Markets to Infer the Costs of Risk Concentration."
- Kiyotaki, Nobuhiro, and John Moore.** 1997. "Credit cycles." *Journal of Political Economy*.
- Krishnamurthy, Arvind, and Wenhao Li.** 2020. "Dissecting Mechanisms of Financial Crises: Intermediation and Sentiment." *SSRN Electronic Journal*.
- Kurlat, Pablo.** 2018. "How I Learned to Stop Worrying and Love Fire Sales." *National Bureau of Economic Research*.
- Li, Wenhao.** 2020. "Public liquidity, bank runs, and financial crises." *SSRN Electronic Journal*.
- Maxted, Peter.** 2020. "A Macro-Finance Model with Sentiment." *SSRN Working Paper*.
- Moll, Benjamin.** 2014. "Productivity losses from financial frictions: Can self-financing undo capital misallocation?" *American Economic Review*, 104(10): 3186–3221.
- Moreira, Alan, and Alexi Savov.** 2017. "The Macroeconomics of Shadow Banking." *Journal of Finance*, 72(6): 2381–2432.

- Muir, Tyler.** 2017. "Financial crises and risk premia." *Quarterly Journal of Economics*, 132(2): 765–809.
- Phelan, Gregory.** 2016. "Financial Intermediation, Leverage, and Macroeconomic Instability." *American Economic Journal: Macroeconomics*, 8(4): 199–224.
- Reinhart, Carmen M., and Kenneth S. Rogoff.** 2009. *This time is different: Eight centuries of financial folly*.
- Settles, Burr.** 2012. "Active learning." *Synthesis Lectures on Artificial Intelligence and Machine Learning*.
- Shiller, Robert J.** 1981. "Do Stock Prices Move Too Much to be Justified by Subsequent Changes in Dividends?" *American Economic Review*, 71(3): 421–436.
- Shleifer, Andrei, and Robert Vishny.** 2011. "Fire sales in finance and macroeconomics." *Journal of Economic Perspectives*, 25(1): 29–48.

A Figures and Tables

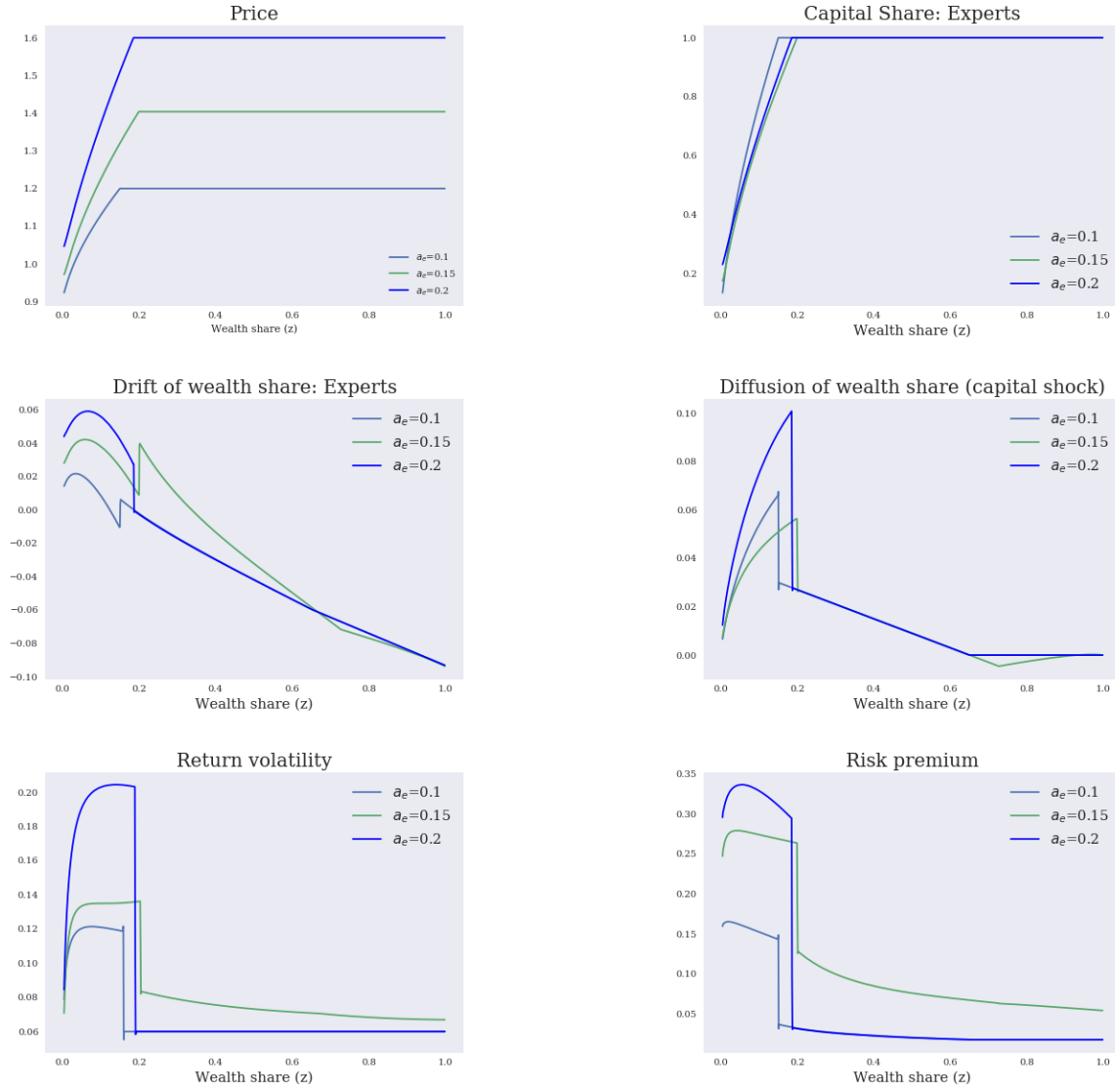
A.1 Figures

Figure 1: Bank failures



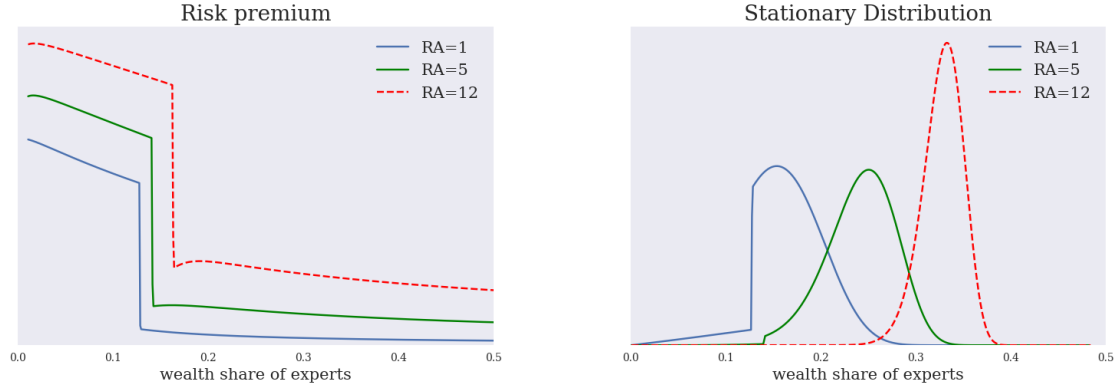
Note: The solid line indicates the number of bank failures and the dashed line indicates the default volume. The shaded region represent the NBER recessionary period. Source: Federal Deposit Insurance Corporation.

Figure 2: Model solution



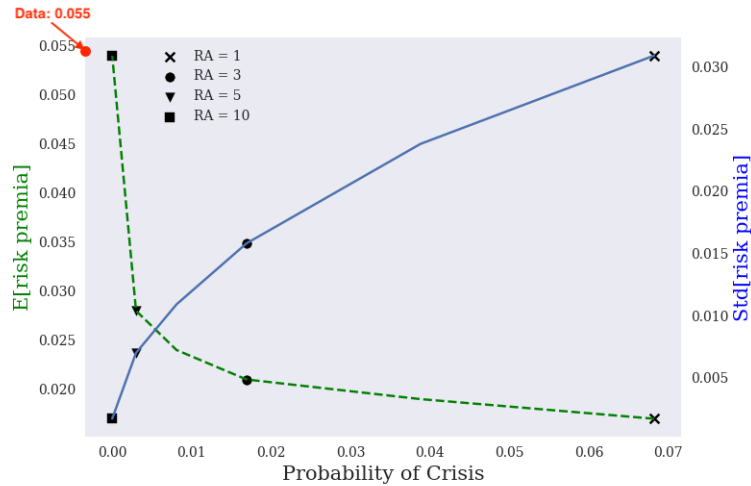
Note: Equilibrium values as functions of the state variable wealth share (z_t) for different values of expert productivity ($a_{e,t}$).

Figure 3: Risk premium and stationary distribution



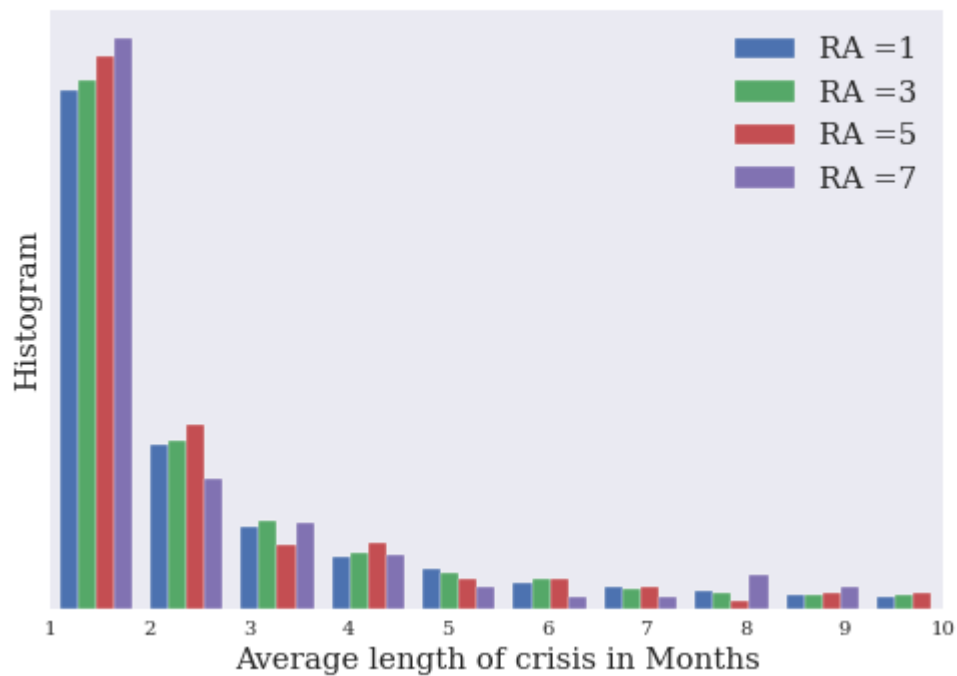
Note: Left panel presents a static comparison of experts risk premium for three different levels of risk aversion. Right panel presents the stationary distribution of expert wealth share for three levels of risk aversion.

Figure 4: Trade-off between risk premium and probability of crisis



Note: Figure shows the trade off between the unconditional asset pricing moments and the probability of crisis for different risk aversion parameters (RA). The dashed line represents expected risk premium (see left axis). The full line represents standard deviation of risk premium (see right axis). Risk aversion decreases from left to right. The risk premium moments and probability of crisis are computed by simulating the model at monthly frequency for 5000 years. The figure displays annualized numbers. The empirical risk premium estimated using regression (32) is 5.5%.

Figure 5: Duration of crisis



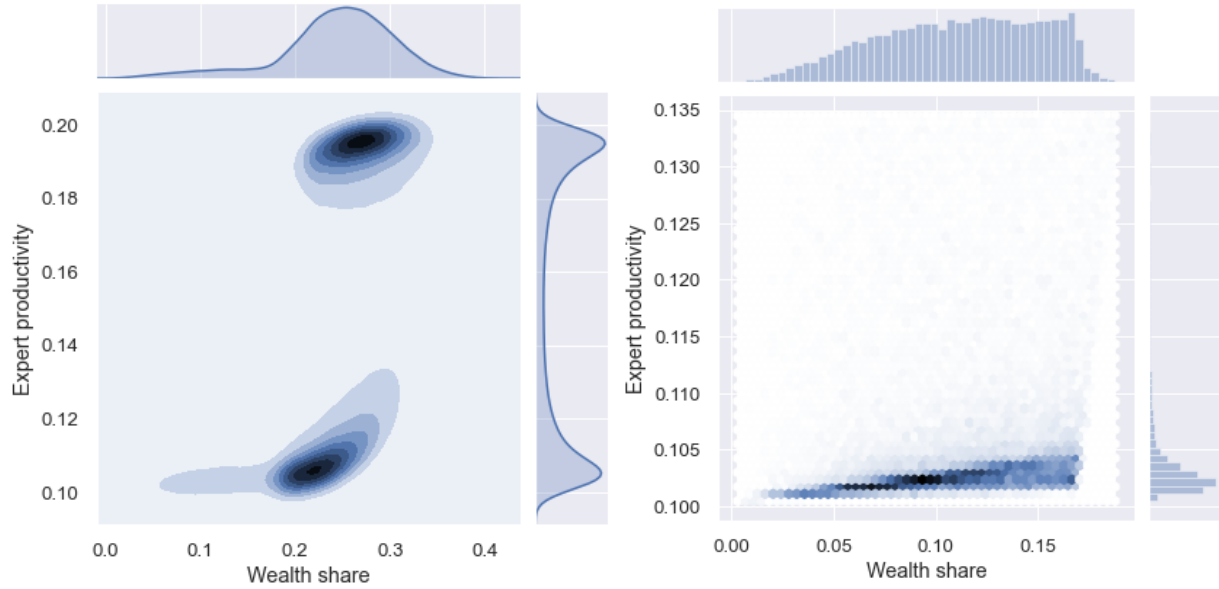
Note: Frequency distribution of average crisis duration for different values of Risk aversion (RA). The graph shows only till months 10 since the frequency for months larger than 10 is negligible. The duration is computed by simulating the model at monthly frequency for 5000 years. The observations are annualized.

Figure 6: Stationary density of wealth share



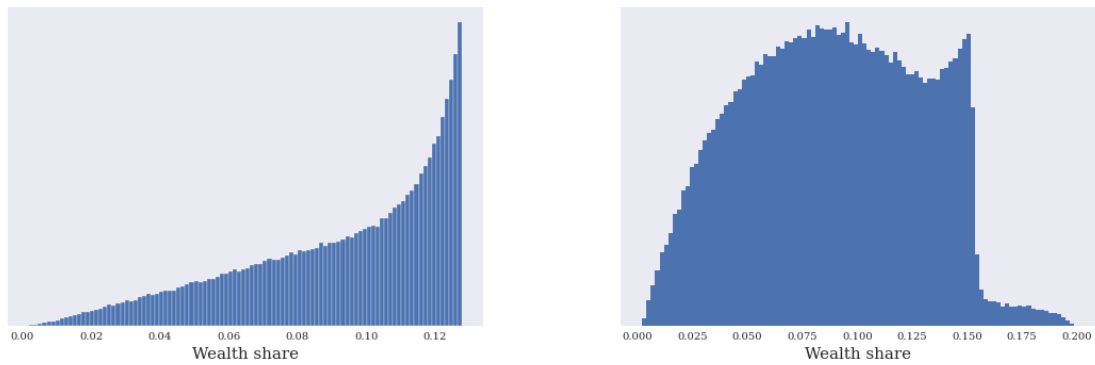
Note: The figure displays stationary marginal density of endogenous wealth share obtained from simulating the model for 5000 years at monthly frequency. The observations are annualized.

Figure 7: Joint density of state variables



Note: Left panel displays the joint density of wealth share and productivity of experts along with respective marginals in the entire state space. Right panel displays the joint density of wealth share and productivity of experts along with respective marginals in crisis region.

Figure 8: Left tail of stationary density



Note: Left panel: Tail of experts wealth share distribution from the benchmark model. Right panel: Tail of experts wealth share distribution from the model with stochastic productivity.

A.2 Tables

Table 1: Calibrated parameters

	Description	Choice	Target
Technology	Volatility of capital (σ)	0.06	Vol (Risk premium)
	Discount rate (ρ)	0.05	Literature
	Depreciation rate of capital (δ)	0.05	GDP growth
	Investment cost (κ)	5	Investment-capital ratio
	Productivity gap ($\hat{a}_e - a_h$)	0.09	Conditional risk premium
	Correlation of shocks (φ)	-0.5	Data
Utility	Risk aversion (γ)	7	Unconditional risk premium
Demographics	Mean proportion of intermediaries (\bar{z})	0.10	Literature
	Turnover (λ_d)	0.03	Literature
Expert Productivity	Mean reversion rate (π)	0.01	Duration of crisis
	Variance (v)	8	Data
Exit rate	Normal state (τ_n)	0.05	Literature
	Crisis state (τ_c)	0.6	Data
Friction	Equity retention ($\underline{\chi}$)	0.65	Literature

Note: All values are annualized.

Table 2: Risk premium estimation

	(I)	(II)	(III)
const	-0.02 (0.00)	0.00 (0.01)	0.00 (0.03)
D_t/P_t	2.13*** (3.52)	1.17** (1.87)	1.15** (0.53)
1_{Rec}		2.21*** (4.15)	1.82*** (0.60)
1_{fin}			2.18*** (2.99)
No. of obs.	906	906	906
Adj. R2	0.02	0.04	0.05

Note: The variables 1_{Rec} and 1_{fin} represents recessionary and financial crisis episodes respectively. Recessionary episodes are taken from NBER, and financial crisis periods are taken from [Reinhart and Rogoff \(2009\)](#). Model (I) excludes both dummy variables to zero. Model (II) excludes financial crisis dummy but includes recession dummy. Model (III) includes both dummy variables.

Table 3: Risk premium moments and probability of crisis

	Data			Benchmark Model (RA=1)		Benchmark Model (RA = 20)	
	All	Recession	Crisis	All	Crisis	All	Crisis
E(Risk premium)	5.5	12.8	25.0	1.7	13.4	5.5	-
Std(Risk premium)	4.7	6.7	7.5	3.1	1.3	0	-
Prob. of Crisis	7.0			6.8		0	

Note: Empirical risk premium moments are computed from the predictive regression (32). Probability of crisis is taken from [Reinhart and Rogoff \(2009\)](#). The model implied moments and probability of crisis is computed by simulating the model at monthly frequency for 5000 years. All values are annualized.

Table 4: Data moments and methodology

	Mean	Std dev	Data source
Risk premium* (%)	5.6	4.7	Predictive regression
Risk free rate* (%)	4.0	0.9	Shiller's website
GDP growth*(%)	3.3	3.9	FRED
Investment rate (%)	14	4.7	He and Krishnamurthy (2019)
BHC Leverage	3.77	-	He and Krishnamurthy (2019)
Corr(BHC Leverage, GDP cycle)	-0.18	-	He, Kelly and Manela (2017)
Probability of Crisis (%)	7	-	Reinhart and Rogoff (2009)
Duration of Crisis	18-months	-	NBER cycle

Note: The Table presents unconditional mean and standard deviation of key variables in the data along with the methodology to compute the variables. The variables marked with asterisk are estimated using quarterly frequency data between 1950Q1 till 2021Q1. All percentage values are annualized.

Table 5: Model success summary

	Quantity of interest	Success level	Comments
Macroeconomic	GDP/Output growth	High	✓
	Investment rate	Low	Low variation and not enough drop in crisis
Intermediary	Leverage	High	✓
	Cyclical of leverage	High	✓
Crisis	Probability of crisis	Moderate	Matching prob. of crisis attenuates crisis dynamics
	Duration of crisis	Low	Matching duration attenuates crisis dynamics
Asset price	Conditional risk premium	High	✓
	Unconditional risk premium	Low	Matching unconditional risk premium attenuates prob. of crisis
	Std. of risk premium	Moderate	-
	Conditional volatility	High	✓
	Unconditional volatility	Low	Shiller puzzle

Note: The model implied moments and probability of crisis is computed by simulating the model at monthly frequency for 5000 years. All values are annualized.

Table 6: Duration of crisis

	Data (NBER)	Benchmark model (RA=1, IES = 1)	Benchmark model (RA=2, IES = 1)	My model (RA=5, IES=1)
10th percentile	8.0	1.0	1.0	1.0
50th percentile	13.5	2.0	2.0	3.0
90th percentile	31.2	13.0	16.0	49.0
Mean	17.5	5.8	6.5	17.0

Note: Data for computing the empirical duration of crisis is from NBER website. The last three columns presents the model implied duration percentiles obtained from simulating each of the benchmark models for 5000 years at monthly frequency.

Table 7: Calibration: Benchmark model

	Parameter	Benchmark Model	Model B1	Model B2	Target
Technology	Volatility (σ)	0.06	0.06	0.06	Volatility of risk premium
	Discount rate (ρ)	0.05	0.05	0.05	Literature
	Depreciation rate (δ)	0.02	0.1	0.1	GDP growth
	Investment cost (κ)	10	5	5	Investment-capital ratio
	Expert Productivity (a_e)	0.11	0.2	0.15	Conditional risk premium
	Household Productivity (a_h)	0.03	0.02	-0.03	Consumption-output ratio
	Correlation of shocks (φ)	-	-0.5	-	Data
Preference	Utility parameters (γ)	2	5	5	Unconditional risk premium
Demographics	Mean expert mass (\bar{z})	0.1	0.1	0.1	Literature
	Turnover (λ_d)	0.03	0.001	0.001	Literature
Expert productivity	Mean reversion rate (π)	-	0.01	-	Duration of crisis
	Variance (ν)	-	4.2	-	Data
Friction	Equity retention (χ)	0.5	0.95	0.95	Literature

Note: Calibrated parameters for the benchmark models along with the target. The benchmark model B1 does not feature stochastic productivity or exit rate. The model B2 considers stochastic productivity but without exit. The model B3 has constant productivity but the experts have a state-dependent exit rate.

Table 8: Summary of key moments

	Data	My model		Benchmark		B1		B2	
	All	All	Crisis	All	Crisis	All	Crisis	All	Crisis
Risk premium (% mean)	5.5	5.0	18.2	1.7	13.4	1.9	14.1	12.7	13.4
Risk premium (% sd)	4.7	4.8	5.2	3.1	1.3	3.5	3.7	2.7	2.9
Investment-capital ratio (% mean)	14	8.3	5.4	10.0	7.7	8.2	7.5	5.5	5.0
BHC Leverage	3.77	4.5	8.8	3.5	5.8	2.7	3.2	3.2	3.5
GDP growth (% mean)	3.2	3.5	-7.1	3.7	-9.9	3.1	-8.2	-6.3	-7.9
Corr(BHC Leverage, GDP)	-0.18	-0.19	-0.01	-0.17	-0.01	-0.15	-0.03	-0.28	-0.05
Probability of Crisis (%)	7.0	8.0		6.8		6.3		90.8	
Duration of Crisis (months)	18.0	17.0		4.0		5.0		13.0	

Note: Comparison of model implied moments. The % values are annualized. The calibrated parameter for my model is given in Table (1). The benchmark model B1 does not feature stochastic productivity or exit. The model B2 considers a stochastic productivity but without exit. The model B3 has constant productivity but the experts have a state-dependent exit rate. The calibrated parameters for the benchmark models are given in Table (7).

B Appendix: Main proofs

B.1 Model with stochastic productivity

B.1.1 Proof of the Asset pricing conditions

The expected return that the experts earn from investing in the capital is given by

$$dr_t^v = (\mu_{e,t}^R - (1 - \chi_t)\epsilon_{h,t})dt + \chi_t(\sigma_t^{q,k} + \sigma) dZ_t^k + \chi_t\sigma_t^{q,a} dZ_t^a$$

where $\epsilon_{h,t} = \zeta_{h,t}^k(\sigma_t^{q,k} + \sigma) + \zeta_{h,t}^a\sigma_t^{q,a} + \varphi(\zeta_{h,t}^a(\sigma + \sigma_t^{q,a}) + \sigma_t^{q,a}\zeta_{h,t}^k)$. That is, $(1 - \chi_t)\epsilon_{h,t}$ is the part of the expected excess return that is paid by the experts to the outside equity holders, which is netted out. Since the experts hold a fraction χ_t of the inside equity, the volatility terms are multiplied by this quantity. Consider a trading strategy of investing \$1 into the capital at time 0. Let v_t be the value of this investment strategy at time t . Then, we have $\frac{dv_t}{v_t} = dr_t^v$, and

$$\frac{d(\xi_e v_t)}{\xi_e v_t} = (-r_t + \mu_{e,t}^R - (1 - \chi_t)\epsilon_{h,t} - \chi_t\epsilon_{e,t})dt + \text{diffusion terms}$$

where $\epsilon_{e,t} = \zeta_{e,t}^k(\sigma + \sigma_t^{q,k}) + \zeta_{e,t}^a\sigma_t^{q,a} + \varphi(\zeta_{e,t}^a(\sigma + \sigma_t^{q,k}) + \zeta_{e,t}^k\sigma_t^{q,a})$, and $\xi_{e,t}$ follows the process in (5). Since $\xi_e v_t$ is a martingale, the drift equals to zero, which implies

$$\mu_{e,t}^R - r_t = \chi_t\epsilon_{e,t} + (1 - \chi_t)\epsilon_{h,t}$$

The households do not issue outside equity but are exposed to the risk from experts through the equity issuance of the latter. Following similar steps, we get the asset pricing condition for the households as

$$\mu_{h,t}^R - r_t = \epsilon_{h,t}$$

where $\epsilon_{h,t} = \zeta_{h,t}^k(\sigma + \sigma_t^{q,k}) + \zeta_{h,t}^a\sigma_t^{q,a} + \varphi(\zeta_{h,t}^a(\sigma + \sigma_t^{q,k}) + \zeta_{h,t}^k\sigma_t^{q,a})$ ■

B.1.2 Proof of Proposition 1

The law of motion of wealth for the experts and the households are given in the optimization problems (7) and (8) respectively. Using the law of large numbers to aggregate

the wealth of individual household and expert, we get

$$\begin{aligned}\frac{dW_{h,t}}{W_{h,t}} &= \left(r_t - \rho_h - \lambda_d + \theta_{h,t}(\mu_{h,t}^R - r_t) + \frac{(1 - \bar{z})\lambda_d}{1 - z_t} + \tau_t \frac{W_{e,t}}{W_{h,t}} \right) dt + \theta_{h,t}(\sigma + \sigma_t^q) dZ_t^k + \theta_{h,t}\sigma_t^a dZ_t^a \\ \frac{dW_{e,t}}{W_{e,t}} &= \left(r_t - \rho_e - \lambda_d + \theta_{e,t}\epsilon_{e,t} + \frac{\bar{z}\lambda_d}{z_t} - \tau_t \right) dt + \theta_{e,t}(\sigma + \sigma_t^{q,k}) dZ_t^k + \theta_{e,t}\sigma_t^{q,a} dZ_t^a\end{aligned}$$

where $W_{h,t} = \int_{j \in H} w_{j,t} dj$ and $W_{e,t} = \int_{j \in E} w_{j,t} dj$ denotes aggregated wealth among respective group, $z_t = \frac{W_{e,t}}{W_{h,t} + W_{e,t}} = \frac{W_{e,t}}{q_t K_t}$, and $\theta_{e,t} := \frac{\chi_t \psi_t}{z_t}$, $\theta_{h,t} := \frac{1 - \chi_t \psi_t}{1 - z_t}$ from the capital market clearing condition.⁵² The terms containing λ_d and \bar{z} are due to the overlapping generations assumption, and the terms with τ_t is due to the exit of the experts. By Ito's lemma, the dynamics of the wealth share becomes

$$\frac{dz_t}{z_t} = \frac{dW_{e,t}}{W_{e,t}} - \frac{d(q_t K_t)}{q_t K_t} + \frac{d\langle q_t K_t, q_t K_t \rangle}{(q_t K_t)^2} - \frac{d\langle q_t K_t, W_{e,t} \rangle}{(q_t K_t W_{e,t})}$$

where⁵³

$$\frac{dK_t}{K_t} = (\phi(\iota_t) - \delta)dt + \sigma dZ_t^k$$

Applying Ito's lemma, we get

$$\begin{aligned}\frac{d(q_t K_t)}{q_t K_t} &= (\epsilon_{e,t}(\sigma + \sigma_t^q) - \frac{(a_{e,t} - \iota_t)}{q_t} + r_t)dt + (\sigma + \sigma_t^{q,k})dZ_t^k + \sigma_t^{q,a} dZ_t^a \\ \frac{d\langle q_t K_t, q_t K_t \rangle}{(q_t K_t)^2} &= ((\sigma_t^{q,k} + \sigma)^2 + (\sigma_t^{q,a})^2 + 2\phi(\sigma_t^{q,k} + \sigma)\sigma_t^{q,a})dt \\ \frac{d\langle q_t K_t, W_{e,t} \rangle}{q_t K_t W_{e,t}} &= (\theta_{e,t}(\sigma_t^{q,k} + \sigma)^2 + \theta_{e,t}(\sigma_t^{q,a})^2 + 2\phi(\sigma_t^{q,k} + \sigma)\sigma_t^{q,a})dt\end{aligned}$$

and the result follows from here after some algebra. ■

Note that we can write $\theta_{e,t}\epsilon_{e,t} = \theta_{e,t}\chi_t^{-1}(\mu_{e,t}^R - r_t - (1 - \chi_t)\epsilon_{h,t})$ from the asset pricing condition in B.1.1, which allows us to write the experts wealth dynamics after aggregat-

⁵²Note that $z_t = \frac{W_{e,t}}{q_t K_t}$ and $\psi_t = \frac{K_{e,t}}{K_t}$. Moreover, $\sigma_{w_{e,t}}(\sigma + \sigma_t^q)z_t + \sigma_{w_{h,t}}(\sigma + \sigma_t^q)(1 - z_t) = (\sigma + \sigma_t^q)$ and similarly for $\sigma_t^{q,a}$. Using these, we can relate $\sigma_{w_{j,t}}$ to $\theta_{j,t}$.

⁵³Since the investment rate is the same for all agents, the evolution of the aggregate capital K_t is the same as the evolution of $k_{j,t}$. To see this, write $\frac{dK_t}{K_t} = \frac{dK_{e,t}}{K_t} + \frac{dK_{h,t}}{K_t} = \psi_t \frac{dK_{e,t}}{K_{e,t}} + (1 - \psi_t) \frac{dK_{h,t}}{K_{h,t}}$ and the rest follows from (2).

ing the optimal policies and using law of large numbers as

$$\begin{aligned} \frac{dW_{e,t}}{W_{e,t}} = & (r_t - \rho - \lambda_d + \frac{\psi_t}{z_t}(\mu_{e,t}^R - r_t) - (1 - \chi_t)\frac{\psi_t}{z_t}\epsilon_{h,t} + \frac{\bar{z}\lambda_d}{z_t} - \tau(a_{e,t}, z_t))dt \\ & + \frac{\chi_t\psi_t}{z_t}(\sigma + \sigma_t^{q,k})dZ_t^k + \frac{\chi_t\psi_t}{z_t}\sigma_t^{q,a}dZ_t^a \end{aligned}$$

B.1.3 Proof of Proposition 2

The value function conjecture is

$$U_{j,t} = \frac{(J_{j,t}(z_t, a_{e,t})K_t)^{1-\gamma}}{1-\gamma}$$

where $J_{j,t}$ follows the stochastic differential equation $\frac{dJ_{j,t}}{J_{j,t}} = \mu_{j,t}^J dt + \sigma_{j,t}^{J,k} dZ_t^k + \sigma_{j,t}^{J,a} dZ_t^a$ whose drift and volatility needs to be determined in the equilibrium. The HJB equation is given by

$$\sup_{C,K} f(C_{j,t}, U_{j,t}) + E[dU_{j,t}] = 0 \quad (33)$$

where $f(C_{j,t}, U_{j,t}) = (1-\gamma)\rho U_{j,t} \left(\log C_{j,t} - \frac{1}{1-\gamma} \log((1-\gamma)U_{j,t}) \right)$. The HJB equation is derived directly in terms of the aggregate capital K_t instead of the wealth share z_t . For ease of notation, I will denote the wealth share of the experts and households as $z_{e,t}$ and $z_{h,t}$ respectively but it is to be understood that $z_{e,t} = z_t$ and $z_{h,t} = 1 - z_t$. The value function derivatives are

$$\begin{aligned} \frac{\partial U_{j,t}}{\partial J_{j,t}} &= K_t^{1-\gamma} J_{j,t}^{-\gamma}; \quad \frac{\partial U_{j,t}}{\partial K_t} = J_{j,t}^{1-\gamma} K_t^{-\gamma} \\ \frac{\partial^2 U_{j,t}}{\partial J_{j,t}^2} &= -\gamma K_t^{1-\gamma} J_{j,t}^{-\gamma-1}; \quad \frac{\partial^2 U_{j,t}}{\partial K_t^2} = -\gamma J_{j,t}^{1-\gamma} K_t^{-(1+\gamma)}; \quad \frac{\partial^2 U_{j,t}}{\partial J_{j,t} \partial K_t} = (1-\gamma)(K_t J_{j,t})^{-\gamma} \end{aligned} \quad (34)$$

Applying Ito's lemma to $U_{j,t}$ and using HJB equation (33), we get

$$\begin{aligned} \sup_C \quad & \rho(J_{j,t}K_t)^{1-\gamma} [\log \frac{C_{j,t}}{W_{j,t}} - \log J_{j,t} + \log(q_t z_{j,t})] + (J_{j,t}K_t)^{1-\gamma} (\Phi(t) - \delta) \\ & - \frac{\gamma}{2} (J_{j,t}K_t)^{1-\gamma} \sigma^2 + (J_{j,t}K_t)^{1-\gamma} \mu_{j,t}^J - (J_{j,t}K_t)^{1-\gamma} \frac{\gamma}{2} ((\sigma_{j,t}^{J,k})^2 + (\sigma_{j,t}^{J,a})^2 + 2\varphi \sigma_{j,t}^{J,k} \sigma_{j,t}^{J,a}) \\ & + (1-\gamma)(J_{j,t}K_t)^{1-\gamma} (\sigma \sigma_{j,t}^{J,k} + \varphi \sigma \sigma_{j,t}^{J,a}) + \tau_t(U_{h,t} - U_{e,t}) = 0 \end{aligned} \quad (35)$$

Writing the value function expression in terms of the wealth, we have

$$U_{j,t} = \frac{(\tilde{J}_{j,t} W_{j,t})^{1-\gamma}}{1-\gamma}; \quad f(C_{j,t}, U_{j,t}) = (1-\gamma)\rho U_{j,t} \left(\log \frac{C_{j,t}}{W_{j,t}} - \tilde{J}_{j,t} \right) \quad (36)$$

where $\tilde{J}_{j,t} = \frac{J_{j,t}}{q_t z_{j,t}}$ and $z_{j,t} = \frac{W_{j,t}}{q_t K_t}$ are used to obtain (36). At the optimum, the marginal utilities of wealth and consumption become equal. Therefore,

$$\begin{aligned} \frac{\partial U_{j,t}}{\partial W_{j,t}} &= \frac{\partial f_{j,t}}{\partial C_{j,t}} \\ \tilde{J}_{j,t}^{1-\gamma} W_{j,t}^{-\gamma} &= (1-\gamma)\rho \frac{U_{j,t}}{C_{j,t}} \implies \frac{C_{j,t}}{W_{j,t}} = \rho \end{aligned}$$

This proves the optimal consumption policy. The stochastic discount factor for recursive utility is given by

$$\xi_{j,t} = \exp \left(\int_0^t \frac{\partial f(C_{j,s}, U_{j,s})}{\partial U} ds \right) \frac{\partial U_{j,t}}{\partial W_{j,t}}$$

From (36), we get

$$\xi_{j,t} = (1-\gamma) \exp \left(\int_0^t [(1-\gamma)\rho (\log \rho - \tilde{J}_{j,t})] ds \right) \frac{U_{j,t}}{W_{j,t}}$$

This implies that $\sigma(\xi_{j,t}) = \sigma \left(\frac{U_{j,t}}{W_{j,t}} \right)$. To compute the R.H.S., we have to obtain $d \left(\frac{U_{j,t}}{W_{j,t}} \right)$. Let $v(J_{j,t}, z_{j,t}, q_t, K_t) := \frac{U_{j,t}}{W_{j,t}}$. Using the derivatives

$$\begin{aligned} \frac{1}{v} \frac{\partial v}{\partial J_{j,t}} &= \frac{1-\gamma}{J_{j,t}}; & \frac{1}{v} \frac{\partial v}{\partial z_{j,t}} &= -\frac{1}{z_{j,t}} \\ \frac{1}{v} \frac{\partial v}{\partial q_t} &= -\frac{1}{q_t}; & \frac{1}{v} \frac{\partial v}{\partial K_t} &= \frac{1-\gamma}{K_t} \end{aligned}$$

and applying Ito's lemma, we get

$$\begin{aligned} \frac{dv}{v} &= \underbrace{[\dots\dots]}_{\text{drift term}} dt + (1-\gamma)(\sigma_{j,t}^{J,k} dZ_t^k + \sigma_{j,t}^{J,a} dZ_t^a) - (\sigma_{j,t}^{z,k} dZ_t^k + \sigma_{j,t}^{z,a} dZ_t^a) \\ &\quad - ((\sigma + \sigma_t^{q,k}) dZ_t^k + \sigma_t^{q,a} dZ_t^a) + (1-\gamma)\sigma dZ_t^k \end{aligned} \quad (37)$$

Applying Ito's lemma to $J_{j,t}(z_t, a_{e,t})$, we have

$$\begin{aligned} dJ_{j,t} &= \frac{\partial J_{j,t}}{\partial z_t} dz_t + \frac{\partial J_{j,t}}{\partial a_{e,t}} da_{e,t} + \frac{1}{2} \frac{\partial^2 J_{j,t}}{\partial z_t^2} d\langle z, z \rangle_t + \frac{1}{2} \frac{\partial^2 J_{j,t}}{\partial a_{e,t}^2} d\langle a_e, a_e \rangle_t \\ &= (\text{drift terms}) + \frac{\partial J_{j,t}}{\partial z_t} z_t (\sigma_t^{z,k} dZ_t^k + \sigma_t^{z,a} dZ_t^a) + \frac{\partial J_{j,t}}{\partial a_{e,t}} \sigma_{ae} dZ_t^a \end{aligned}$$

Comparing with the SDE (20) and matching the diffusion coefficients, we have

$$\begin{aligned} \sigma_{j,t}^{J,k} J_{j,t} &= \frac{\partial J_{j,t}}{\partial z_t} z_t \sigma_t^{z,k} = \frac{\partial J_{j,t}}{\partial z_t} z_t \left(\frac{\chi_t \psi_t}{z_t} - 1 \right) (\sigma + \sigma_t^{q,k}) \\ \sigma_{j,t}^{J,a} J_{j,t} &= \frac{\partial J_{j,t}}{\partial a_{e,t}} \sigma_{ae} + \frac{\partial J_{j,t}}{\partial z_t} z_t \sigma_t^{z,a} = \frac{\partial J_{j,t}}{\partial a_{e,t}} \sigma_{ae} + \frac{\partial J_{j,t}}{\partial z_t} z_t \left(\frac{\chi_t \psi_t}{z_t} - 1 \right) \sigma_t^{q,a} \end{aligned}$$

Collecting the diffusion terms, using $\sigma_{e,t}^{z,i} = \sigma_t^{z,i}$, $\sigma_{h,t}^{z,i} = -\frac{z_t}{1-z_t} \sigma_t^{z,i}$; $i \in \{k, a\}$ in equation (37), and comparing it to the SDF equation

$$\frac{d\xi_{j,t}}{\xi_{j,t}} = -r_t dt - \zeta_{j,t}^k dZ_t^k - \zeta_{j,t}^a dZ_t^a$$

we get the desired result. ■

Plugging in the optimal consumption-wealth ratio into the HJB equation (35), we obtain the expressions for $\mu_{j,t}^J$

$$\begin{aligned} \mu_{e,t}^J &= (\gamma - 1)(\sigma \sigma_{e,t}^{J,k} + \varphi \sigma \sigma_{e,t}^{J,a}) - (\Phi(\iota_t) - \delta) - \rho(\log \rho - \log J_{e,t} + \log(z_t q_t)) \\ &\quad + \frac{\gamma}{2} \left((\sigma_{e,t}^{J,k})^2 + (\sigma_{e,t}^{J,a})^2 + 2\varphi \sigma_{e,t}^{J,k} \sigma_{e,t}^{J,a} + \sigma^2 \right) - \frac{\tau_t}{1-\gamma} \left(\left(\frac{J_{h,t}}{J_{e,t}} \right)^{1-\gamma} - 1 \right) \end{aligned} \quad (38)$$

$$\begin{aligned} \mu_{h,t}^J &= (\gamma - 1)(\sigma \sigma_{h,t}^{J,k} + \varphi \sigma \sigma_{h,t}^{J,a}) - (\Phi(\iota_t) - \delta) - \rho(\log \rho - \log J_{h,t} + \log((1 - z_t) q_t)) \\ &\quad + \frac{\gamma}{2} \left((\sigma_{h,t}^{J,k})^2 + (\sigma_{h,t}^{J,a})^2 + 2\varphi \sigma_{h,t}^{J,k} \sigma_{h,t}^{J,a} + \sigma^2 \right) \end{aligned} \quad (39)$$

B.1.4 Proof of Proposition 3

Applying Ito's lemma to $q(z_t, a_{e,t})$, we have

$$dq_t = \frac{\partial q_t}{\partial z_t} dz_t + \frac{\partial q_t}{\partial a_{e,t}} da_{e,t} + \frac{1}{2} \frac{\partial^2 q_t}{\partial z_t^2} d\langle z_t, z_t \rangle + \frac{1}{2} \frac{\partial^2 q_t}{\partial a_{e,t}^2} d\langle a_{e,t}, a_{e,t} \rangle + \frac{\partial^2 q_t}{\partial z_t \partial a_{e,t}} d\langle z_t, a_{e,t} \rangle$$

Matching the drift and the volatility terms, we get

$$\begin{aligned}\mu_{q,t} &= \frac{\partial q_t}{\partial z_t} \frac{1}{q_t} \mu_t^z + \frac{\partial q_t}{\partial a_{e,t}} \mu_{ae,t} + \frac{1}{2} \frac{\partial^2 q_t}{\partial z_t^2} ((\sigma_t^{z,k})^2 + (\sigma_t^{z,a})^2 + 2\varphi \sigma_t^{z,k} \sigma_t^{z,a}) \\ &\quad + \frac{1}{2} \frac{\partial^2 q_t}{\partial a_{e,t}^2} \sigma_{ae,t}^2 + \frac{\partial^2 q_t}{\partial z_t \partial a_{e,t}} (\varphi \sigma_t^{z,k} \sigma_{ae,t} + \sigma_t^{z,a} \sigma_{ae,t}) \\ \sigma_t^{q,k} &= \frac{\partial q_t}{\partial z_t} \frac{1}{q_t} \sigma_t^{z,k} \\ \sigma_t^{q,a} &= \frac{\partial q_t}{\partial z_t} \frac{1}{q_t} \sigma_t^{z,a} + \frac{\partial q_t}{\partial a_{e,t}} \frac{1}{q_t} \sigma_{ae,t}\end{aligned}$$

where $\sigma_{ae,t} = v(\bar{a}_e - a_{e,t})(a_{e,t} - \underline{a}_t)$ and $\mu_{ae,t} = \pi(\hat{a}_e - a_{e,t})$. Plugging in the expression for $\sigma_t^{z,k}$ and $\sigma_t^{z,a}$ from the dynamics of wealth share (18) in the above equation and rearranging, we get the result. ■

B.1.5 Numerical solution

Static step: We need to solve for the equilibrium quantities $\{\psi_t, (\sigma + \sigma_t^{q,k}), \sigma_t^{q,a}, q_t\}$. The other equilibrium quantities $\theta_{e,t}, \theta_{h,t}, \zeta_{e,t}^k, \zeta_{e,t}^a, \zeta_{h,t}^k, \zeta_{h,t}^a, r_t, \mu_{e,t}^R, \mu_{h,t}^R, l_t$ can be derived from the goods market clearing and the HJB first order conditions. To solve for these four quantities, four equations are required. The first equation is given by subtracting the expected return of each type of the agent. That is, we have

$$\chi_t(\epsilon_{e,t} - \epsilon_{h,t}) = \mu_{e,t}^R - \mu_{h,t}^R$$

The experts will issue maximum outside equity $\underline{\chi}$ whenever their risk premium is larger than that of households. Thus, we can replace χ_t by $\underline{\chi}$ whenever $\psi < 1$. Plugging in the expression for the return processes from (4), and using (12), (11), and Proposition 2, we get

$$\begin{aligned}\frac{a_{e,t} - a_h}{q_t} &= \underline{\chi} \left((\underline{\chi} \psi_t - z_t) ((\sigma_t^{q,k} + \sigma)^2 + (\sigma_t^{q,a})^2 + 2\varphi(\sigma + \sigma_t^{q,k})) \right. \\ &\quad \times \left((1 - \gamma) \left(\frac{\partial J_{h,t}}{\partial z_t} \frac{1}{J_{h,t}} - \frac{\partial J_{e,t}}{\partial z_t} \frac{1}{J_{e,t}} \right) + \frac{1}{z_t(1 - z_t)} \right) \\ &\quad \left. + (1 - \gamma) \left(\frac{\partial J_{h,t}}{\partial a_{h,t}} \frac{1}{J_{h,t}} - \frac{\partial J_{e,t}}{\partial a_{e,t}} \frac{1}{J_{e,t}} \right) \sigma_{ae,t} (\sigma_t^{q,a} + \varphi(\sigma + \sigma_t^{q,k})) \right) \end{aligned} \quad (40)$$

The second condition comes from the goods market clearing

$$\rho q_t = \psi_t(a_{e,t} - \iota_t) + (1 - \psi_t)(a_h - \iota_t) \quad (41)$$

The third and fourth conditions are the return variance components

$$\sigma_t^{q,k} + \sigma = \frac{\sigma}{1 - \frac{1}{q_t} \frac{\partial q_t}{\partial z_t} (\underline{\chi} \psi_t - z_t)} \quad (42)$$

$$\sigma_t^{q,a} = \frac{\frac{1}{q_t} \frac{\partial q_t}{\partial a_{e,t}} \sigma_{ae,t}}{1 - \frac{1}{q_t} \frac{\partial q_t}{\partial z_t} (\underline{\chi} \psi_t - z_t)} \quad (43)$$

which are partial differential equations solved using a Newton-Raphson scheme. The algorithm is as follows. Consider tensor grids of size N_z and N_a with step size Δ_i , and Δ_j where $\{i\}_1^{N_z}, \{j\}_1^{N_a}$ denote the dimensions for the wealth share and the expert productivity respectively. There are three following regions in the state space

- $\psi_t < 1$ and $\chi_t = \underline{\chi}$
- $\psi_t = 1$ and $\chi_t = \underline{\chi}$
- $\psi_t = 1$ and $\chi_t > \underline{\chi}$

In the first region, the households also hold capital and hence equation (15) holds with equality. In this case, the equations (40), (41), (42), and (43) are used to solve for ψ_t , q_t , $(\sigma + \sigma_t^{q,k})$, and $\sigma_t^{q,a}$. In the second region, the households do not hold capital and hence the equation (15) holds with an inequality. In this case, set $\psi_t = 1$, and use (40), (42), (43), and (41) to solve for χ_t, q_t , $(\sigma + \sigma_t^{q,k})$, and $\sigma_t^{q,a}$. If $\chi_t < \underline{\chi}$, then set $\chi_t = \underline{\chi}$, otherwise the third region is entered.

- For the first iteration on the wealth share $\{i = 1, \forall j\}$, set $\psi_t = 0$, and take the limiting case of the goods market clearing condition to get q_t . That is

$$\inf_{z \rightarrow 0^+} q_t = \frac{a_h \kappa + 1}{\rho \kappa + 1} \quad (44)$$

- For iterations $i > 1, \forall j$, use the discretized versions of the equations (42) and (43)

$$(\sigma^{q,k} + \sigma)_{i,j} = \sigma \left(1 - \frac{1}{q_{i,j}} \left(\frac{q_{i,j} - q_{i-1,j}}{\Delta_i} z_i \left(\frac{\psi_{i,j}}{z_i} - 1 \right) \right) \right)^{-1} \quad (45)$$

$$(\sigma^{q,a})_{i,j} = \left(\frac{q_{i,j} - q_{i,j-1}}{\Delta_j} \sigma_{ae,j} \right) \left(1 - \frac{1}{q_{i,j}} \left(\frac{q_{i,j} - q_{i-1,j}}{\Delta_i} z_i \left(\frac{\psi_{i,j}}{z_i} - 1 \right) \right) \right)^{-1} \quad (46)$$

along with the equations (40), and (41) to solve for $q_{i,j}, \psi_{i,j}, (\sigma + \sigma^q)_{i,j}, (\sigma^{q,a})_{i,j}$.⁵⁴ Note that in this region, $\chi_t = \underline{\chi}$ since the risk premium of experts is larger than that of households. The set of non-linear equations is solved using the Newton-Raphson method. Repeat this procedure until $\psi_t = 1$, in which case the system enters the second region. Then, use (40), (41), (45), and (46) to solve for $\chi_{i,j}, q_{i,j}, (\sigma + \sigma^{q,k})_{i,j}$ and $(\sigma^{q,a})_{i,j}$. If $\chi_{i,j} < \underline{\chi}$, set $\chi_{i,j}^* = \underline{\chi}$, otherwise set $\chi_{i,j}^* = \chi_{i,j}$. When $\chi_{i,j} > \underline{\chi}$, the system is in the third region where all capital is held by the experts ($\psi_{i,j} = 1$), and risk is perfectly shared between the experts and the households by setting $\epsilon_{e,t} = \epsilon_{h,t}$. The value of χ_t^* is obtained such that $\chi_t^* = \underset{\chi}{argsolve} \quad \epsilon_{e,t} - \epsilon_{h,t} = 0$. Since the premiums $\epsilon_{e,t}, \epsilon_{h,t}$ depend on the χ_t , I iterate between these two quantities until $|\chi_t^{new} - \chi_t^{old}| < tol$ for some tolerance level.

Time step: Applying Ito's lemma to $J_{j,t}(z_t, a_{e,t})$, matching the drift terms, and augmenting the resulting coupled PDEs with a time step (falst-transient method), we get

$$\begin{aligned} \mu_{j,t}^J J_{j,t} = & \frac{\partial J_{j,t}}{\partial t} + \frac{\partial J_{j,t}}{\partial z_t} \mu_t^z + \frac{\partial J_{j,t}}{\partial a_{e,t}} \mu_t^a + \frac{1}{2} \frac{\partial^2 J_{j,t}}{\partial z_t^2} \left((\sigma_{j,t}^{z,k})^2 + (\sigma_{j,t}^{z,a})^2 + 2\varphi \sigma_{j,t}^{z,k} \sigma_{j,t}^{z,a} \right) + \frac{1}{2} \frac{\partial^2 J_{j,t}}{\partial a_{e,t}^2} \sigma_{ae,t}^2 \\ & + \frac{\partial^2 J_{j,t}}{\partial z_t \partial a_{e,t}} (z_t \sigma_{j,t}^{z,k} \sigma_{ae,t} \varphi + \sigma_a \sigma_{j,t}^{z,a}) \end{aligned} \quad (47)$$

The coefficients μ_t^z and σ_t^z can be computed from the equilibrium quantities in the static step and $\mu_{j,t}^J$ is computed from the equations in (38). The PDEs are solved using the neural network method explained in Section B.1.6. Using the updated function $J_{j,t}$, the static step is performed again. The procedure is repeated until the function $J_{j,t}$ converges upto a pre-specified tolerance level.

⁵⁴For $j = 1$, set $\frac{\partial q_t}{\partial a_{e,t}} = 0$ since $a_{e,t} \in [\underline{a}_e, \bar{a}_e]$. That is, the lower and the upper boundaries \underline{a}_e and \bar{a}_e respectively act as reflecting barriers forcing the derivative of the price to be zero.

B.1.6 Neural network solution method

The outer loop involves solving for a de-coupled system of quasi-linear PDEs- one for the households and one for the experts, taking as given the equilibrium quantities that are determined from the static loop. The PDE obtained at kth time iteration by applying Ito's lemma to $J_{j,t}(z_t, a_{e,t})$ and using the HJB equation (23) is⁵⁵

$$\begin{aligned} \mu^J J = & \frac{\partial J}{\partial t} + \frac{\partial J}{\partial z} \mu^z + \frac{\partial J}{\partial a} \mu^a + \frac{1}{2} \frac{\partial^2 J}{\partial z^2} \left((\sigma^{z,k})^2 + (\sigma^{z,a})^2 + 2\varphi \sigma^{z,k} \sigma^{z,a} \right) + \frac{1}{2} \frac{\partial^2 J}{\partial a^2} \sigma_a^2 \\ & + \frac{\partial^2 J}{\partial z_t \partial a} (z \sigma^{z,k} \sigma_a \varphi + \sigma_a \sigma^{z,a}); \quad \forall (t, z, a) \in [T - \Delta t, T - (k - 1)\Delta t] \times \Omega \end{aligned} \quad (48)$$

with the boundary conditions

$$\begin{aligned} J(z, a, t) &= \tilde{J}; \quad \forall (t, z, a) \in (T - (k - 1)\Delta t) \times \Omega \\ \frac{\partial J(0, a, t)}{\partial z_t} &= \frac{\partial J(1, a, t)}{\partial z_t} = 0; \quad \forall (t, a) \in (T - (k - 1)\Delta t) \times \partial\Omega_a \\ \frac{\partial J(z, \underline{a}_e, t)}{\partial a_{e,t}} &= \frac{\partial J(z, \bar{a}_e, t)}{\partial a_{e,t}} = 0; \quad \forall (t, z) \in (T - (k - 1)\Delta t) \times \partial\Omega_z \end{aligned} \quad (49)$$

where Ω_z and Ω_a are the domains of state variables z and a_e respectively, and $\Omega = \Omega_z \times \Omega_a$. I take advantage of the universal approximation theorem that states that a neural network with at least one hidden layer can approximate any Borel measurable function, and solve for the function $J(z, a, T - k\Delta t)$ that is governed by the PDE (48). Starting from an arbitrary terminal value at time T , the task is to solve for $J(z, a, T - \Delta t)$ in the first time iteration. More generally, in kth time iteration, the function $J(z, a, T - k\Delta t)$ is found such that it respects (48) satisfying the given boundary conditions at time $T - (k - 1)\Delta t$. Equivalently, we can start from $J(z, a, t + \Delta t)$ for some time period t , and solve for $J(z, a, t)$. In this case, the initial condition \tilde{J} denotes the value from the previous time step $J(z, a, t + \Delta t)$. The PDE coefficients and the terminal value are in the form of a grid but not all grid points are required in the algorithm as will be explained. While the space of admissible solutions to the function given the sample data from terminal value and other boundary conditions is potentially large, I use the residuals from PDE and the boundary conditions as *regularizers* that constrain the space to a manageable size. This encoding of prior information into the learning algorithm amplifies the information

⁵⁵I ignore the time and agent indices in order to avoid cluttering of notations. The productivity of the expert $a_{e,t}$, and the volatility $\sigma_{a_{e,t}}$ are denoted as a and σ_a for simplicity in the PDEs.

content from the economic problem and makes it possible for the deep neural network to head towards the correct solution even with the limited training sample. Consider the PDE residual from (48)

$$f := \frac{\partial J}{\partial t} + \frac{\partial J}{\partial z} \mu^z + \frac{\partial J}{\partial a} \mu^a + \frac{1}{2} \frac{\partial^2 J}{\partial z^2} \left((\sigma^{z,k})^2 + (\sigma^{z,a})^2 + 2\varphi \sigma^{z,k} \sigma^{z,a} \right) + \frac{1}{2} \frac{\partial^2 J}{\partial a^2} \sigma_a^2 + \frac{\partial^2 J}{\partial z \partial a} (z \sigma^{z,k} \sigma_a \varphi + \sigma_a \sigma^{z,a}) - \mu^J J \quad (50)$$

Starting from a neural network $\hat{J}(z, a, t; \Theta)$ parameterized by an arbitrary Θ , the optimal parameter Θ^* that ensures that $\hat{J}(z, a, t; \Theta)$ is close to J is obtained by minimizing the following loss function

$$\mathcal{L} = \lambda_f \mathcal{L}_f + \lambda_j \mathcal{L}_j + \lambda_b \mathcal{L}_b + \lambda_c^1 \mathcal{L}_c^1 + \lambda_c^2 \mathcal{L}_c^2 \quad (51)$$

where⁵⁶

$$\text{PDE loss} \quad \mathcal{L}_f = \frac{1}{N_f} \sum_{i=1}^{N_f} |f(z_f^i, a_f^i, t_f^i)|^2 \quad (52)$$

$$\text{Bounding loss-1} \quad \mathcal{L}_j = \frac{1}{N_j} \sum_{i=1}^{N_j} |\hat{J}(z_j^i, a_j^i, t_j^i) - \tilde{J}^i|^2 \quad (53)$$

$$\text{Bounding loss-2} \quad \mathcal{L}_b = \frac{1}{N_b} \sum_{i=1}^{N_b} |\nabla \hat{J}(z_b^i, a_b^i, t_b^i)|^2 \quad (54)$$

$$\text{Crisis loss-1} \quad \mathcal{L}_c^1 = \frac{1}{N_c^1} \sum_{i=1}^{N_c^1} |\hat{J}(z_c^i, a_c^i, t_c^i) - \tilde{J}^i|^2 \quad (55)$$

$$\text{Crisis loss-2} \quad \mathcal{L}_c^2 = \frac{1}{N_c^2} \sum_{i=1}^{N_c^2} |f(z_c^i, a_c^i, t_c^i)|^2 \quad (56)$$

The parameters $(\lambda_f, \lambda_j, \lambda_b, \lambda_c)$ are weights attached to the corresponding losses, $(z_j^i, a_j^i, t_j^i, \tilde{J}^i)_{i=1}^{N_j}$ and $(z_b^i, a_b^i, t_b^i)_{i=1}^{N_b}$ denote the boundary training data, and $(z_f^i, a_f^i, t_f^i)_{i=1}^{N_f}$ denote the collocation points for the PDE residual $f(z, a, t)$. The crisis boundary collocation points $(z_c^i, a_c^i, t_c^i)_{i=1}^{N_c}$ are sampled from the neighborhood of state space where fire-sale gets initiated, that is endogenously determined in the static inner loop. The quantities $(N_f, N_j, N_b, N_c^1, N_c^2)$

⁵⁶I write $\nabla \hat{J}$ to denote $\left[\frac{\partial \hat{J}}{\partial z} \quad \frac{\partial \hat{J}}{\partial a} \right]^T$.

denote the number of points to minimize the PDE loss, the two bounding losses, and the two crisis boundary losses respectively. By encoding the crisis boundary loss, the neural network is forced to learn better around the crisis threshold which is where the policy functions are highly non-linear. The sampling is done uniformly with replacement in each domains. The construction of crisis loss is inspired from *active machine learning* (Settles (2012)), a budding area in the artificial intelligence literature. Active learning algorithms work by providing better training samples at each iteration to ensure quick convergence. At every iteration, the points in the state space where crisis occurs might change, and sampling more points from around this region dynamically provides better training samples. I consider artificial collocation points for time such that $\{t^i\} \in [t^i, t^i + \Delta t^i]$ are sampled uniformly so as to reduce errors in numerical derivatives with respect to the time dimension. The number of collocation points $(N_j, N_b, N_f, N_c^1, N_c^2, N_t)$ in total need not be large and is taken to be 10% of the total grid size. This makes the algorithm mesh-free and scalable to higher dimensions.

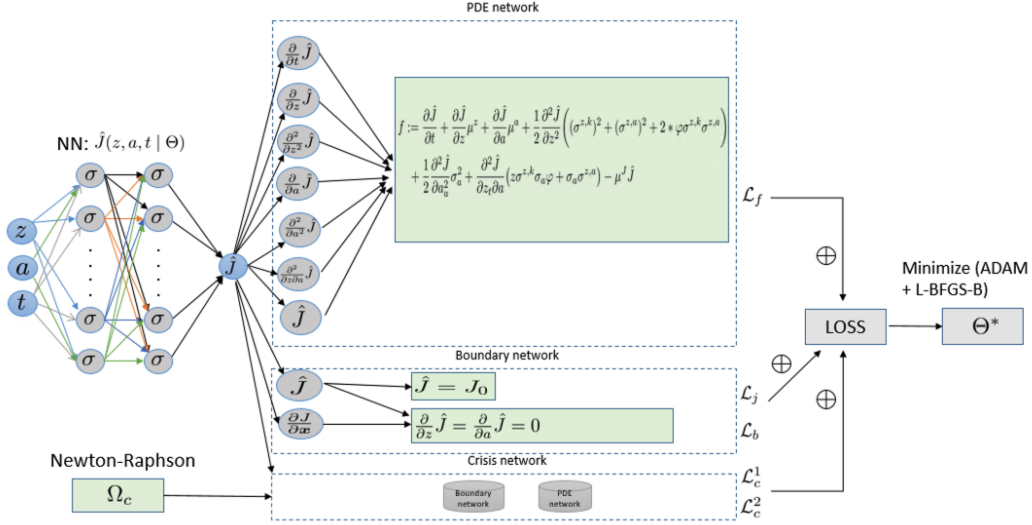
Table 9: Network architecture.

Parameters	Choices
No. of hidden layers	4
Hidden units	[30,30,30,30]
Activation functions	Tanh (Hidden), Linear (Output)
Optimizer	ADAM + L-BFGS-B
Learning rate	0.01
Loss function weights($\lambda_f, \lambda_j, \lambda_b, \lambda_c^1, \lambda_c^2$)	$\{1, 1, 0.001, 1, 1\}$
Batch size	Full batch

Opening the black box The success of a deep neural network model often relies on the network architecture and the hyperparameters. The machine learning models in finance literature use extensive hyperparameter search in the tuning process to select the ‘right’ model (see Gu, Kelly and Xiu (2020), Chen, Pelger and Zhu (2019), etc.). The deep learning model used in this paper does not suffer from this problem for two reasons. First, there is no training/test/validation set really which means that one does not have to worry about the classical overfitting problem.⁵⁷ Second, and more importantly, the proposed regularization mechanism encodes the economic problem into the learning

⁵⁷The boundary conditions provide us with data points which can be thought of as training sample, but it does not carry the same meaning as it does in supervised machine learning.

Figure 9: Neural network architecture



Note: The quantities I and Ω denote the domain of the state space pertaining to the initial and boundary conditions respectively. The domain Ω_c refers to the crisis neighborhood and is endogenously determined in the inner static loop.

algorithm by building a meaningful loss function which enables a simple feed-forward network to arrive at the right solution. Using complex architectures such as Convolution neural network, LSTM, etc. create a ‘black-box’ problem which limits the ability to understand what makes the algorithm succeed. On the contrary, using a simple feed-forward network and encoding the economic information as regularizers provides a lot more visibility on how the model steers towards the right solution.

The proliferation of deep learning application in the past decade can be largely attributed to the *automatic differentiation* which has enabled reduced computation time of the derivatives of functions. In the deep learning literature, the parameters of a network are optimized through backpropagation by taking the derivative of a loss function with respect to the parameters. The approach presented in this paper explicitly uses automatic differentiation to take derivatives with respect to the space and the time dimensions. In Figure (9), the left most part of the neural network ($NN : \hat{J}(z, a, t | \Theta)$) is the familiar simple feed-forward architecture. The output from this network (\hat{J}) is fed into the PDE, boundary, and crisis network respectively that utilizes automatic differentiation in the customized loss functions. The separation of fundamental neural network with a simple architecture and the informed PDE network allows us to peek into the black-box and witness the automatic differentiation fully in action, which is the key driver of the algorithm’s learning in both low and high dimensions.

Hyperparameter choices: Table (9) presents the chosen hyperparameters of the model. I use 4 hidden layers with 30 neurons each since a deep layer is empirically observed to be better than a wide layer. While a rectified linear unit is the common choice for activation function, I use a hyperbolic tangent function based on its superior performance for the problem at hand. The optimizers are chosen based on empirical observation. I use an adaptive momentum (ADAM) optimizer with a learning rate of 0.01 until error is minimized to the order of $1e-4$ and then use a quasi-newton method called L-BFGS-B until convergence is ensured. The network weights and biases are initialized using Xavier initialization in order to avoid the ubiquitous vanishing/exploding gradient problem in deep learning (see [Glorot and Bengio \(2010\)](#)). The weights of loss functions ($\lambda_f, \lambda_j, \lambda_c$) are uniform to give equal importance for each of these components. I use a smaller weight for the second bounding loss \mathcal{L}_b . Since the training sample size is much smaller than the full grid size, full batch is used in optimizer as opposed to mini-batches which is common in deep learning algorithms.

B.1.7 Three-dimensional plots

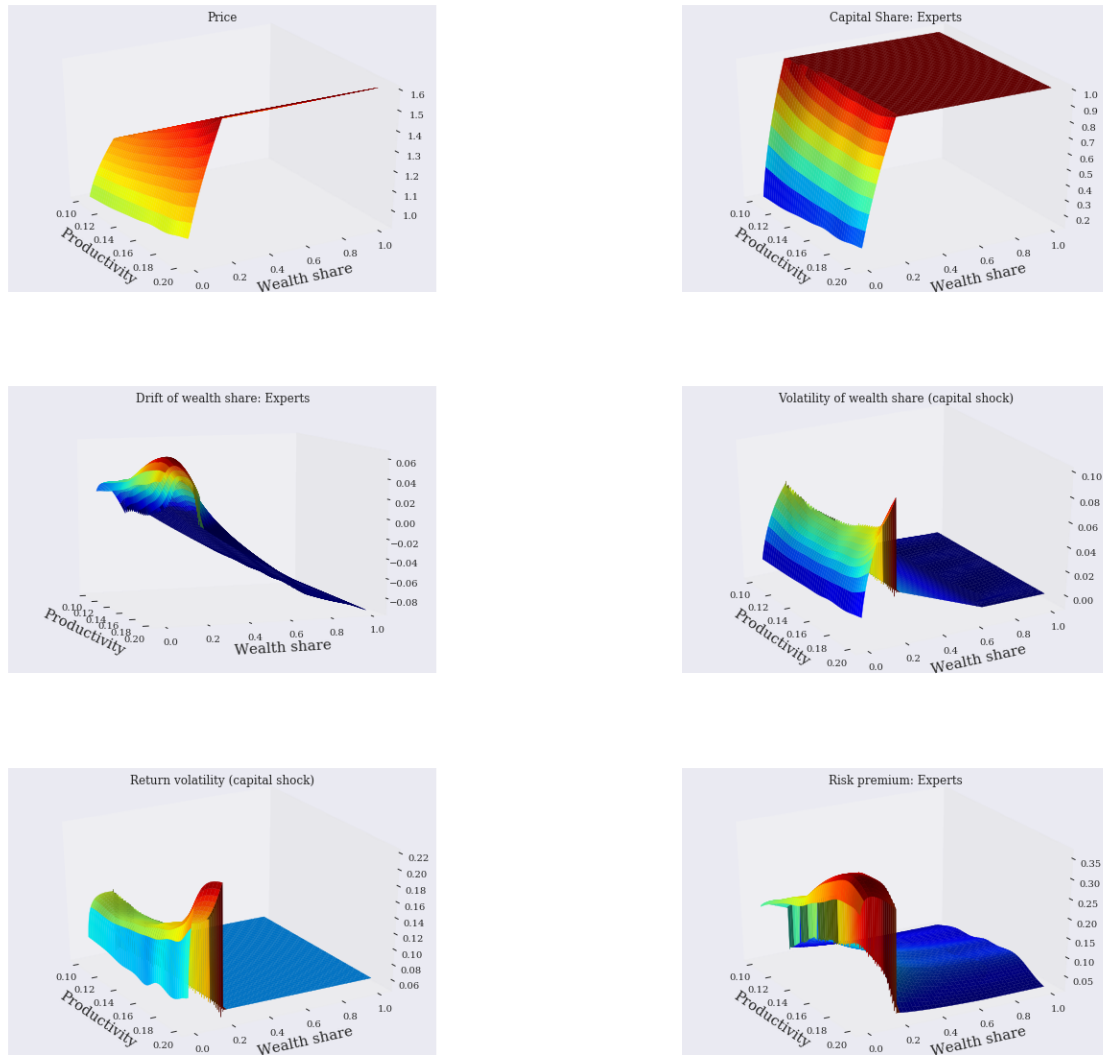


Figure 10: Equilibrium values as functions of state variables z_t and a_t for the stochastic productivity model.

C Appendix: Benchmark model

C.1 Benchmark model

The capital price per unit q_t follows the process

$$\frac{dq_t}{q_t} = \mu_t^q dt + \sigma_t^q dZ_t^k$$

The terms μ_t^q , and σ_t^q are endogenously determined in the equilibrium. Note that the productivity shocks are absent in the benchmark model. Using this dynamics for the price, the return process can be written as

$$dR_{j,t} = \underbrace{\left(\frac{a_j - l_{j,t}}{q_t} + \Phi(l_{j,t}) - \delta + \mu_t^q + \sigma \sigma_t^q \right)}_{\mu_{j,t}^R} dt + (\sigma + \sigma_t^q) dZ_t^k \quad (57)$$

Let $\xi_{e,t}$ and $\xi_{h,t}$ denote the SDF of the experts and the households respectively that follows

$$\frac{d\xi_{j,t}}{\xi_{j,t}} = -r_t dt - \zeta_{j,t} dZ_t^k \quad (58)$$

where, $\zeta_{j,t}$ is the market price of risk for agent j . Similar to the stochastic productivity model, both agents invest in the risk-free asset, and hence the drift of the SDF process is the same for all agents. The asset pricing conditions for the experts and the households respectively take the simpler form⁵⁸

$$\frac{\frac{a_e - l_t}{q_t} + \Phi(l_t) - \delta + \mu_t^q + \sigma \sigma_{q,t} - r_t}{\sigma + \sigma_{q,t}} = \chi_t \zeta_{e,t} + (1 - \chi_t) \zeta_{h,t} \quad (59)$$

$$\frac{\frac{a_h - l_t}{q_t} + \Phi(l_t) - \delta + \mu_t^q + \sigma \sigma_{q,t} - r_t}{\sigma + \sigma_{q,t}} \leq \zeta_{h,t} \quad (60)$$

⁵⁸This can be proved using the Martingale argument similar to the model with stochastic productivity. See Appendix C.1.1 for the proof.

The equality holds in (60) if the households own some amount of capital ($\psi_t < 1$). The optimal investment rate is the same as before and is given in (13). The agents solve

$$\begin{aligned} \sup_{c_{j,t}, \chi_{j,t}, k_{j,t}} \quad & E_t \left[\int_t^\infty f(c_{j,s}, U_{j,s}) ds \right] \\ \text{s.t.} \quad & \frac{dw_{j,t}}{w_{j,t}} = \left(r_t - \frac{c_{j,t}}{w_{j,t}} + \frac{q_t k_{j,t}}{w_{j,t}} (\mu_{j,t}^R - r_t - (1 - \chi_{j,t})(\sigma + \sigma_t^q) \zeta_{j',t}) \right) dt + \sigma_{w_{j,t}} (\sigma + \sigma_t^q) dZ_t^k \end{aligned} \quad (61)$$

where the aggregator $f(c_{j,s}, U_{j,s})$ is given in (6) and the index j' denotes the other type of agent. The households do not issue outside equity and hence $\chi_{h,t} = 1$. On the other hand, the experts issue outside equity but are constrained to hold at least a fraction $\underline{\chi}$ of equity in their balance sheet. Thus, $\chi_{e,t} \in [\underline{\chi}, 1]$. Moving forward, I denote $\chi_{e,t}$ as simply χ_t for notation brevity. The expressions for $\sigma_{w_{j,t}}$ is the same as in the stochastic productivity model given in (9) and (10). Since all agents within the group j are identical as before, I solve for the decentralized economy with wealth share of the experts z_t as the sole state variable. The wealth share is defined as

$$z_t = \frac{W_{e,t}}{W_{e,t} + W_{h,t}} = \frac{W_{e,t}}{q_t K_t}$$

where $W_{e,t} = \int_{\mathbb{E}} w_{j,t} dj$ and $K_t = \int_{\mathbb{E}} k_{j,t} dj + \int_{\mathbb{H}} k_{j,t} dj$. Moving forward, I denote $X_{e,t}$ to mean $\int_{\mathbb{E}} x_{j,t} dj$, and similarly for the households.

Proposition 4. *The law of motion of the wealth share of experts is given by*

$$\frac{dz_t}{z_t} = \mu_t^z dt + \sigma_t^z dZ_t^k \quad (62)$$

where

$$\begin{aligned} \mu_t^z &= \frac{a_e - \iota_t}{q_t} - \frac{C_{e,t}}{W_{e,t}} + \left(\frac{\chi_t \psi_t}{z_t} - 1 \right) (\sigma + \sigma_{q,t}) (\zeta_{e,t} - (\sigma + \sigma_t^q)) + (1 - \chi_t) (\sigma + \sigma_t^q) (\zeta_{e,t} - \zeta_{h,t}) + \frac{\lambda_d}{z_t} (\bar{z} - z_t) \\ \sigma_t^z &= \left(\frac{\chi_t \psi_t}{z_t} - 1 \right) (\sigma + \sigma_t^q) \end{aligned}$$

Proof: The law of motion of wealth for the households and the experts are given by equation (61). Using the law of large numbers to aggregate the wealth of individual

household and expert, we get

$$\begin{aligned}\frac{dW_{h,t}}{W_{h,t}} &= \left(r_t - \frac{C_{h,t}}{W_{h,t}} - \lambda_d + \frac{1 - \chi_t \psi_t}{1 - z_t} (\mu_{h,t}^R - r_t) + \frac{(1 - \bar{z})\lambda_d}{1 - z_t} \right) dt + \frac{1 - \chi_t \psi_t}{1 - z_t} (\sigma + \sigma_t^q) dZ_t \\ \frac{dW_{e,t}}{W_{e,t}} &= \left(r_t - \frac{C_{e,t}}{W_{e,t}} - \lambda_d + \frac{\chi_t \psi_t}{z_t} \zeta_{e,t} (\sigma + \sigma_t^q) + \frac{\bar{z}\lambda_d}{z_t} \right) dt + \frac{\chi_t \psi_t}{z_t} (\sigma + \sigma_t^q) dZ_t\end{aligned}$$

where $W_{h,t} = \int_{j \in H} w_{j,t} dj$ and $W_{e,t} = \int_{j \in E} w_{j,t} dj$ denotes the aggregated wealth among respective group. Similar to the stochastic productivity model, the volatility terms $\frac{\chi_t \psi_t}{z_t} (\sigma + \sigma_t^q)$ and $\frac{1 - \chi_t \psi_t}{1 - z_t} (\sigma + \sigma_t^q)$ can be derived using the definitions of z_t, ψ_t and the market clearing condition $\sigma_{w_{e,t}} z_t (\sigma + \sigma_t^q) + \sigma_{w_{h,t}} (1 - z_t) (\sigma + \sigma_t^q) = (\sigma + \sigma_t^q)$. By Ito's lemma, the dynamics of the wealth share becomes

$$\frac{dz_t}{z_t} = \frac{dW_{e,t}}{W_{e,t}} - \frac{d(q_t K_t)}{q_t K_t} + \frac{d\langle q_t K_t, q_t K_t \rangle}{(q_t K_t)^2} - \frac{d\langle q_t K_t, W_{e,t} \rangle}{(q_t K_t W_{e,t})}$$

where

$$\frac{d(q_t K_t)}{q_t K_t} = ((\chi_t \zeta_{e,t} + (1 - \chi_t) \zeta_{h,t}) (\sigma + \sigma_t^q) - \frac{(a_e - \iota_t)}{q_t} + r_t) dt + (\sigma + \sigma_t^q) dZ_t$$

and the result follows from here after some algebra. ■

The expression for the wealth share dynamics is similar to the model with stochastic productivity except that only the price of risk for capital shock matters, and the exit rate τ_t disappears from the drift. The solution methodology is also the same as before where equilibrium policies are determined in the static inner step and the value function is solved in the outer time step by solving a couple of PDEs. I use an implicit finite difference method with up-winding to solve the PDEs. The up-winding preserves the monotonicity of the PDEs and helps achieve convergence. In section C.4.1, I show that the solution to the PDEs obtained using the finite difference method is the same as the solution obtained from the neural network method.

C.1.1 Asset pricing conditions

The expected return that the experts earn from investing in the capital is given by

$$dr_t^v = (\mu_{e,t}^R - (1 - \chi_t) \epsilon_{h,t}) dt + \chi_t (\sigma_t^{q,k} + \sigma) dZ_t^k$$

where $\epsilon_{h,t} = \zeta_{h,t}(\sigma_t^q + \sigma)$. That is, $(1 - \chi_t)\epsilon_{h,t}$ is the part of the expected excess return that is paid by the experts to the outside equity holders, which is netted out. Consider a trading strategy of investing \$1 into the capital at time 0. Denoting v_t as the value of this investment strategy at time t , we have $\frac{dv_t}{v_t} = dr_t^v$, and

$$\frac{d(\xi_e v_t)}{\xi_e v_t} = (-r_t + \mu_{e,t}^R - (1 - \chi_t)\epsilon_{h,t} - \chi_t \epsilon_{e,t})dt + \text{diffusion terms}$$

where $\epsilon_{e,t} = \zeta_{e,t}(\sigma + \sigma_t^q)$, and $\xi_{e,t}$ follows the process in (58). Since $\xi_e v_t$ is a martingale, the drift equals to zero, which implies $\mu_{e,t}^R - r_t = \chi_t \epsilon_{e,t} + (1 - \chi_t)\epsilon_{h,t}$. It follows similarly for the households with the difference that since they do not issue outside equity, their asset pricing condition is $\mu_{h,t}^R - r_t = \epsilon_{h,t}$ \blacksquare

While the quantitative analysis of the benchmark model in main text assumes that agents have recursive utility and IES=1, I present and solve the model for a broader range of preference specifications. I consider four different types of utility functions. Let

$$f(c_{j,s}, U_{j,s}) = \begin{cases} \rho_j \log(c_{j,t}) - \rho_j U_{j,t} & \text{if } \gamma_j = 1, \varrho_j = 1 \\ \frac{c_{j,t}^{1-\gamma_j}}{1-\gamma_j} - \rho_j U_{j,t} & \text{if } \gamma_j = \varrho_j^{-1} \neq 1 \\ (1 - \gamma_j) \rho_j U_{j,t} \left(\log(c_{j,t}) - \frac{1}{1-\gamma_j} \log((1 - \gamma_j) U_{j,t}) \right) & \text{if } \gamma_j \neq 1, \varrho_j = 1 \\ \frac{1-\gamma_j}{1-\frac{1}{\varrho_j}} U_{j,t} \left[\left(\frac{c_{j,t}}{((1-\gamma_j) U_{j,t})^{1/(1-\gamma_j)}} \right)^{1-\frac{1}{\varrho_j}} - \rho_j \right] & \text{if } \gamma_j \neq 1, \varrho_j \neq 1 \end{cases} \quad (63)$$

I allow for preference heterogeneity in risk aversion and discount rate for generality. I solve for a Markov equilibrium in the state variable $z_t \in (0,1)$ for a representative household and expert by aggregating all agents within their respective group.

Proposition 5. *The optimal consumption policy and price of risk are given by*

$$\hat{C}_{e,t} = \begin{cases} \rho_e & \text{if (log or Recursive (IES=1))} \\ J_{e,t}^{-1/\gamma_e} (z_t q_t)^{\frac{1-\gamma_e}{\gamma_e}} & \text{if CRRA} \\ \frac{J_{e,t}^{\frac{1-\varrho_j}{1-\gamma_e}}}{(z_t q_t)^{1-\varrho_j}} & \text{if Recursive (IES} \neq 1) \end{cases} \quad (64)$$

$$\hat{C}_{h,t} = \begin{cases} \rho_h & \text{if (log or Recursive (IES=1))} \\ J_{h,t}^{-1/\gamma_h} ((1-z_t)q_t)^{\frac{1-\gamma_h}{\gamma_h}} & \text{if CRRA} \\ \frac{J_{h,t}^{\frac{1-\varrho_j}{1-\gamma_h}}}{((1-z_t)q_t)^{1-\varrho_j}} & \text{if Recursive (IES} \neq 1) \end{cases} \quad (65)$$

$$\zeta_{e,t} = \begin{cases} \frac{\chi_t \psi_t}{z_t} (\sigma + \sigma_t^q) & \text{if log} \\ -\sigma_{e,t}^J + \sigma_t^z + \sigma_t^q + \gamma_e \sigma & \text{if (CRRA or Recursive)} \end{cases} \quad (66)$$

$$\zeta_{h,t} = \begin{cases} \frac{(1-\chi_t \psi_t)}{1-z_t} (\sigma + \sigma_t^q) & \text{if log} \\ -\sigma_{h,t}^J - \frac{z_t}{1-z_t} \sigma_t^z + \sigma_t^q + \gamma_h \sigma & \text{if (CRRA or Recursive)} \end{cases} \quad (67)$$

Proof: The HJB equation is given by

$$\sup_{c,K} f(c_{j,t}, U_{j,t}) + E[dU_{j,t}] = 0 \quad (68)$$

I consider three cases of utility functions separately.

(a) Log utility The value function conjecture takes a logarithmic form

$$U_{j,t} = \log K_t + J_{j,t}(z_t) = \log W_{j,t} + \tilde{J}_{j,t}$$

and where the second equality follows from $z_t = \frac{W_{e,t}}{q_t K_t} = 1 - \frac{W_{h,t}}{q_t K_t}$. Also, $f(C_{j,t}, U_{j,t}) = \rho_j \log(C_{j,t}) - \rho_j U_{j,t}$. The value function derivatives are

$$\frac{\partial U_{j,t}}{\partial W_{j,t}} = \frac{dW_{j,t}}{W_{j,t}}; \quad \frac{\partial^2 U_{j,t}}{\partial W_{j,t}^2} = -\frac{d\langle W_{j,t}, W_{j,t} \rangle}{W_{j,t}^2}; \quad \frac{\partial U_{j,t}}{\partial \tilde{J}_{j,t}} = 1; \quad \frac{\partial^2 U_{j,t}}{\partial \tilde{J}_{j,t}^2} = \frac{\partial^2 \tilde{J}_{j,t}}{\partial \tilde{J}_{j,t}^2 \partial W_{j,t}} = 0$$

Applying Ito's lemma and using the HJB, we get

$$\sup_{C, \theta_{j,t}} \rho_j \log C_{j,t} - \rho(\log W_{j,t} + \tilde{J}_{j,t}) + r_t - \frac{C_{j,t}}{W_{j,t}} + \theta_{j,t}(\sigma + \sigma_t^q) \zeta_{j,t} - \frac{1}{2} \theta_{j,t}^2 (\sigma + \sigma_t^q)^2 + \mu_t^{\tilde{J}} = 0$$

where $\theta_{e,t} = \frac{\chi_t \psi_t}{z_t}$ and $\theta_{h,t} = \frac{1 - \chi_t \psi_t}{1 - z_t}$. Taking the first order conditions, we get the following result for log utility.

$$\hat{c}_{j,t} = \rho_j \quad (69)$$

$$\zeta_{e,t} = \frac{\chi_t \psi_t}{z_t} (\sigma + \sigma_t^q) \quad (70)$$

$$\zeta_{h,t} = \frac{1 - \chi_t \psi_t}{1 - z_t} (\sigma + \sigma_t^q) \quad (71)$$

(b) CRRA Utility The value function conjecture is

$$U_{j,t} = J_{j,t}(z_t) \frac{K_t^{1-\gamma_j}}{1 - \gamma_j}$$

where $J_{j,t}$ follows the stochastic differential equation $\frac{dJ_{j,t}}{J_{j,t}} = \mu_{j,t}^J dt + \sigma_{j,t}^J dZ_t$ whose drift and volatility needs to be determined in the equilibrium. The HJB equation is derived directly in terms of the capital k_t instead of the wealth share z_t . The value function derivatives are

$$\begin{aligned} \frac{\partial U_{j,t}}{\partial J_{j,t}} &= \frac{K_t^{1-\gamma_j}}{1 - \gamma_j}; \quad \frac{\partial U_{j,t}}{\partial K_t} = J_{j,t} K_t^{-\gamma_j} \\ \frac{\partial^2 U_{j,t}}{\partial J_{j,t}^2} &= 0; \quad \frac{\partial^2 U_{j,t}}{\partial K_t^2} = -\gamma_j J_{j,t} K_t^{-(1+\gamma_j)}; \quad \frac{\partial^2 U_{j,t}}{\partial J_{j,t} \partial K_t} = K_t^{-\gamma_j} \end{aligned} \quad (72)$$

Applying Ito's lemma and using HJB, we get

$$\begin{aligned} \sup_{C, K} & -\rho \frac{J_{j,t} K_t^{1-\gamma_j}}{1 - \gamma_j} + \frac{C_t^{1-\gamma_j}}{1 - \gamma_j} + \frac{J_{j,t} K_t^{1-\gamma_j}}{1 - \gamma_j} \mu_{j,t}^J + J_{j,t} K_t^{1-\gamma_j} (\Phi(\iota_t) - \delta) \\ & - \sigma^2 \frac{\gamma_j}{2} J_{j,t} K_t^{1-\gamma_j} + J_{j,t} K_t^{1-\gamma_j} \sigma \sigma_{j,t}^J = 0 \end{aligned} \quad (73)$$

At the optimum, the marginal utilities of consumption and wealth become equal. Rewriting the value function in terms of the wealth and using the mapping $q_t k_t = \frac{W_{e,t}}{z_t} = \frac{W_{h,t}}{1 - z_t}$,

we get the equilibrium consumption-wealth ratio

$$\frac{C_{e,t}}{W_{e,t}} = \frac{(z_t q_t)^{\frac{1-\gamma_e}{\gamma_e}}}{J_{e,t}^{\frac{1}{\gamma_e}}}; \quad \frac{C_{h,t}}{W_{h,t}} = \frac{((1-z_t)q_t)^{\frac{1-\gamma_h}{\gamma_h}}}{J_{h,t}^{\frac{1}{\gamma_h}}} \quad (74)$$

The risk premium of the experts and the households can be derived from the stochastic discount factor which is given by

$$\xi_{j,t} = \xi_{j,0} e^{-\rho_j t} \left(\frac{C_{j,t}}{C_{j,0}} \right)^{-\gamma_j}$$

This gives a relationship between the volatility of SDF and consumption: $\sigma_{j,t}^\xi = -\gamma_j \sigma_{j,t}^c$. The consumption-capital ratio for the households and the experts is given by $\frac{C_{h,t}}{K_t} = \frac{((1-z_t)q_t)^{1/\gamma_h}}{J_{h,t}^{1/\gamma_h}}$ and $\frac{C_{e,t}}{K_t} = \frac{(z_t q_t)^{1/\gamma_e}}{J_{e,t}^{1/\gamma_e}}$. Combining this with the differential equation for SDF

$$\frac{d\xi_{j,t}}{\xi_{j,t}} = -r_t dt - \zeta_{j,t} dZ_t$$

we get

$$\zeta_{e,t} = \gamma_e \sigma_{e,t}^c = -\sigma_{e,t}^J + \sigma_t^z + \sigma_t^q + \gamma_e \sigma; \quad \zeta_{h,t} = \gamma_h \sigma_{h,t}^c = -\sigma_{h,t}^J - \frac{z_t}{1-z_t} \sigma_t^z + \sigma_t^q + \gamma_h \sigma \quad (75)$$

Plugging in the optimal consumption-wealth ratio from (74) into HJB equation (73), we get the expressions for $\mu_{j,t}^J$

$$\mu_{e,t}^J = \rho_e - \frac{(z_t q_t)^{\frac{1-\gamma_e}{\gamma_e}}}{J_{e,t}^{1/\gamma_e}} - (1-\gamma_e)(\Phi(\iota_t) - \delta - \frac{\gamma_e}{2} \sigma^2 + \sigma_{e,t}^J \sigma) \quad (76)$$

$$\mu_{h,t}^J = \rho_e - \frac{((1-z_t)q_t)^{\frac{1-\gamma_h}{\gamma_h}}}{J_{h,t}^{1/\gamma_h}} - (1-\gamma_h)(\Phi(\iota_t) - \delta - \frac{\gamma_h}{2} \sigma^2 + \sigma_{h,t}^J \sigma) \quad (77)$$

(c) Recursive Utility (IES=1) The value function conjecture is the same as that of CRRA utility, and $f(C_{j,t} U_{j,t}) = (1-\gamma_j) \rho_j U_{j,t} \left(\log C_{j,t} - \frac{1}{1-\gamma_j} \log((1-\gamma_j) U_{j,t}) \right)$. Plugging in the conjecture for value function in HJB equation (33) and applying Ito's lemma⁵⁹,

⁵⁹The value function derivatives are the same as in the CRRA case given by (72).

we get

$$\begin{aligned} \sup_{C,K} \quad & \rho J_{j,t} K_t^{1-\gamma_j} \left[\log \frac{C_{j,t}}{W_{j,t}} - \frac{1}{1-\gamma_j} \log J_{j,t} + \log(q_t z_t) \right] + J_{j,t} \frac{K_t^{1-\gamma_j}}{1-\gamma_j} \mu_{j,t}^J \\ & + J_{j,t} K_t^{1-\gamma_j} (\Phi(\iota_t) - \delta) - J_{j,t} K_t^{1-\gamma_j} \frac{1}{2} \gamma_j \sigma^2 + J_{j,t} K_t^{1-\gamma_j} \sigma \sigma_{j,t}^J = 0 \end{aligned} \quad (78)$$

As before, at the optimum, the marginal utilities of the wealth and the consumption become equal. Using the value function expression in terms of wealth, we have

$$\begin{aligned} \frac{\partial U_{j,t}}{\partial W_{j,t}} &= \frac{\partial f}{\partial C_{j,t}} \\ \tilde{J}_{j,t} W_{j,t}^{-\gamma_j} &= (1-\gamma_j) \rho_j \frac{U_{j,t}}{C_{j,t}} \implies \frac{C_{j,t}}{W_{j,t}} = \rho_j \end{aligned}$$

The stochastic discount factor for recursive utility is given by

$$\xi_{j,t} = \exp \left(\int_0^t \frac{\partial f(C_{j,s}, U_{j,s})}{\partial U} ds \right) \frac{\partial U_{j,t}}{\partial W_{j,t}}$$

Writing the value function conjecture in terms of the wealth instead of the capital, we have

$$U_{j,t} = \tilde{J}_{j,t} \frac{W_{j,t}^{1-\gamma_j}}{1-\gamma_j}; \quad f(C_{j,t}, U_{j,t}) = (1-\gamma_j) \rho_j U_{j,t} \left(\log \rho_j - \frac{1}{1-\gamma_j} \tilde{J}_{j,t} \right)$$

where $\tilde{J}_{j,t} = \frac{J_{j,t}}{(q_t z_t)^{1-\gamma_j}}$. The SDF then becomes

$$\xi_{j,t} = (1-\gamma_j) \exp \left(\int_0^t \left[\rho_j ((1-\gamma_j) \log C_{j,s} - \log((1-\gamma_j) U_{j,s}) - 1) \right] ds \right) \frac{U_{j,t}}{W_{j,t}}$$

This implies that $\sigma(\xi_{j,t}) = \sigma \left(\frac{U_{j,t}}{W_{j,t}} \right)$. Computing the R.H.S and using

$$\frac{d\xi_{j,t}}{\xi_{j,t}} = -r_t dt - \zeta_{j,t} dZ_t$$

we get the desired result. Plugging in the consumption-wealth ratio and the market price of risk into the HJB equation (78), we obtain the expressions for $\mu_{j,t}^J$

$$\mu_{e,t}^J = (\gamma_e - 1)(\rho_e \log \rho_e + \log(q_t z_t)) + \rho_e \log J_{e,t} - (1 - \gamma_e)(\Phi(\iota_t) - \delta - \frac{\gamma_e}{2} \sigma^2 + \sigma \sigma_{e,t}^J) \quad (79)$$

$$\mu_{h,t}^J = (\gamma_h - 1)(\rho_h \log \rho_h + \log(q_t(1 - z_t))) + \rho_h \log J_{h,t} - (1 - \gamma_h)(\Phi(\iota_t) - \delta - \frac{\gamma_h}{2} \sigma^2 + \sigma \sigma_{h,t}^J) \quad (80)$$

(d) Recursive Utility (IES different from unity) The optimization problem is

$$\sup_{C_{j,t}, \theta_{j,t}, \iota_t} f(C_{j,t}, U_{j,t}) + E[dU_{j,t}] = 0$$

where

$$f(c_{j,t}, U_{j,t}) = \frac{1 - \gamma_j}{1 - \frac{1}{\varrho_j}} U_{j,t} \left[\left(\frac{C_{j,t}}{((1 - \gamma_j) U_{j,t})^{1/(1 - \gamma_j)}} \right)^{1 - \frac{1}{\varrho_j}} - \rho_j \right]$$

where ϱ_j denotes the IES parameter. The conjecture for the value function is

$$U_{j,t} = J_{j,t}(z_t) \frac{K_t^{1 - \gamma_j}}{1 - \gamma_j}$$

where $J_{j,t}$ follows the stochastic differential equation $\frac{dJ_{j,t}}{J_{j,t}} = \mu_{j,t}^J dt + \sigma_{j,t}^J dZ_t$ whose drift and volatility needs to be determined in the equilibrium.⁶⁰

As before, the HJB equation is derived directly in terms of the capital K_t instead of the wealth share z_t . Applying Ito's lemma and using the HJB, we get

$$\begin{aligned} \sup_{c,K} \quad & \frac{1}{1 - \frac{1}{\varrho_j}} \left(\frac{C_{j,t}^{1 - \frac{1}{\varrho_j}}}{J_{j,t}^{\frac{1 - \frac{1}{\varrho_j}}{1 - \gamma_j}} K_t^{1 - \frac{1}{\varrho_j}}} - \rho_j \right) J_{j,t} K_t^{1 - \gamma_j} + \frac{J_{j,t} K_t^{1 - \gamma_j}}{1 - \gamma_j} \mu_{j,t}^J + J_{j,t} K_t^{1 - \gamma_j} (\Phi(\iota_t) - \delta) \\ & - \sigma^2 \frac{\gamma_j}{2} J_{j,t} K_t^{1 - \gamma_j} + J_{j,t} K_t^{1 - \gamma_j} \sigma \sigma_{j,t}^J = 0 \end{aligned} \quad (81)$$

At the optimum, the marginal utilities of the consumption and the wealth become equal. Rewriting the value function in terms of the wealth and using the mapping $q_t K_t = \frac{W_{e,t}}{z_t} =$

⁶⁰Since the value function conjecture is the same as in CRRA case, the value function derivatives are given by (72).

$\frac{W_{h,t}}{1-z_t}$, we have

$$\begin{aligned}\frac{\partial f_{e,t}}{\partial C_{e,t}} &= C_{e,t}^{-\frac{1}{\varrho_e}} J_{e,t}^{\frac{1}{\varrho_e}-\gamma_e} (z_t q_t)^{\gamma_j-\frac{1}{\varrho_e}} \\ \frac{\partial f_{h,t}}{\partial C_{h,t}} &= C_{h,t}^{-\frac{1}{\varrho_h}} J_{h,t}^{\frac{1}{\varrho_h}-\gamma_h} ((1-z_t)q_t)^{\gamma_j-\frac{1}{\varrho_h}} \\ \frac{\partial U_{e,t}}{\partial W_{e,t}} &= \frac{J_{e,t}}{(z_t q_t)^{1-\gamma_e}} W_{e,t}^{1-\gamma_e} \\ \frac{\partial U_{h,t}}{\partial W_{h,t}} &= \frac{J_{h,t}}{((1-z_t)q_t)^{1-\gamma_h}} W_{h,t}^{1-\gamma_h}\end{aligned}$$

Equating the marginal values, we get the respective optimal consumption-wealth ratios

$$\frac{C_{e,t}}{W_{e,t}} = \frac{J_{e,t}^{\frac{1-\varrho_e}{1-\gamma_e}}}{(z_t q_t)^{1-\varrho_e}}; \quad \frac{C_{h,t}}{W_{h,t}} = \frac{J_{h,t}^{\frac{1-\varrho_h}{1-\gamma_h}}}{((1-z_t)q_t)^{1-\varrho_h}} \quad (82)$$

The stochastic discount factor for recursive utility is given by

$$\xi_{j,t} = \exp\left(\int_0^t \frac{\partial f(C_{j,s}, U_{j,s})}{\partial U} ds\right) \frac{\partial U_{j,t}}{\partial w_{j,t}}$$

Writing the value function conjecture in terms of the wealth instead of the capital, we have

$$U_{j,t} = \tilde{J}_{j,t} \frac{W_{j,t}^{1-\gamma_j}}{1-\gamma_j}; \quad f(C_{j,t}, U_{j,t}) = \frac{\tilde{J}_{j,t} W_{j,t}^{1-\gamma_j}}{1-\frac{1}{\varrho_j}} \left[\left(\frac{C_{j,t}}{W_{j,t}} \right)^{1-\frac{1}{\varrho_j}} \tilde{J}_{j,t}^{\frac{1-\frac{1}{\varrho_j}}{\gamma_j-1}} - \rho_j \right]$$

where $\tilde{J}_{j,t} = \frac{J_{j,t}}{(q_t z_t)^{1-\gamma_j}}$. Plugging in the above expression in the stochastic discount factor, we notice that $\sigma(\xi_{j,t}) = \sigma\left(\frac{U_{j,t}}{W_{j,t}}\right)$. Computing the R.H.S and using

$$\frac{d\xi_{j,t}}{\xi_{j,t}} = -r_f dt - \zeta_{j,t} dZ_t$$

we get the following result.

$$\zeta_{e,t} = -\sigma_{e,t}^J + \sigma_t^z + \sigma_t^q + \gamma_e \sigma \quad (83)$$

$$\zeta_{h,t} = -\sigma_{h,t}^J - \frac{z_t}{1-z_t} \sigma_t^z + \sigma_t^q + \gamma_h \sigma \quad (84)$$

Substituting the consumption-wealth ratio into the HJB equation (81), we the expression

for $\mu_{j,t}^J$

$$\begin{aligned}\mu_{e,t}^J &= \frac{(\gamma_e - 1)}{1 - \frac{1}{\varrho_e}} \left((q_t z_t)^{\varrho_e - 1} J_{e,t}^{\frac{1-\varrho_e}{1-\gamma_e}} - \rho_e \right) - (1 - \gamma_e)(\Phi(l_t) - \delta - \frac{\gamma_e}{2}\sigma^2 + \sigma\sigma_{e,t}^J) \\ \mu_{h,t}^J &= \frac{(\gamma_h - 1)}{1 - \frac{1}{\varrho_h}} \left((q_t(1 - z_t))^{\varrho_h - 1} J_{h,t}^{\frac{1-\varrho_h}{1-\gamma_h}} - \rho_h \right) - (1 - \gamma_h)(\Phi(l_t) - \delta - \frac{\gamma_h}{2}\sigma^2 + \sigma\sigma_{h,t}^J)\end{aligned}\quad (85)$$

This proves the proposition. ■

C.2 Numerical solution method

C.2.1 Model solution: Log utility

I rely on the solution technique from BS2016 and [Hansen, Khorrami and Tourre \(2018\)](#) that solves the partial differential equations using an up-winding finite difference scheme. The method involves a static inner loop that solves for the equilibrium quantities $\{\psi_t, (\sigma_{q,t} + \sigma), q_t\}$, and an outer loop that updates the value function from $J_{j,t+\Delta t}$ to $J_{j,t}$ using a finite difference method, similar to the model with stochastic productivity.

Static step: To solve for the quantities in inner loop, three equations are required. The first equation is given by subtracting the portfolio choices of the households and the experts. That is, we have

$$(\theta_{e,t} - \theta_{h,t})(\sigma_t^q + \sigma)^2 = \mu_{e,t}^R - (\mu_{h,t}^R)$$

Plugging in the expressions for $\mu_{e,t}^R, \mu_{h,t}^R$ from the return process (57), and using $\theta_{e,t} = \frac{\chi_t \psi_t}{z_t}$ as well as from the capital market clearing condition $\theta_{h,t} = \frac{1 - \chi_t \psi_t}{1 - z_t}$, we get

$$\frac{\underline{\chi} \psi_t - z_t}{z_t(1 - z_t)} (\sigma_t^q + \sigma)^2 = \frac{a_e - a_h}{q_t} \quad (86)$$

Note that $\underline{\chi}$ is used in place of χ_t because of similar reasoning as in the model of stochastic productivity. When the wealth share z_t is low, the experts issue maximum equity possible to the households since their expected rate of return is much higher than that

of households. The second equation comes from the goods market clearing condition

$$(z_t \hat{c}_{e,t} + (1 - z_t) \hat{c}_{h,t}) q_t = \psi_t (a_e - \iota_t) + (1 - \psi_t) (a_h - \iota_t) \quad (87)$$

where $\iota_t = \frac{q_t - 1}{\kappa}$. For the third equation, apply Ito's lemma to $q(z_t)$ and match the drift and the volatility terms to get $\sigma_t^q = \frac{\partial q_t}{\partial z_t} \frac{1}{q} \sigma_t^z$. Combining this with the volatility of wealth share, we get

$$\sigma_t^q + \sigma = \frac{\sigma}{1 - \frac{\partial q_t}{\partial z_t} \frac{1}{q} \left(\frac{\chi_t \psi_t}{z_t} - 1 \right)} \quad (88)$$

Equations (86), (87), and (88) are solved using the Newton-Raphson method⁶¹ yielding $\{\psi_t, (\sigma_{q,t} + \sigma), q_t\}$. Similar to Brunnermeier and Sannikov (2016), there are three regions in the state space. In the first region, the risk premium of the households is lower than that of the experts and hence the experts issue maximum outside equity (i.e., $\chi_t = \underline{\chi}_t$). In the second region, the experts hold all capital ($\psi_t = 1$) but their risk premium is still larger than that of households and hence $\chi_t = \underline{\chi}$. In the third region, perfect risk sharing is achieved between the experts and households by setting $\chi_t = z_t$. In the case of log utility, the static step is enough to compute the equilibrium policies since the consumption-wealth share is equal to the discount rate and the capital share is not dependent on $J_{j,t}$.

C.2.2 Model solution: CRRA and Recursive utility

The portfolio choice in the case of CRRA and recursive utility includes the hedging demand that needs to be taken into account. From equations (59) and (60), we get

$$\frac{a_e - a_h}{q_t(\sigma + \sigma_t^q)} \geq \underline{\chi}(\zeta_{e,t} - \zeta_{h,t})$$

⁶¹BS2016 and Hansen, Khorrami and Tourre (2018) provide details of the algorithm. The state space is segmented into the crisis region and the normal region. The static step is solved for iteratively until the system enters the crisis region in which case the capital share ψ is set to 1 and the remaining quantities (q_t, σ_t^q) are solved for using equations (87) and (88).

with equality if $\psi_t = 1$. Plugging in the expressions for $\zeta_{e,t}$ and $\zeta_{h,t}$ from proposition (5), we have

$$\begin{aligned}\frac{a_e - a_h}{q_t} &= \underline{\chi} \left(\frac{1}{J_{h,t}} \frac{\partial J_{h,t}}{\partial z_t} - \frac{1}{J_{e,t}} \frac{\partial J_{e,t}}{\partial z_t} + \frac{1}{z_t(1-z_t)} \right) (\chi \psi_t - z_t)(\sigma + \sigma_t^q)^2 \\ \frac{a_e - a_h}{q_t} &= \underline{\chi} \left(\sigma_{h,t}^J - \sigma_{e,t}^J + \frac{\sigma_t^z}{1-z_t} \right) (\sigma + \sigma_t^q)\end{aligned}$$

where the second expression comes from using the dynamics of the wealth share (62).⁶² The goods market clearing condition (87) and return volatility (88) remain the same. Similar to the case of log utility, the Newton-Raphson method is used to solve for the $\{\psi_t, q_t, (\sigma + \sigma_t^q)\}$. Given these equilibrium functions, $J_{j,t}$ needs to be solved for, which is done in the dynamic time step.

Time step: Applying Ito's lemma to $J_{j,t}(z_t)$, matching the drift terms, and augmenting the resulting coupled PDEs with a time step (falst-transient method), we get

$$\mu_{h,t}^J J_{h,t} = \frac{\partial J_{h,t}}{\partial z_t} \mu_t^z + \frac{1}{2} \frac{\partial^2 J_{h,t}}{\partial z_t^2} (\sigma_t^z)^2 \quad (89)$$

$$\mu_{e,t}^J J_{e,t} = \frac{\partial J_{e,t}}{\partial z_t} \mu_t^z + \frac{1}{2} \frac{\partial^2 J_{e,t}}{\partial z_t^2} (\sigma_t^z)^2 \quad (90)$$

The coefficients μ_t^z and σ_t^z can be computed from the equilibrium quantities in the static step and $\mu_{j,t}^J$ is computed from the equations in (79). The PDEs are solved using an implicit method with an up-winding scheme explained in the next part.

C.2.3 Up-winding scheme

The PDEs (89) are solved by considering artificial time-derivatives. To be specific, the modified system

$$0 = \frac{\partial J_{h,t}}{\partial t} - \mu_{h,t}^J J_{h,t} + \frac{\partial J_{h,t}}{\partial z_t} \mu_t^z + \frac{1}{2} \frac{\partial^2 J_{h,t}}{\partial z_t^2} (\sigma_t^z)^2 \quad (91)$$

$$0 = \frac{\partial J_{e,t}}{\partial t} - \mu_{e,t}^J J_{e,t} + \frac{\partial J_{e,t}}{\partial z_t} \mu_t^z + \frac{1}{2} \frac{\partial^2 J_{e,t}}{\partial z_t^2} (\sigma_t^z)^2 \quad (92)$$

⁶²Note that by Ito's lemma, we have $\sigma_{j,t} = \frac{1}{J_{j,t}} \frac{\partial J_{j,t}}{\partial z_t} \sigma_t^z = \frac{1}{J_{j,t}} \frac{\partial J_{j,t}}{\partial z_t} (\theta_{e,t} - 1)(\sigma + \sigma_t^q)^2$

is solved backwards in time with the corresponding terminal conditions $(J_{h,T}, J_{e,T})$. Consider a general quasi-linear PDE of the form

$$A\left(z, g, \frac{\partial g}{\partial z}\right) + tr\left[B\left(z, g, \frac{\partial g}{\partial z}\right) \frac{\partial^2 g}{\partial z^2} B\left(z, g, \frac{\partial g}{\partial z}\right)'\right] + \frac{\partial g}{\partial t} = 0$$

Consider a two-dimensional grid of size N_z and N_t with step sizes Δ_i and Δ_j respectively where $\{i\}_1^{N_z}, \{j\}_1^{N_t}$ denote the dimensions for space and time respectively. The function $g(z_t, t)$ evaluated at (i, j) is denoted as $g_{i,j}$. The derivatives of the function are discretized as

$$\begin{aligned}\frac{\hat{\partial} g_{i,j}}{\hat{\partial} z} &= (\mu_j^z)^+ \frac{g_{i+1,j} - g_{i,j}}{\Delta_i} + (\mu_j^z)^- \frac{g_{i,j} - g_{i-1,j}}{\Delta_i} \\ \frac{\hat{\partial}^2 g_{i,j}}{\hat{\partial} z^2} &= \frac{g_{i+1,j} - 2g_{i,j} + g_{i-1,j}}{\Delta_i^2} \\ \frac{\hat{\partial} g_{i,j}}{\hat{\partial} t} &= \frac{g_{i,j+1} - g_{i,j}}{\Delta_j}\end{aligned}$$

where

$$(\mu_j^z)^+ = \begin{cases} \mu_t^z & \text{if } \mu_t^z > 0 \\ 0 & \text{if otherwise} \end{cases} \quad (\mu_j^z)^- = \begin{cases} \mu_t^z & \text{if } \mu_t^z < 0 \\ 0 & \text{if otherwise} \end{cases}$$

Discretizing the derivatives at $j + 1$ and applying it to the PDE, we get

$$g_{i,j+1} = g_{i,j} + \Delta_j \left\{ A\left(z, g_{i,j+1}, \frac{\hat{\partial} g_{i,j+1}}{\hat{\partial} z}\right) + tr\left[B\left(z, g_{i,j+1}, \frac{\hat{\partial} g_{i,j+1}}{\hat{\partial} z}\right) \frac{\hat{\partial}^2 g_{i,j+1}}{\hat{\partial} z^2} B\left(z, g_{i,j+1}, \frac{\hat{\partial} g_{i,j+1}}{\hat{\partial} z}\right)'\right] \right\}$$

Solving for $g_{i,j+1}$ requires solving a linear system of equations which can be done using a standard procedure such as the Richardson method. The up-winding scheme ensures monotonicity of the numerical scheme (see [D'Avernas and Vandeweyer \(2019\)](#)). Since the method is implicit, a large time step can be set which considerably reduces the computation time.

	Description	Symbol	Value
Technology / Preferences	Volatility of output	σ	0.06
	Discount rate (experts)	ρ_e	0.06
	Discount rate (households)	ρ_h	0.04
	Depreciation rate of capital	δ	0.02
	Investment cost	κ	10
	Productivity (experts)	a_e	0.11
	Productivity (households)	a_h	0.03
Utility	CRRA utility	γ_e, γ_h	[1, 15]
	Recursive utility	γ_e, γ_h	[1, 15]
Demographics	Mean proportion of experts	\bar{z}	0.10
	Turnover	λ_d	0.03
Friction	Equity retention	$\underline{\chi}$	0.5

Table 10: Calibrated parameters for the benchmark model. All values are annualized.

C.2.4 Equilibrium policies

The equilibrium plots for the benchmark model is given in Figure (11).

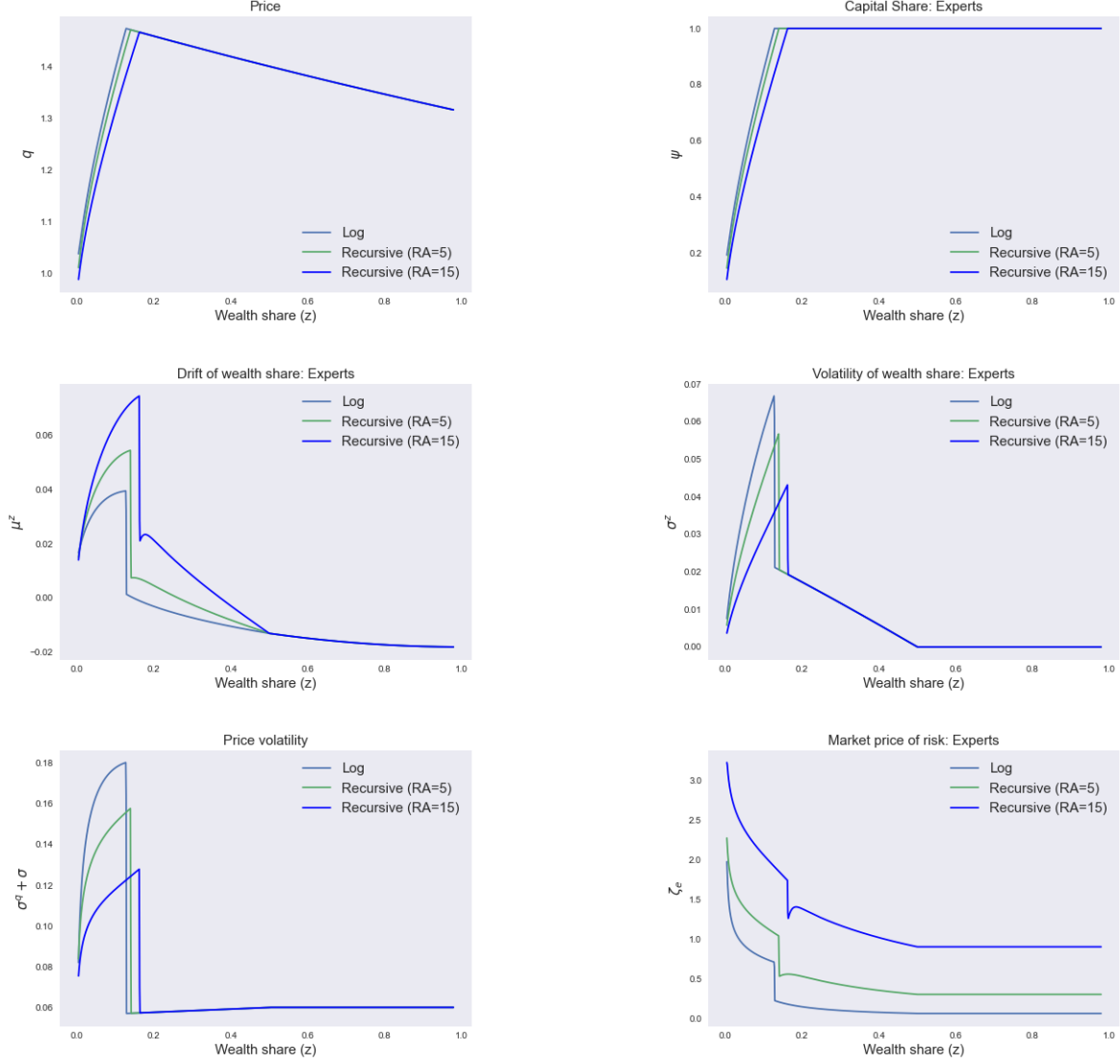


Figure 11: Equilibrium values as functions of state variable z_t . The recursive utility plots have IES equal to 1. Log utility has RA=1 by construction.

C.2.5 Numerical simulation

The state variable in the model is z_t whose law of motion is governed by the equation (62). Once the mapping between z_t and (μ_t^z, σ_t^z) are determined numerically from the previous section, we can simulate z_t using an Euler-Maruyama scheme. Specifically, the task is to simulate

$$dz_t = \mu_t^z dt + \sigma_t^z dZ_t$$

where the shock dZ_t is the standard Brownian motion. The law of motion is discretized as

$$z_{t+\Delta t} = z_t + \mu_z(z_t)\Delta t + \sigma_t^z(z_t) * \sqrt{\Delta t} Z$$

where $Z \sim N(0,1)$. The steps are as follows

1. Set z_0 to an arbitrary initial value, say 0.5.
2. Simulate Z from the standard normal distribution and compute $z_{t+\Delta t}$ using the discretized equation for $\Delta = 1/12$. The mapping between z_t and (μ_t^z, σ_t^z) is in a grid since it is solved for numerically and hence I use a spline interpolation to obtain the intermediate values.
3. Repeat the procedure for z_1, z_2, \dots and obtain $\{z_t\}_1^{60,000}$. That is, the simulation is done for 5000 years at monthly frequency.

The first 1000 years are eliminated so as to reduce the dependency on the initial condition. I experiment with different initial values to make sure that the obtained distribution is indeed stationary. The procedure is repeated for 1000 times and Figure (12) plots the resulting distributions.

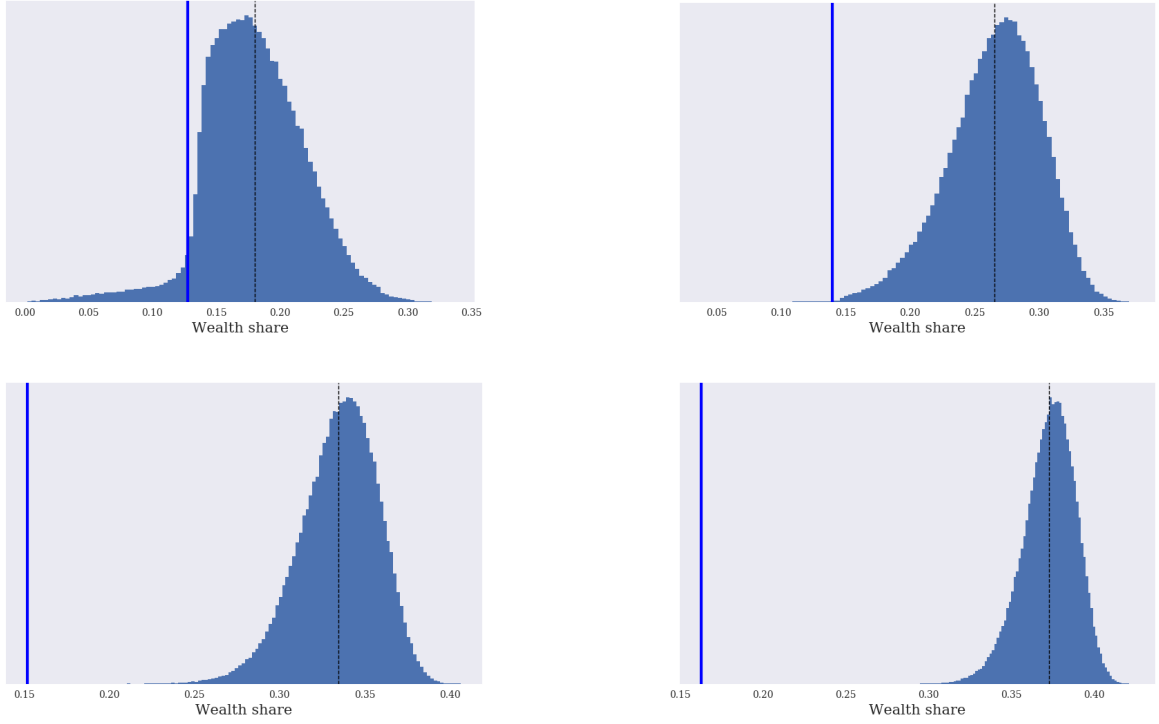


Figure 12: Stationary distribution of wealth share.

Figure 13: Plots (a), (b), (c), and (d) represent benchmark model with risk aversion parameter set to 1, 5, 10, and 20 respectively. The vertical blue line and the vertical dotted line represent the endogenous crisis boundary z^* and the steady state \hat{z} of the wealth share respectively.

Comparison with Fokker-Planck equation The density of wealth share $g(z_t, t)$ can be expressed in the form of Fokker-Planck (or Kolmogorov Forward Equation) equation

$$\frac{\partial g(z_t, t)}{\partial t} = -\frac{\partial}{\partial z_t}(\mu_t^z g(z_t, t)) + \frac{1}{2} \frac{\partial^2}{\partial z_t^2}((\sigma_t^z)^2 g(z_t, t))$$

We have $\lim_{z_t \rightarrow 0^+, z_t \rightarrow 1^-} \sigma_t^z = 0$ by construction and $(\lim_{z_t \rightarrow 0^+} \mu_t^z > 0, \lim_{z_t \rightarrow 1^-} \mu_t^z < 0)$ due to the overlapping generations assumption. This forces the distribution to be non-degenerate. Also, a stationary density implies that $\frac{\partial g}{\partial t} = 0$. Thus, we can integrate the Fokker-Planck equation to obtain

$$0 = \text{constant} - (\mu_t^z g(z_t)) + \frac{1}{2} \frac{\partial}{\partial z_t}((\sigma_t^z)^2 g(z_t))$$

I solve this equation numerically using an explicit finite difference scheme and compare it with the stationary distribution obtained through the simulation. Figure (14) shows that the density obtained from the simulation is a good approximation for the

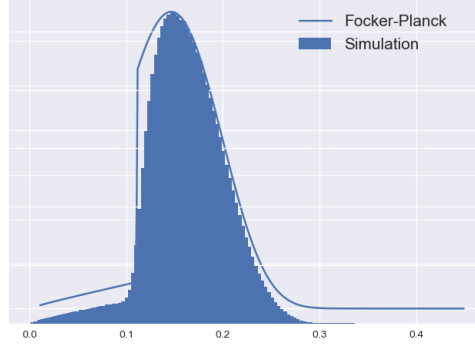


Figure 14: Comparison of the stationary density obtained from Fokker-Planck equation and the simulation for the benchmark model with $RA=1$.

theoretical density dictated by the Fokker-Planck equation. The simulated wealth share is annualized so as to make the comparison with the empirical data. The proportion of annualized wealth share that fall below the theoretically obtained crisis boundary z^* is taken to be the probability of crisis implied by the model. Table (11) presents the moments of equilibrium quantities obtained using the annualized wealth share

C.3 Other trade-offs in the benchmark model

One key quantity that governs the time spent in the crisis region is the drift of the wealth share. The parameter λ_d controls the death rate of experts which is necessary to ensure model stationarity. As the death rate increases, all else equal, the system stays in the crisis region longer. A similar effect is observed when the mean proportion of experts \bar{z} is decreased. Figure (15) presents the static comparison of the drift of the wealth share for different values of λ_d and \bar{z} . A higher death rate pushes the system into the crisis region by making the drift of wealth share more negative in the normal regime. However, there is only a minimal effect on the drift once the system enters the crisis region. The second panel varies the mean population share of experts by keeping the death rate fixed. As the population share decreases, the drift becomes more negative making the crisis more likely. Once the system enters the crisis region, the drift becomes less positive pushing the system back into the normal regime at a slower rate. Both of

these effects work towards increasing the frequency of crisis.

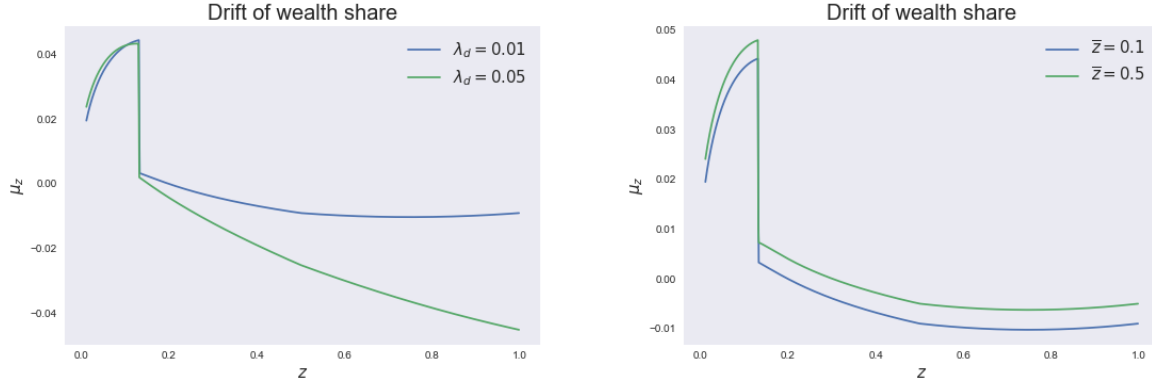


Figure 15: Left panel shows the drift of wealth share for two different values of death rate λ_d for \bar{z} fixed at 0.1. The second panel shows the drift of wealth share for two different values of mean expert population for λ_d fixed at 0.02. The risk aversion is set to 2 for both the plots.

Figure (16) shows the probability of crisis for several values of λ_d and \bar{z} for the recursive utility model with IES=1 and risk aversion equal to 2. To obtain a 7% probability of crisis, the population share of experts have to be less than 10%, with a death rate of 3%. Since the discount rate assumed in the model is inclusive of death rate, a 3% death rate means that the households do not discount at all. The second panel of Figure (16) reveals that changing the OLG parameters doesn't affect unconditional risk premium much. While it is possible to achieve a realistic probability of crisis and unconditional risk premium simultaneously, this comes at the cost of extremely high death risk, and more importantly, it still does not generate persistent recessions. This is because the duration of the crisis is unaffected by a high death risk and thus leads to a quick recovery.

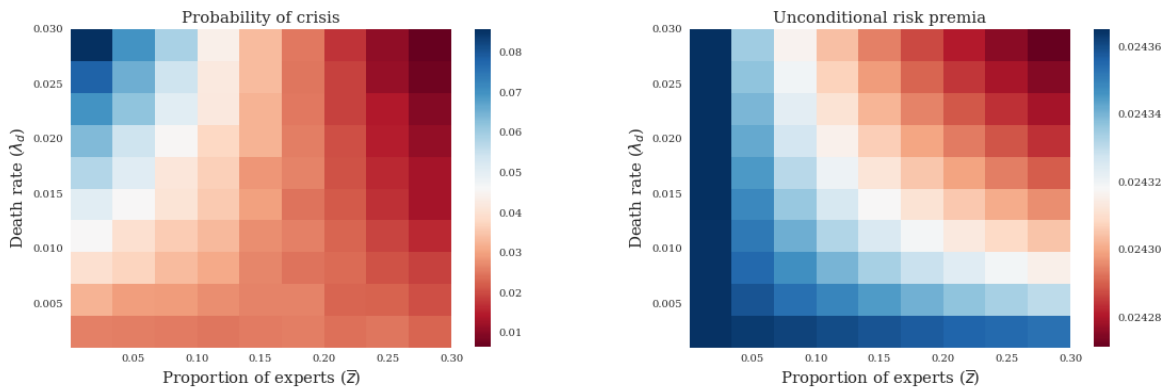


Figure 16: Left panel shows the drift of wealth share for two different values of exit rate λ_d for \bar{z} fixed at 0.1. The right panel shows the drift of wealth share for two different values of mean expert population for λ_d fixed at 0.02. Both plots are from recursive utility model with risk aversion equal 2 and IES=1.

Tightening financial constraint: One of the key assumptions of the model is the inability

of experts to fully issue outside equity. The parameter $\underline{\chi}$ governs how much equity the experts are forced to retain and hence it is of interest to study the model by varying this parameter. As the financial constraint tightens, the probability of crisis increases. The left panel of Figure (17) plots the risk premium of experts for three different values of the skin-in-the-game constraint. As the constraint increases, the crisis boundary shifts to the right but the unconditional risk premium is lower. This effect can be seen in the simulation result on the right panel of Figure (17). While a higher value of $\underline{\chi}$ leads to a higher probability of the crisis, the conditional risk premium drops drastically leading to only a marginal increase in the unconditional premium.

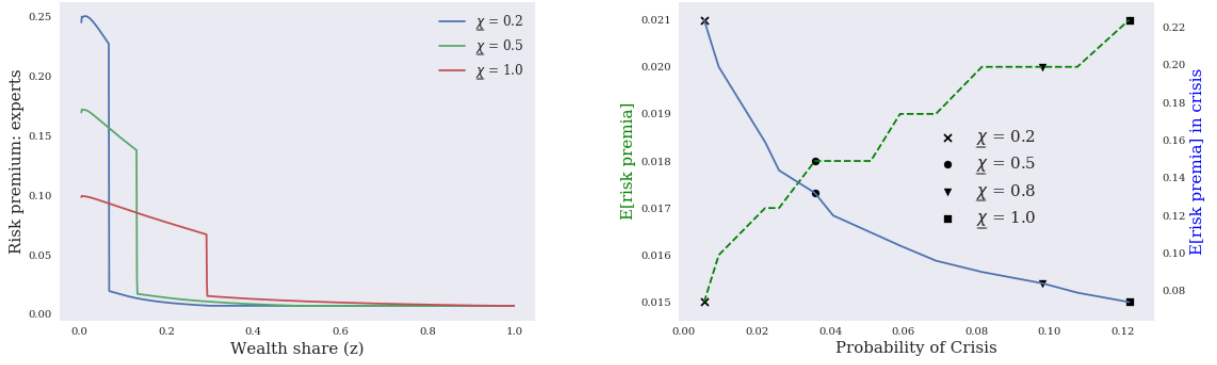


Figure 17: Left panel: Static comparison of the risk premium by changing the skin-in-the game constraint for the baseline model with $RA=1$ and $IES=1$. Right panel: Trade off between the conditional risk premium and the probability of crisis by varying the skin-in-the-game constraint. The parameter $\underline{\chi}$ increases from left to right. Left (dashed line) and right (blue line) axes correspond to the unconditional and the conditional risk premium respectively.

C.4 Deep learning methodology

C.4.1 One-dimensional model

I first present the solution to the benchmark model using deep learning method and then demonstrate how and why it is easy to scale to higher dimensions by presenting the solution to richer model with two state variables. I consider the case of recursive utility with $IES=1$ and $RA=2$ for demonstration.⁶³ The PDE that needs to be solved is

⁶³The deep learning algorithm works for any type of utility function. For larger risk aversion values, it takes longer to achieve convergence due to the highly non-linear value function near the boundaries.

given in (91). Construct a neural network $\hat{J}(z, t | \Theta)$ and define the PDE residual to be

$$f := \frac{\partial \hat{J}}{\partial t} + \frac{\partial \hat{J}}{\partial z} \mu^z + \frac{1}{2} \frac{\partial^2 \hat{J}}{\partial z^2} (\sigma^z)^2 - \mu^J \hat{J}$$

The network architecture is given in Figure (19) with the hyperparameters in Table (9).⁶⁴ Figure (18) plots the full grid and the training sample. The inner static loop uses a grid size of 1000 points in space dimension while the neural network only uses 300 points for training. In the case of a single space dimensional model, sampling one-third of the grid points is enough to find the right solution. In higher dimensions, the proportion of grid points required as training sample can be set much lower than one-third.

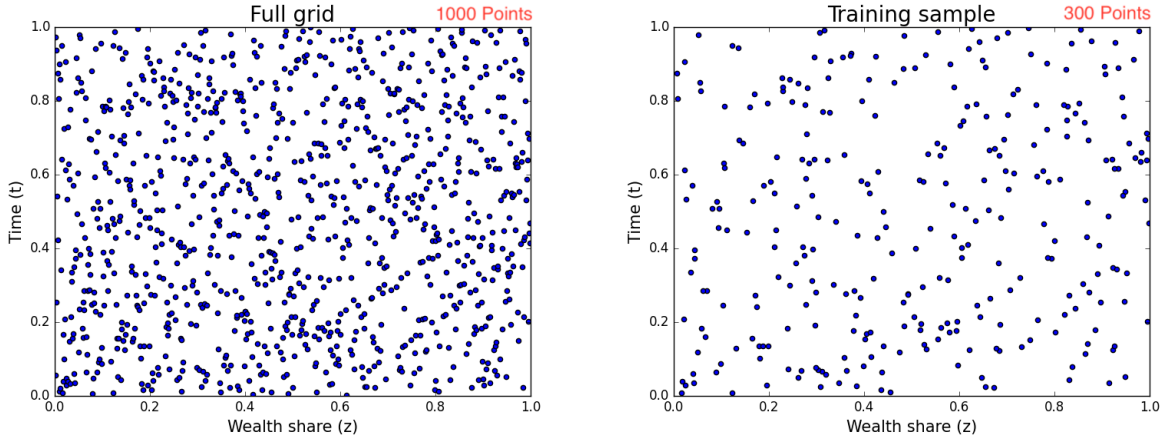


Figure 18: Grid used in numerical procedure: 1D model.

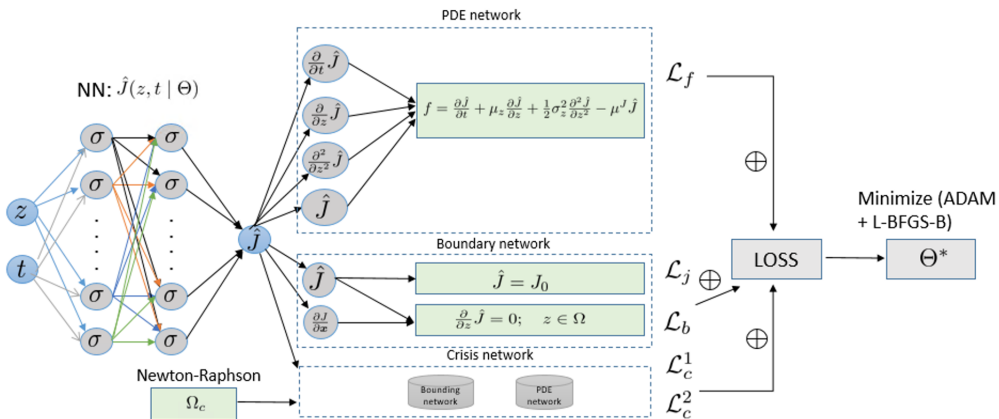


Figure 19: Network architecture: benchmark model.

⁶⁴The algorithm works even for 2 hidden layers with 30 neurons each instead of 4 hidden layers but may be prone to instabilities for some extreme parameter values such as setting $\chi = 0.1$. It is recommended to have four layers to capture the non-linearity well.

I illustrate the simplicity of coding the neural network solution using code snippets that uses Tensorflow library. The first step is to construct a neural network \hat{J} using the space and time dimensions as training data, and weights and biases as parameters initialized arbitrarily.⁶⁵ This is illustrated in the code snippet (1) and it corresponds to the left most feed-forward neural network ($NN : \hat{J}(z, t | \Theta)$) in Figure (19). The next step is to construct the regularizers using PDE residual as given in code snippet (2). This forms the PDE network in Figure (19). The PDE coefficients (advection, diffusion, and linear terms) are taken as given and form part of the training sample. The automatic differentiation in Tensorflow (*tf.gradients*) enables fast computation of derivatives in the regularizers which guides the parameterized neural network \hat{J} towards the right solution even when the training sample is small. In addition to the PDE bounding loss, one can easily set up the boundary loss and crisis region loss in a similar fashion.

```

1 def J(z,t):
2     J = neural_net(tf.concat([z,t],1),weights,biases)
3     return J
4

```

Listing 1: Approximating J using a neural network: 1D model

```

1 def f(z,t):
2     J = J(z,t)
3     J_t = tf.gradients(J,t)[0]
4     J_z = tf.gradients(J,z)[0]
5     J_zz = tf.gradients(J_z,z)[0]
6     f = J_t + advection * J_z + diffusion * J_zz - linearTerm * J
7     return f

```

Listing 2: Constructing regularizer: 1D model

Since the analytical solution to the benchmark model is not available, I compare the neural network solution with the those obtained from the finite difference method explained in Appendix (C.2.3). Figure (20) shows the comparison. They are not only

⁶⁵I use Xavier initialization to avoid the vanishing gradient problem.

qualitatively similar, they are quantitatively the same up to the order of $1e-4$.

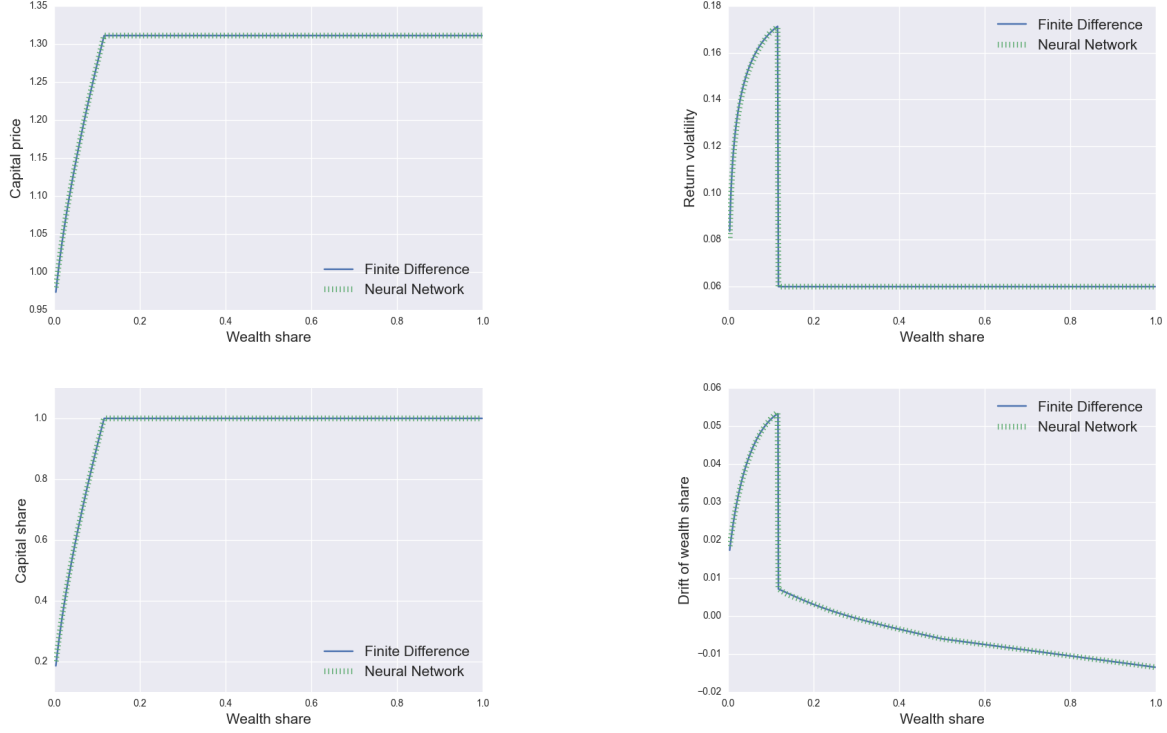


Figure 20: Comparison of equilibrium quantities using finite difference and neural network in one-dimensional benchmark model.

C.4.2 Two-dimensional model

The PDE that needs to be solved in the two-dimensional model is given in (48). As in the case of one-dimensional model, construct the neural network $\hat{J}(z, a, t \mid \Theta)$ with the PDE residual taking the form

$$f := \frac{\partial \hat{J}}{\partial t} + \frac{\partial \hat{J}}{\partial z} \mu^z + \frac{\partial \hat{J}}{\partial a} \mu^a + \frac{1}{2} \frac{\partial^2 \hat{J}}{\partial z^2} \left((\sigma^{z,k})^2 + (\sigma^{z,a})^2 + 2\varphi \sigma^{z,k} \sigma^{z,a} \right) + \frac{1}{2} \frac{\partial^2 \hat{J}}{\partial a^2} \sigma_a^2 + \frac{\partial^2 \hat{J}}{\partial z \partial a} (z \sigma^{z,k} \sigma_a \varphi + \sigma_a \sigma^{z,a}) - \mu^J \hat{J}$$

The network architecture and hyperparameters are given in Figure (9) and (9) respectively. The grid size becomes larger compared to the one-dimensional model but the chosen training sample size is 3000 which is much smaller than the full grid size of 30,000 as is illustrated in Figure (21). To appreciate the simplicity involved in scaling to higher dimensions, I present the code snippets for the 2D model in (3) and (4). Similar to the 1D model, the neural network J is parameterized the same way except that the network takes three inputs- two space dimensions (z, a) and one time dimension

(t). This corresponds to the leftmost feed-forward neural network in Figure (9) where three neurons enter the network instead of two as in Figure (19). The construction of regularizer as shown in code snippet (4) simply adds new derivative terms to the PDE network taking as given the coefficients (advection, diffusion, linear, and cross terms). Moving from one to two dimensions in an implicit finite difference method is not trivial since one has to set up the system of linear equations to be solved numerically. In even higher dimensions, as demonstrated in [Gopalakrishna \(2021\)](#), the PDE network simply adds further derivative terms. This is easier to do in comparison with setting up the system of equations. In dimensions more than two with correlated state variables, preserving monotonicity of the numerical schemes adds further complications, which the neural network method sidesteps. The literature has used advanced C++ tools like Paradiso (see [Hansen, Khorrami and Tourre \(2018\)](#)) which requires much more effort than simply augmenting the PDE network. Since most of the heavy lifting is done by the automatic differentiation in the regularizers, learning in high dimensions is accomplished effectively through a few lines of coding.

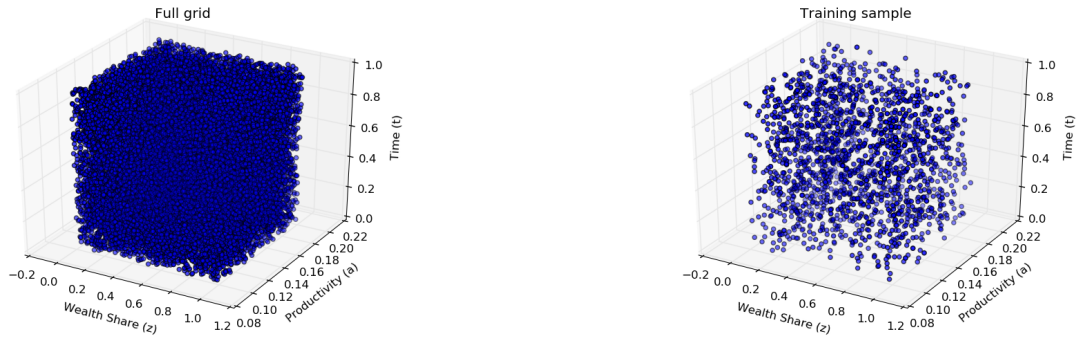


Figure 21: Grid used in numerical procedure: 2D model. The full grid contains 30,000 points and the training sample contains 3000 points.

```

1 def J(z,a,t):
2     J = neural_net(tf.concat([z,a,t],1),weights,biases)
3     return J
4

```

Listing 3: Approximating J using a neural network: 2D model

```

1 def f(z,a,t):
2     J = J(z,a,t)
3     J_t = tf.gradients(J,t)[0]
4     J_z = tf.gradients(J,z)[0]
5     J_a = tf.gradients(J,a)[0]
6     J_zz = tf.gradients(J_z,z)[0]
7     J_aa = tf.gradients(J_a,a)[0]
8     J_az = tf.gradients(J_a,z)[0]
9     f = J_t + advection_z * J_z + advection_a * J_a + diffusion_z * J_zz +
10         diffusion_a * J_aa + crossTerm * J_az - linearTerm * J
11     return f

```

Listing 4: Constructing regularizer: 2D model

	All	Crisis	Normal	All	Crisis	Normal	All	Crisis	Normal	All	Crisis	Normal
E[leverage]	3.22	5.50	3.09	2.08	4.36	2.08	1.57	1.57	1.57	1.29		1.29
E[inv. rate]	6.00%	4.90%	6.00%	5.80%	5.60%	5.80%	5.50%	5.50%	5.50%	5.30%		5.30%
E[risk premia]	1.70%	13.50%	1.00%	2.70%	16.50%	2.70%	4.50%	4.50%	4.50%	8.00%		8.00%
E[return volatility]	6.20%	15.90%	5.70%	5.80%	14.30%	5.80%	5.80%	5.80%	5.80%	5.90%		5.90%
E[GDP growth rate]	2.30%	-7.90%	2.90%	2.10%	-10.70%	2.10%	1.90%	1.90%	1.90%	1.80%		1.80%
Std[inv. rate]	3.10%	1.30%	0.11%	0.13%	0.23%	0.12%	0.08%	0.08%	0.08%	0.04%		0.04%
Std[risk premia]	2.84%	0.91%	0.23%	0.43%	0.56%	0.21%	0.17%	0.17%	0.17%	0.10%		0.10%
Corr(leverage, shock)	-0.27	-0.04	-0.24	-0.19	0.29	-0.19	-0.21	-0.21	-0.21	-0.26		-0.26
Prof. of crisis	7.80%			0.10%			0.01%	0.01%	0.01%	0.00%		0.00%
Risk aversion	1			5			10	10	10	20		20

Table 11: Benchmark model implied moments for different risk aversion levels with parameters from Table (10).

D Online Appendix

D.1 Benchmark model

Solving the incomplete market capital misallocation model with fire-sales and endogenous regimes involves numerical techniques that are non-standard from the asset pricing literature viewpoint. In addition to the complexity involving in solving the PDEs, the coefficients of the PDEs change with respect to the form of utility function. Thus, comparing model solutions across different utility specifications require manual intervention to modify the equations in static step, and the PDE coefficients. Part of the contribution of this paper is to offer a simpler way to perform comparative valuation dynamics through numerical libraries made available⁶⁶ at <https://github.com/goutham-epfl/MacroFinance>. The simplicity of using the library is that model can be solved and simulated in a few lines facilitating comparative valuation. Code snippet (5) presents an example of solving the model with different utility specifications. Code snippet (6) shows examples of simulating different models from the general framework.

```
1 from model_recursive_class import model_recursive
2 from model_class import model
3 from model_general_class import model_recursive_general
4 import matplotlib.pyplot as plt
5
6 #Input parameters
7 params={'rhoE': 0.06, 'rhoH': 0.03, 'aE': 0.11, 'aH': 0.03,
8         'alpha':0.5, 'kappa':7, 'delta':0.025, 'zbar':0.1,
9         'lambda_d':0, 'sigma':0.06, 'gammaE':2, 'gammaH':2, 'IES=1.5'}
10
11 #solve model1
12 model1 = model_recursive_general(params)
13 model1.solve()
14
15 #solve model2
16 #switch to model with unitary IES
17 params['IES'] =1.0
18 #solve model
19 model2 = model_recursive(params)
20 model2.solve()
21
22 #plot capital price (Q) from the model1 and model2
23 plt.plot(model1.Q), plt.plot(model2.Q)
```

Listing 5: Solving the model using Python library

```
1 from model_recursive_class import model_recursive
2 from simulation_model_class import simulation_benchmark
3
4
5 #Input parameters
6 params={'rhoE': 0.06, 'rhoH': 0.03, 'aE': 0.11, 'aH': 0.03,
7         'alpha':0.5, 'kappa':7, 'delta':0.025, 'zbar':0.1,
8         'lambda_d':0, 'sigma':0.06, 'gammaE':2, 'gammaH':2, 'IES=1.0'}
9 #set number of simulations
```

⁶⁶Advanced users can also choose among implicit and explicit finite difference schemes to solve the model, use different interpolation methods, and modify the frequency of time used in the simulation.

```

10 params['nsim'] = 500
11 params['utility'] = 'recursive'
12 #simulate model1
13 simulate_model1 = simulation_benchmark(params)
14 simulate_model1.compute_statistics()
15 print(simulate_model1.stats) #print key statistics
16 simulate_model1.write_files() #store key statistics for later use
17
18 #simulate model2
19 #change volatility
20 params['sigma'] = 0.10
21 simulate_model2 = simulation_benchmark(params)
22 simulate_model2.compute_statistics()
23
24 #compare stationary distribution from two models
25 plt.plot(simulate_model1.z_sim.reshape(-1))
26 plt.hist(simulate_model2.z_sim.reshape(-1))

```

Listing 6: Simulating the model using Python library